

Functional characterization of  
leucine-rich repeat kinase 2 (LRRK2)  
dimerization

Dissertation

zur Erlangung des Grades eines Doktors  
der Naturwissenschaften

der Fakultät für Biologie  
und  
der Medizinischen Fakultät  
der Eberhard-Karls-Universität Tübingen

vorgelegt

von

Christian Klein  
aus Dachsbach, Deutschland

September 2008

Tag der mündlichen Prüfung: 1. Dezember 2008

Dekan der Fakultät für Biologie: Prof. Dr. H. A. Mallot

Dekan der Medizinischen Fakultät: Prof. Dr. I. B. Autenrieth

1. Berichterstatter: Prof. Dr. T. Gasser

2. Berichterstatter: Prof. Dr. T. Stehle

Prüfungskommission:  
Prof. Dr. T. Gasser  
Prof. Dr. T. Stehle  
Prof. Dr. B. Schloßhauer  
Prof. Dr. P. J. Kahle  
Prof. Dr. O. Rieß

MEINER FAMILIE GEWIDMET



AND IF WE ARE HERE  
JUST TO EASE GOD'S SORROW  
LORD COME TO ME  
AND I'LL EASE YOUR MIND

PSYCHOTIC WALTZ *Into The Everflow* (1992)



---

<b>1</b>	<b>SUMMARY .....</b>	<b>1</b>
<b>2</b>	<b>INTRODUCTION .....</b>	<b>3</b>
<b>2.1</b>	<b>Parkinson's disease.....</b>	<b>3</b>
2.1.1	Clinical definition.....	3
2.1.2	Epidemiology and economic impact .....	4
2.1.3	Neuropathology .....	5
2.1.4	Etiology.....	7
2.1.5	Pathogenesis.....	12
<b>2.2</b>	<b>PARK8: Leucine-rich repeat kinase 2 (LRRK2) .....</b>	<b>15</b>
2.2.1	Phenotype and neuropathology.....	15
2.2.2	Structure .....	16
2.2.3	Expression and localization .....	18
2.2.4	Mutations.....	18
2.2.5	Putative functions and effects of mutations .....	19
<b>2.3</b>	<b>The ROCO protein family.....</b>	<b>23</b>
<b>2.4</b>	<b>Goals of this study .....</b>	<b>24</b>
<b>3</b>	<b>RESULTS .....</b>	<b>27</b>
<b>3.1</b>	<b>Characterization of the <math>\alpha</math>Mid LRRK2 antibody .....</b>	<b>27</b>
<b>3.2</b>	<b>LRRK2 homodimerizes via its ROCO domain .....</b>	<b>29</b>
<b>3.3</b>	<b>LRRK1 homodimerizes via its ROCO domain .....</b>	<b>33</b>
<b>3.4</b>	<b>LRRK2 and LRRK1 heterodimerize via their ROCO domains .....</b>	<b>35</b>
<b>3.5</b>	<b>DAPK1 demonstrates homodimerization capability and shows heterodimerization potential with LRRK ROCO kinases .....</b>	<b>37</b>
<b>3.6</b>	<b>The ROCO<sup>LRRK2</sup> homodimerization is independent of GTP .....</b>	<b>38</b>
<b>3.7</b>	<b>Familial PD mutations in the ROCO<sup>LRRK2</sup> domain alter ROCO homo- and heterodimerization.....</b>	<b>41</b>
<b>3.8</b>	<b>The ROCO<sup>LRRK2</sup> fragment exerts an inhibitory effect on LRRK2 kinase activity.....</b>	<b>43</b>
<b>3.9</b>	<b>Influence of familial and artificial mutations in the ROCO<sup>LRRK2</sup> fragment on the LRRK2 kinase inhibiting effect.....</b>	<b>47</b>
<b>4</b>	<b>DISCUSSION .....</b>	<b>51</b>
<b>4.1</b>	<b>The ROCO<sup>LRRK2</sup> domain directs LRRK2 dimerization.....</b>	<b>51</b>
<b>4.2</b>	<b>Predicted model of the ROCO<sup>LRRK2</sup> self-interaction.....</b>	<b>53</b>

4.3	<b>LRRK1 homodimerization and LRRK2/LRRK1 heterodimerization ....</b>	<b>55</b>
4.4	<b>Putative functions of the mammalian ROCO domain .....</b>	<b>56</b>
4.5	<b>Influence of artificial and familial PD mutations on LRRK dimerization .....</b>	<b>57</b>
4.6	<b>ROCO<sup>LRRK2</sup> exerts an inhibitory effect on LRRK2 kinase activity .....</b>	<b>59</b>
4.7	<b>Predicted model of the ROCO<sup>LRRK2</sup>-mediated LRRK2 kinase inhibition .....</b>	<b>61</b>
4.8	<b>Outlook.....</b>	<b>63</b>
<b>5</b>	<b>MATERIALS AND METHODS.....</b>	<b>67</b>
5.1	<b>Chemicals .....</b>	<b>67</b>
5.2	<b>Solutions and buffers .....</b>	<b>69</b>
5.2.1	Molecular biology.....	69
5.2.2	Yeast two-hybrid (Y2H).....	70
5.2.3	Protein biochemistry .....	70
5.2.4	Cell biology .....	72
5.3	<b>Vectors and oligonucleotides .....</b>	<b>72</b>
5.4	<b>Antibodies.....</b>	<b>73</b>
5.5	<b>Molecular cloning.....</b>	<b>74</b>
5.5.1	PCR, agarose gel electrophoresis and extraction of DNA .....	74
5.5.2	Enzymatic digestion of DNA fragments and plasmid DNA .....	74
5.5.3	Ligation of digested DNA fragments and transformation of DNA by electroporation.....	75
5.5.4	Production of electrocompetent cells.....	75
5.5.5	Amplification, purification and validation of plasmid DNA .....	76
5.5.6	Cloned constructs.....	77
5.6	<b>MBP-Mid fusion protein expression and purification .....</b>	<b>78</b>
5.7	<b>Y2H interaction study .....</b>	<b>80</b>
5.8	<b>Cell culture, transfection, cell harvest and cell lysis .....</b>	<b>81</b>
5.9	<b>Immunoprecipitation, GTP-sepharose affinity purification and nucleotide competition assays .....</b>	<b>81</b>
5.10	<b>SDS-PAGE, Coomassie staining, Western blotting and densitometry .....</b>	<b>82</b>
5.11	<b><i>In vitro</i> kinase assay .....</b>	<b>82</b>
<b>6</b>	<b>REFERENCES .....</b>	<b>83</b>



Figure 2-1	Scheme of the nigrostriatal pathway in health and PD.	6
Figure 2-2	LB pathology.	7
Figure 2-3	Pathways leading to PD.	13
Figure 2-4	Domain architectures of mammalian ROCO kinases.	17
Figure 2-5	Mutations in LRRK2.	19
Figure 3-1	Characterization of the $\alpha$ Mid LRRK2 antibody.	26
Figure 3-2	The Mid LRRK2 antibody immunoprecipitates LRRK2 protein.	27
Figure 3-3	LRRK2 homodimerizes via its ROCO domain.	29
Figure 3-4	LRRK2 does not interact with ArmAnk, MidLRR, LRR or WD40 domains in co-IP assays.	31
Figure 3-5	LRRK1 homodimerizes via its ROCO domain.	32
Figure 3-6	LRRK2 and LRRK1 heterodimerize via their ROCO domain.	34
Figure 3-7	DAPK1 shows potential for homo- and heterodimerization.	36
Figure 3-8	The ROCO <sup>LRRK2</sup> homodimerization is independent of GTP.	37
Figure 3-9	Familial PD mutations in the ROCO <sup>LRRK2</sup> domain alter ROCO homo- and heterodimerization.	40
Figure 3-10	The ROCO <sup>LRRK2</sup> fragment exerts an inhibitory effect on LRRK2 kinase activity.	43
Figure 3-11	Effects of familial and artificial mutations in the ROCO <sup>LRRK2</sup> fragment on LRRK2 kinase activity.	46
Figure 4-1	Predicted model of the ROCO <sup>LRRK2</sup> interaction.	52
Figure 4-2	Homegenic dimerization is a prerequisite for LRRK2 kinase activity.	58
Figure 4-3	Possible mechanisms of the ROCO <sup>LRRK2</sup> mediated inhibitory effect on LRRK2 kinase activity.	60
Table 2-1	Genetic loci associated to PD.	9

°C	degree celcius
μ	micro
aa	amino acid
AD	Alzheimer's disease
ANK	ankyrin
ARM	armadillo
ASK1	apoptosis signal-regulatng kinase 1
BCA	Bicinchoninic Acid Assay
BSA	bovine serum albumine
<i>C. elegans</i>	<i>Caenorhabditis elegans</i>
COR	C-terminal of ROC
<i>D. melanogaster</i>	<i>Drosophila melanogaster</i>
DA	dopaminergic
DAPK1	death-associated protein kinase 1
DD	death domain
DMEM	Dulbecco's Minimal Essential Medium
<i>E. coli</i>	<i>Escherichia coli</i>
ER	endoplasmatic reticulum
ERK	extracellular signal regulated kinase
ERM	ezrin/radixin/moesin
<i>g</i>	gravitation constant
g	gram
h	hour
HEK	human embryonal kidney
HEPES	4-(2-hydroxyethyl)-1-piperazineethanesulfonic acid
HRP	<i>horseradish</i> -peroxidase
HSP	heat shock protein
IP	immunoprecipitation
IPTG	isopropyl-β-D-thiogalactopyranoside
kD	kilodalton
KSR	kinase suppressor of Ras
l	liter
LB	Luria-Bertani
LB	Lewy Body
LRR	leucine-rich repeat
LRRK2/1	leucine-rich repeat kinase 2/1

m	milli
M	molar
MAPKKK	mitogen activated kinase kinase kinase
MBP	maltose binding protein
MEK	MAP/ERK kinase
MFHAS1	malignant fibrous histiocytomas-amplified sequences with leucine-rich tandem repeats 1
min	minute
MLK	mixed-lineage kinase
MPTP	1-methyl-4-phenyl, 1, 2, 3, 6-tetrahydropyridine
mRNA	messenger ribonucleic acid
MSA	multiple system atrophy
n	nano
PAGE	polyacrylamide gelelectrophoresis
PBS	phosphate buffered saline
PCR	polymerase chain reaction
PD	Parkinson's disease
PINK1	phosphatase and tensin [PTEN] homolog-induced putative kinase 1
RCK	ROC-COR-kinase
RCKW	ROC-COR-kinase-WD40
ROC	Ras of complex proteins
ROCO	ROC-COR
ROS	reactive oxygen species
rpm	rounds per minute
RT	room temperature
SDS	sodium dodecyl sulfate
SN	substantia nigra
U	units
UPS	ubiquitin-proteasome-system
Y2H	yeast two-hybrid
Δ	deletion



# 1 SUMMARY

Parkinson's disease (PD), the second most common neurodegenerative disorder, afflicts 1 – 2% of people over age 50. During the last decade, several genes associated to familial forms of PD have been discovered and have led to a greatly improved understanding of the molecular pathways putatively involved in the pathogenesis of PD. Recently, mutations in the gene encoding leucine-rich repeat kinase 2 (LRRK2) were revealed to be the most common genetic cause for late-onset PD.

LRRK2 is a large multidomain protein kinase with a ROC-COR (ROCO) domain tandem archetypal for the ROCO protein family, providing a ROC domain capable of GTP binding and hydrolysis. Given the frequent dimerization of protein kinases, this study sought to shed light on putative LRRK2 dimerization, meanwhile an emerging theme in the field. Employing different experimental assays, the ROCO domain was mapped as the core interface directing LRRK2 dimerization. Moreover, homodimerization potential mediated by the respective ROCO domain was similarly revealed for the related ROCO kinases LRRK1 and DAPK1 (death-associated protein kinase 1). Intriguingly, heterodimerization potential among ROCO domains discovered in this study suggested a regulatory interplay between all three mammalian ROCO kinases. Whereas familial PD mutations in the ROCO<sup>LRRK2</sup> domain uniformly weakened ROCO<sup>LRRK2</sup> homodimerization, regular self-interaction of GTP binding deficient ROCO<sup>LRRK2</sup> mutants indicated independence from GTP. Most interestingly, challenging regular full length LRRK2 dimerization by co-expression of the ROCO<sup>LRRK2</sup> fragment, a significant inhibitory effect on LRRK2 autophosphorylation was disclosed. Importantly, the pathological augmented kinase activity of G2019S PD mutant LRRK2 was decreased identically. Consistent with weakened homodimerization, ROCO<sup>LRRK2</sup> fragments containing familial PD mutations accordingly showed a reduced LRRK2 kinase inhibiting effect.

Taken together, these findings suggest a general dimerization function for the ROCO domain, a notion supported by recent identification of bacterial ROCO domain dimerization. By virtue of its kinase inhibiting effect, the artificial ROCO fragment could serve as a blueprint for LRRK2 dimerization/kinase inhibitors, ultimately providing new therapeutic perspectives in the treatment of PD.



## 2 INTRODUCTION

### 2.1 Parkinson's disease

Aged individuals, the fastest growing proportion in the western populations, are threatened by neurodegenerative diseases. As life expectancy rises, so does the occurrence of these foremost age-related disorders. Posing not only a major problem to public health systems, illnesses like Alzheimer's or Parkinson's also deprive the benefit of a longer life. Ongoing research efforts for elucidating principle causes and mechanisms underlying these debilitating brain diseases are essential to develop successful therapeutic strategies.

What started out nearly 200 years ago with James Parkinson's (1755 – 1824) observance of only six patients with distinct symptoms (1) these days is well recognized as the second most common neurodegenerative disorder after Alzheimer's disease (AD). Putting at risk the ever increasing fraction of elderly people, Parkinson's disease (PD) has made its way beyond science into lay media, economy and politics. While there is still no cure, the past two centuries have seen an enormous advance in the diagnosis, treatment and molecular understanding of this devastating neurologic disorder.

#### 2.1.1 Clinical definition

PD is a chronic progressive neurodegenerative movement disorder clinically defined by tremor at rest, rigidity, bradykinesia and postural instability. The clinical symptoms – which were already accurately described by James Parkinson in his 1817 monograph “An essay on the shaking palsy” (1) – also can occur in a variety of other neurological disorders and thus, the clinical entity delineated by James Parkinson is referred to as parkinsonism or the parkinsonian syndrome (2, 3). Essentially, PD is the most common cause of parkinsonism, accounting for ~80% of cases (4).

For the vast majority of PD cases (~95%), etiology is unknown and thus the term idiopathic PD has been used. Confusingly, parkinsonism of known cause – if not part of another neurological disorder – is also called PD (familial PD if hereditary), even if

symptoms and pathology are not always strictly identical to idiopathic PD. Moreover, autopsy studies and genetic testing are not always available to ultimately confirm the clinical diagnosis. Thus, the term PD is commonly used to classify the four cardinal symptoms tremor at rest, rigidity, bradykinesia and postural instability, regardless of the exact etiology and pathology (5).

Approximately 70% of patients notice tremor as the first symptom, usually starting in one of the hands (6, 7). Rigidity, which is an increased resistance to passive movement, initially is also often asymmetrical. Bradykinesia is a general term to describe the overall slowness of voluntary movements and comprises akinesia (absence of movements) and hypokinesia (reduced amplitude of movement). Impairment of postural reflexes and disturbances of gait are a rather late manifestation of PD, occurring about 5 years from onset of disease (8). However, an accurate diagnosis of PD is complicated by several issues. In the first years of disease, the symptoms can be present intermittent. As PD is foremost a disease of the elderly, symptoms can also be mistaken as signs of normal aging. Indeed, parkinsonian features are known in the human aging process (9-11). Moreover, PD is a slowly progressing disorder, with disease symptoms being faint in the initial stages. Furthermore, parkinsonism also appears as part of other neurological disorders such as progressive supranuclear palsy, cortical-basal ganglionic degeneration, or multiple system atrophy (MSA), thus requiring a careful differential diagnosis (reviewed in (12)).

### **2.1.2 Epidemiology and economic impact**

PD has a mean age of onset of 55 years, and the incidence (the number of new cases per year per 100000 population) increases with age, from 20/100,000 to 120/100,000 at age 70 (4). Roughly, 1 – 2% of the ‘over 50’ population is affected, adding up to a current estimation of 1.5 million patients in the U.S. (13). Given similar demographic preconditions, up to 500,000 people are affected in Germany. Prevalence (the number of cases in a screened population) also increases with age, rising from 1.4 to 3.4% from age 55 to age 75 (14).

PD itself is not fatal. However, it leads to physical disabilities that eventually can result in premature death (e.g. deep vein thrombosis, pulmonary embolism, aspiration, falls) (15). Before the use of levodopa, mean survival of PD patients was



approximately 9.42 years, whereas now, with the application of levodopa, patients live five years longer. Most studies suggest that this increase in life expectancy is indeed due to treatment and not because of socioeconomic and medical advancement that leads to a general increase in life span. Yet, life expectancy among PD patients remains shortened in comparison to the normal population, not to mention the severe disability patients suffer from in late stages of the disease (reviewed in (16)).

Health care expenses are on the rise, and so are costs for PD. The economic burden caused by PD comprises not only direct cost like medication and other treatment, but also indirect cost like loss of productivity or informal care by family members. The few available studies suggest that these indirect costs account for the main part of the overall economic burden of PD. Moreover, expenses increase with disease stage. Estimates in the U.S. assessed the economic impact of PD to roughly \$25.4 billion in 1998, compared to \$116 billion for dementing diseases and \$697 million for epilepsy (17). The Parkinson's disease foundation calculated the per-individual yearly cost of PD at \$24,425 in 1998, with about one third being direct medical costs (18). In Germany, a study estimated the three-month mean direct health care costs to 5210 DM (2664 EUR) in 1995 (19). Introduction of new anti-PD drugs will be also increasingly charging health care systems. Thus, it is crucial to carefully evaluate the effectiveness of new treatments, which should at the same time alleviate the patient's suffering and be affordable for health care systems.

### **2.1.3 Neuropathology**

The pathological hallmarks of PD are the profound and selective loss of dopaminergic (DA) neurons in the substantia nigra pars compacta (SNpc), and the occurrence of cytoplasmatic proteinacious inclusions called Lewy bodies (LBs). While the clinical diagnosis of PD relies on the cardinal symptoms, postmortem identification of both SNpc dopaminergic neuron loss and LBs is required for a definite diagnosis of PD (4).

DA neurons project from the SNpc primarily to the putamen (Fig. 2-1), and their demise leads to a pronounced putamenal dopamine deficiency, which is causal for the motor symptoms of PD (20). It is estimated that dopamine in the putamen is depleted ~80% at the onset of symptoms, with ~60% of DA neurons already lost (4).

Importantly, the pattern of DA neuron loss in PD is distinct from that in normal aging (21). The lack of dopamine can be compensated with levodopa, a precursor of dopamine which crosses the blood brain barrier and is metabolized to dopamine. To date, there is no therapy which halts neurodegeneration, and levodopa is the gold standard in PD symptomatic therapy since its approval 40 years ago.

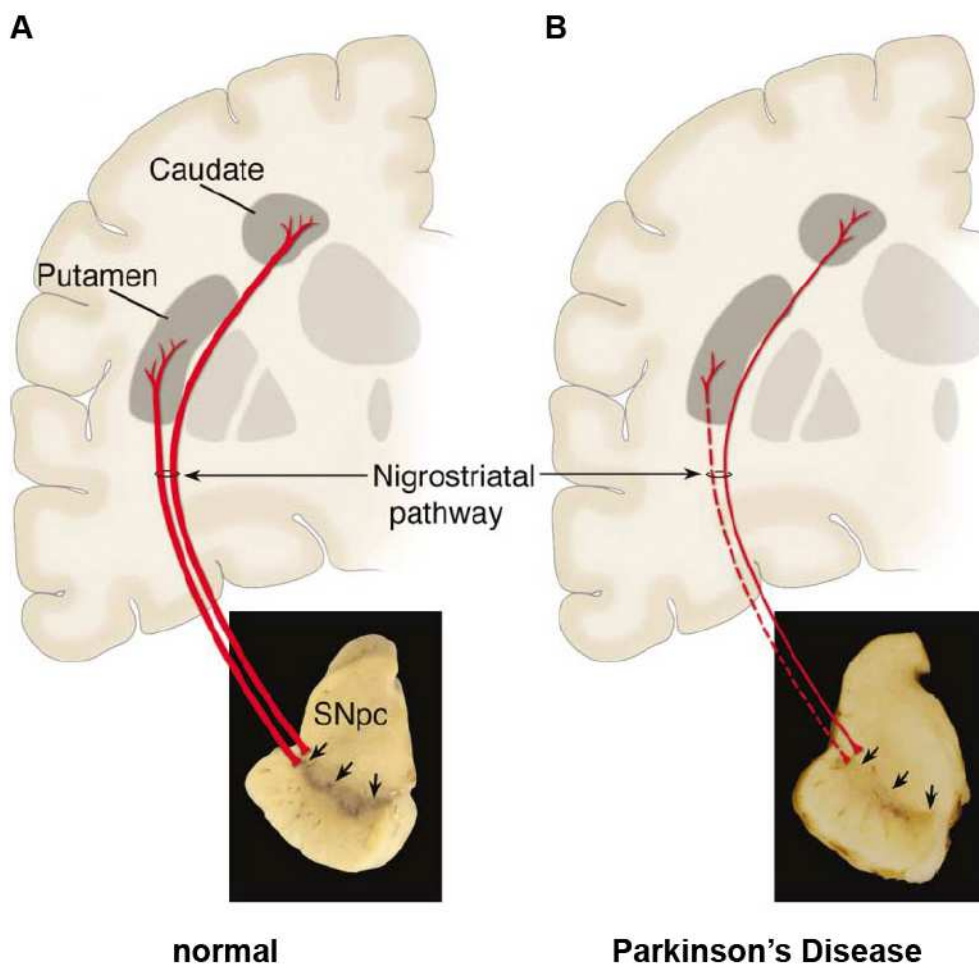


**Figure 2-1. Scheme of the nigrostriatal pathway in health and PD (modified from (4)).**

(A) In health, dopaminergic neurons project from the substantia nigra pars compacta (SNpc) to the putamen and caudate nuclei of the striatum (red lines). Neuromelanin production in the cell bodies of the dopaminergic neurons of the SNpc is demonstrated by normal pigmentation (see arrows in photograph). (B) In PD, dopaminergic neurons in the SNpc degenerate (pigmentation disappears, see arrows in the photograph). Neurons projecting to the putamen are more heavily affected than neurons projecting to the caudate nucleus (dashed red line vs. thin red line).

The archetypal LB is found as a round or spherical eosinophilic inclusion in brainstem sites of PD patients (Fig. 2-2), but LBs are also detected in other brain regions such as the cerebral cortex (22, 23). However, LBs are not specific for PD and are encountered in normal aging and other brain disorders, and thus the role of LBs in

cell death and PD is discussed controversial. LBs are aggregates consisting of various proteins including  $\alpha$ -synuclein (the main constituent), ubiquitin, neurofilaments and chaperones, and they are found in all affected brain regions (24, 25). Indeed, neurodegeneration in PD goes well beyond the commonly mentioned dopaminergic system and can affect noradrenergic, serotonergic and cholinergic systems as well (26). Furthermore, there is an overall increase of iron content in the PD brain, whereas the iron binding protein ferritin is reduced. This results in a higher fraction of non-ferritin-bound iron, which is potentially toxic and capable of catalyzing free radical formation (27). Thus, the main lesion in the SN differentially affects the whole brain metabolism.

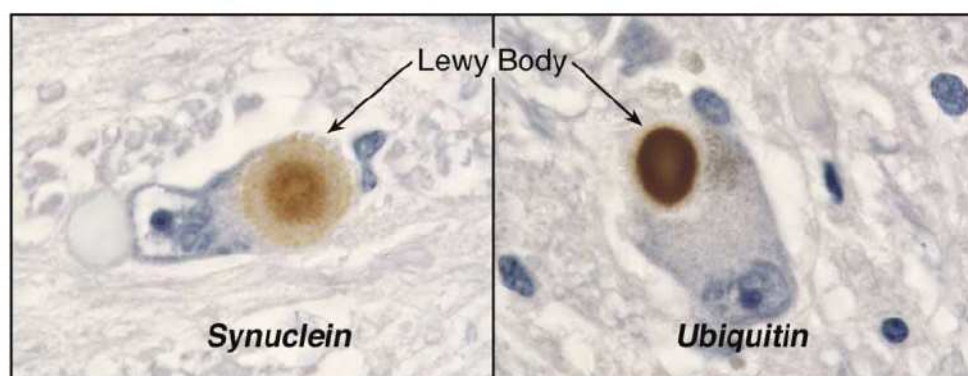


**Figure 2-2. LB pathology (modified from (4)).**

Immunohistochemical labeling of intracellular inclusions termed Lewy bodies (LBs) with antibodies against  $\alpha$ -synuclein (left photograph) and ubiquitin (right photograph).

#### **2.1.4 Etiology**

The cause for idiopathic PD remains obscure. Whereas the environmental toxin hypothesis prevailed for much of the 20<sup>th</sup> century, the discovery of inherited PD due to gene mutations provided much understanding of mechanisms underlying neurodegeneration in PD. However, it remains unknown if mechanistic concepts delineated from familial cases will also hold true for sporadic PD. Most probably, both environmental and hereditary factors play a role in the etiology of PD.

##### ***Environmental factors***

According to the environmental toxin hypothesis, exposure to an exogenous dopaminergic toxin leads to PD-related neurodegeneration. Actually, epidemiological

studies list a number of factors increasing the risk to contract PD, among them pesticides and herbicides, farming-associated exposures, as well as residence in a rural environment (28). Moreover, smoking cigarettes and drinking coffee seem to be inversely related to the risk for development of PD (29).

The environmental toxin hypothesis was strongly supported by the finding that people intoxicated with MPTP (1-methyl-4-phenyl, 1, 2, 3, 6-tetrahydropyridine, a byproduct originating from drug synthesis) developed a clinical syndrome nearly identical to PD (30). The lipophilic MPTP readily crosses the blood-brain barrier (31) and is metabolized in glial and serotonergic cells to its active neurotoxic form MPP<sup>+</sup>. Following uptake into nerve terminals by dopamine transporter (32, 33), it is concentrated in mitochondria (34) and blocks oxidative phosphorylation and ATP production by inhibiting complex I of the respiratory chain (35). Subsequently, ATP depletion as well as oxidative stress (through generation of reactive oxygen species (ROS) due to complex I inhibition) could lead to neurodegeneration. Interestingly, the herbicide paraquat is structurally similar to MPP<sup>+</sup>, and the insecticide rotenone similarly inhibits mitochondrial complex I, and both compounds are used to model PD in animals. Thus, a chronic exposure to MPTP-like agents may lead to PD, however, no such substances could be detected in the brain of PD patients (4).

### ***Genetic factors***

A contribution of genetic factors to PD was long denied, as many studies did not find significant differences in concordance rates of parkinsonism between mono- and dizygotic twins (36-41). However, these studies did not account for subclinical PD, possibly resulting in lowered concordance rates. In contrast, a study assessing dopaminergic dysfunction with positron emission spectroscopy (PET) applying [<sup>18</sup>F]-DOPA detected significant higher concordance rates among monozygotic twins, suggesting a genetic contribution in PD (42).

Concordantly, genetic studies could reveal genetic linkage of PD to distinct genetic loci in families with hereditary PD. To date, eleven genes with mutations associated to familial PD have been identified, five of which have been clearly confirmed to cause monogenic disease similar or identical to idiopathic PD ((5), table 2-1). An overview of current knowledge about the function of these genes is given in the following section.

Acronym	Mode of inheritance	Locus	Gene/protein
<i>PARK1</i>	autosomal-dominant	4q21-q23	<i>SNCA</i> / $\alpha$ -synuclein
<i>PARK2</i>	autosomal-recessive	6q25.2-q27	<i>Parkin</i>
<i>PARK6</i>	autosomal-recessive	1p35-p36	<i>PINK1</i>
<i>PARK7</i>	autosomal-recessive	1p36	<i>DJ-1</i>
<i>PARK8</i>	autosomal-dominant	12q12	<i>LRRK2</i>

**Table 2-1. Genetic loci associated to PD.**

#### *PARK1: $\alpha$ -synuclein*

In 1997, the first mutation causing PD was detected in the gene encoding  $\alpha$ -synuclein (43), leading to a substitution of alanine to threonine at amino acid (aa) position 53 (A53T). To date, two more missense mutations (A30P and E46K) as well as gene duplications and triplications have been found (44-46), the latter resulting in heightened  $\alpha$ -synuclein expression levels. *PARK1* PD is a very rare condition with a clinical appearance similar to idiopathic disease, but may have an earlier age of onset (47). Interestingly,  $\alpha$ -synuclein protein dosis seems to correlate with disease severity, as patients with a gene triplication show an earlier age of onset and a aggravated phenotype compared to persons with a gene duplication (48, 49).

The physiological function of  $\alpha$ -synuclein is still a matter of intense research. Among the proposed roles for this natively unfolded presynaptic protein have been synaptic vesicle recycling, storage and compartmentalization of neurotransmitters (50-52). Due to its hydrophobic non-amyloid- $\beta$  component (NAC) domain,  $\alpha$ -synuclein has an increased propensity to aggregate. Indeed, fibrillar  $\alpha$ -synuclein was found to be the main constituent of LBs, suggesting a role for  $\alpha$ -synuclein aggregation in the pathogenesis of PD (24). This assumption is supported by recent *in vivo* data showing  $\alpha$ -synuclein aggregation is dependent on its NAC domain (53). Moreover, C-terminally truncated human  $\alpha$ -synuclein expressed in mice (on a  *$\alpha$ -synuclein* null background) similarly induced formation of pathological inclusions, suggesting that C-terminal truncation could be an important regulator of aggregation (54). Furthermore, phosphorylation at Ser129 apparently promotes aggregation, and  $\alpha$ -synuclein phosphorylated at S129 is a major component of LBs (55). However, it is currently unclear whether LB-like aggregation of misfolded proteins in PD is toxic or protective

for the neuron. There is evidence suspecting oligomeric rather than fibrillar protein species to be the pathogenic agent. For instance, hydrophobic oligomeric  $\alpha$ -synuclein could generate membrane pores leading to neurotransmitter leakage and toxicity (56).

Interestingly, mice transgenic for human A53T  $\alpha$ -synuclein develop mitochondrial pathology, suggesting another link to PD pathogenesis. Moreover, biochemical analyses have demonstrated involvement of  $\alpha$ -synuclein in cellular pathways crucial for the integrity of dopaminergic neurons (reviewed in (13)).

### *PARK2: Parkin*

Mutations in the gene encoding Parkin are the most common genetic cause for early-onset PD, being responsible for ~49% of familial and ~19% of sporadic early-onset PD cases (57, 58). Whereas patients present with PD-typical nigrostriatal neuron loss, they usually do not show classic LB pathology (59-61). The disease was initially described to be inherited in an autosomal-recessive manner. However, certain missense mutations seem to be inherited in an autosomal-dominant way, and controversial evidence suggests that possession of a single Parkin mutation raises the likelihood of developing PD (62, 63).

Parkin functions as an E3 ubiquitin protein ligase by targeting misfolded ubiquitin-tagged proteins to the proteasome for degradation, and loss of this enzymatic activity due to mutations leads to early-onset PD (58, 64, 65). Thus, accumulation of misfolded proteins due to missing proteasome targeting is suggested to play a role in PD pathogenesis. Concordantly, some substrates of Parkin have been found to accumulate in Parkin and sporadic PD patients as well as parkin knock out mice (66, 67). Moreover, Parkin appears as a neuroprotective protein (68) implicated in pro-survival pathways important for dopaminergic neuron integrity (69, 70). Several studies revealed a functional connection to other PD genes. For instance, Parkin rescues mitochondrial dysfunction, muscle degeneration and dopaminergic cell loss due to PINK1 (see next page) inactivation in flies (71-73). Whereas age-dependent dopaminergic neurodegeneration due to mutant Parkin in flies argues for a toxic gain-of-function mechanism, Parkin knock out mice as a loss-of-function model did not show nigral degeneration (74, 75). Thus, Parkin can be considered as a multipurpose neuroprotective protein with a rather selective neuroprotective efficiency.

*PARK7: DJ-1*

Loss-of-function mutations (exonic deletions, truncations, homo- and heterozygous point mutations) in the DJ-1 gene cause 1-2% of all early-onset PD cases (76, 77). DJ-1 is a homodimeric protein with ubiquitous expression in various mammalian tissues including brain (78). A fraction of DJ-1 is localized at the mitochondrion (79). Whereas DJ-1 co-localizes with tau and  $\alpha$ -synuclein in other neurodegenerative disorders like AD and MSA, it is not present in LBs (80).

The precise functional role of DJ-1 is unclear so far. Among proposed functions are antioxidant, transcriptional co-activator and chaperone activity. Antioxidant, redox sensor-like features of DJ-1 are supported by data proposing a ROS (reactive oxygen species) scavenging function through eliminating hydrogen peroxide via self oxidation. Moreover, overexpression of wild type protein both *in vitro* and *in vivo* protects against injuries due to oxidative stress, most probably mediated by stabilizing transcription of antioxidant genes (81-84). Redox-dependent chaperone activity of DJ-1 was reported to inhibit  $\alpha$ -synuclein aggregation and subsequent cell death, and under conditions of oxidative stress, DJ-1 interacts with  $\alpha$ -synuclein *in vitro* (85-87). Mutant and oxidized DJ-1 tends to be unstable at the protein level. A contribution of DJ-1 to PD pathogenesis is supported by mouse models lacking DJ-1, which are sensitized to MPTP toxicity. Finally, transcriptional upregulation of tyrosine hydroxylase expression by DJ-1 may be important for maintenance and survival of dopaminergic neurons (reviewed in (88)).

*PARK6: PINK1*

In 2004, mutations in the *PINK1* (phosphatase and tensin [PTEN] homolog-induced putative kinase 1) gene were found to cause early-onset familial PD (89). Patients show disease onset at an average age of 35 years, with a phenotype indistinguishable from other forms of early-onset PD (90, 91). Similar to Parkin-related PD, inheritance is autosomal-recessive, and a single *PINK1* mutation seems to predispose an individual to PD (92). PARK6-related PD is a rather rare condition, with 2 – 3% of early-onset patients showing *PINK1* (homozygous) mutations (90, 93). Currently, the precise function of PINK1 remains elusive. Its mitochondrial localization and a clustering of mutations in the kinase domain suggest roles in mitochondrial dysfunction and kinase pathways relevant for PD pathogenesis (94, 95). The highly conserved kinase domain belongs to the Ser/Thr kinases of the

Ca<sup>2+</sup>/calmodulin family and undergoes autophosphorylation, yet no putative kinase substrates have been identified so far. In contrast to PINK1 with familial PD mutations, wild type protein confers protection from stress- or toxin-induced mitochondrial dysfunction and apoptosis *in vitro*, suggesting a pathologic loss-of-function mechanism leading to PINK1-related PD (89). Concordantly, PINK1 mutations affect protein stability (96). Furthermore, proteasomal stress reportedly enables altered cleavage of PINK1, impairing its function and possibly promoting its aggregation in LBs (96-98). In flies, PINK1 loss-of-function leads to muscle and dopaminergic degeneration due to mitochondrial dysfunction, a phenotype rescued by overexpression of Parkin (71-73). Thus, PINK1 and Parkin could act in a common biochemical pathway.

### 2.1.5 Pathogenesis

The discovery of gene mutations causing PD greatly advanced the understanding of pathological molecular mechanisms leading to hereditary parkinsonism and complemented knowledge from anatomical and histological studies. However, genetic defined PD is rare, and the vast majority of cases are sporadic. If mechanistic knowledge from familial PD is suited to develop treatment strategies for sporadic PD can be questioned; yet, the nearly identical neuropathology argues for a similar pathogenesis of both PD forms and provides a solid basis for further attempts to delineate the molecular cascade leading to familial PD.

From a multitude of studies analyzing toxic PD models as well as sporadic and familial PD, two major hypotheses about the pathogenesis of PD have emerged. One states that abnormal folding and aggregation of proteins lead to dopaminergic cell death, whereas the other suspects mitochondrial dysfunction and the resulting oxidative stress as the perpetrator. A closer inspection reveals a possible mutual influence of both hypotheses (Fig. 2-3). Thus, it will be a demanding scientific task to disentangle the strongly intertwined events leading to PD.



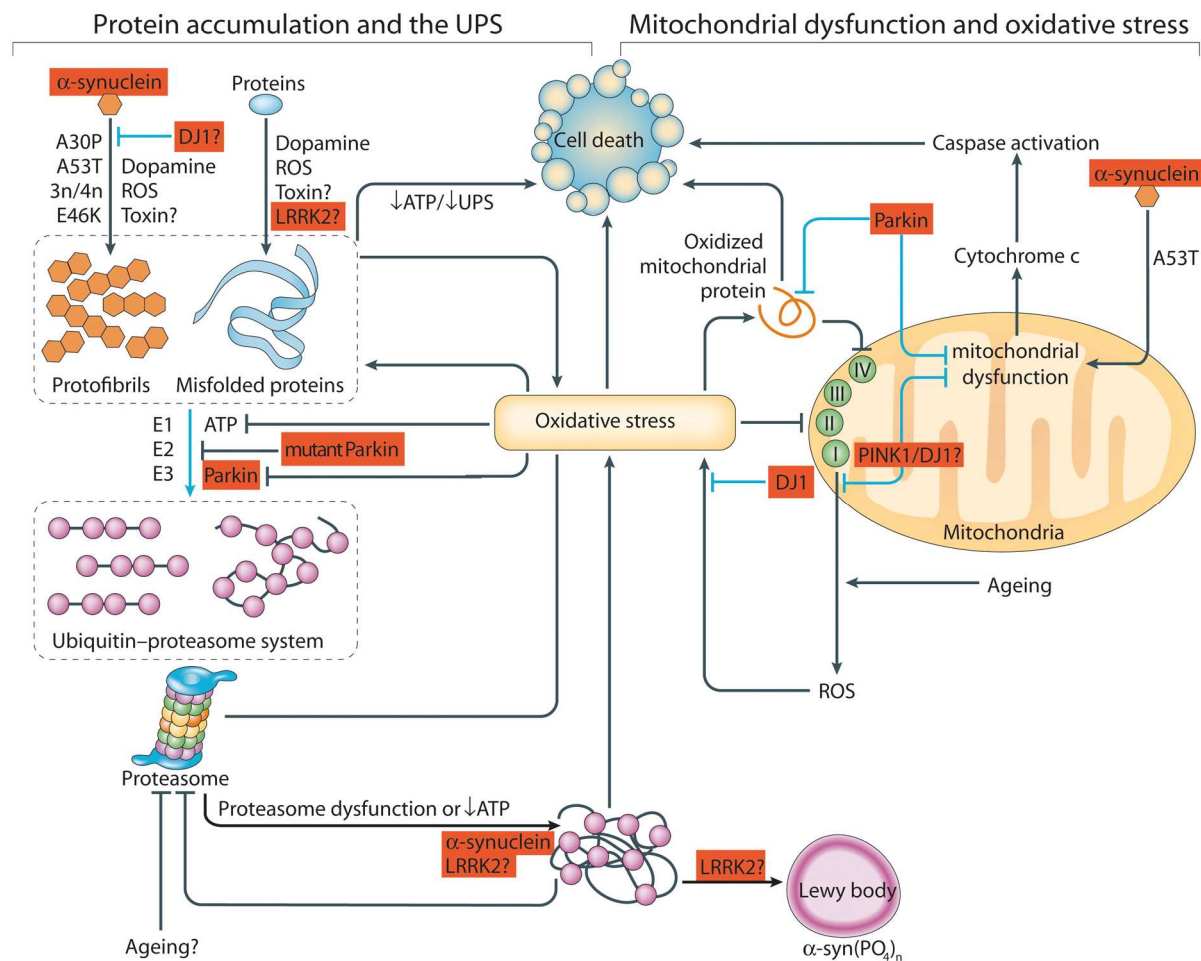


**Figure 2-3. Pathways leading to PD (modified from (88)).**

One main pathway to parkinsonism arises from protein accumulation and impairment of the ubiquitin-proteasome-system (UPS), whereas mitochondrial dysfunction and oxidative stress are engaged in the other prominent track to PD-associated cell death. Both pathways have a multitude of putative interaction points, as most familial genes are thought to impact on both sides. Beyond, PD genes seem to be closely intertwined themselves. For instance,  $\alpha$ -synuclein misfolds and aggregates, accordingly challenging the UPS. Concurrently, it has deleterious effects on the mitochondrion, which in turn can result in oxidative stress. Accumulation of  $\alpha$ -synuclein is suspected to be inhibited by DJ-1, and Parkin could detoxify aberrant  $\alpha$ -synuclein via the proteasome. In contrast to  $\alpha$ -synuclein, Parkin is preventing protein accumulation by targeting misfolded ubiquitin-tagged proteins to the proteasome for degradation. Simultaneously, it is suggested to have a protective effect on mitochondria, similar to the other recessive PD genes DJ-1 and PINK1. The positioning of LRRK2 in this complicated meshwork is not yet clear. Aberrant protein phosphorylation by overactive LRRK2 could lead to protein accumulation or induce pro-apoptotic pathways (for a more detailed overview of PD gene functions, see text). Besides the function of PD genes, the main components of both pathways are interrelated by feedback and feedforward mechanisms. For example, oxidative stress is generated by UPS failure and mitochondrial dysfunction, both of which in turn lead to oxidative stress. Activating and inhibiting effects are depicted by arrows and bars, respectively. Protective impact is colored blue, deleterious influence is colored black. PD genes are highlighted in red.

### ***Protein accumulation and the ubiquitin-proteasome-system (UPS)***

Abnormal deposition of proteins in brain tissue is encountered in several neurodegenerative diseases. Besides PD, typical examples comprise AD and Huntington disease. Although localization of aggregates differs (intra vs. extracellular), this common feature suggests that excessive protein accumulation is toxic to neurons. Toxicity could be conferred either directly (by deforming the cell or impairing intracellular trafficking) or indirectly (by sequestering proteins needed for normal cellular function) (4). However, it is still debated which conformation of accumulated proteins is toxic. Recent data suggests that soluble aggregates (oligomers) may be the neurotoxic species, whereas inclusion formation could be an attempt to detoxify soluble misfolded proteins. This view is supported by the finding that chaperones can protect from neurodegeneration (99-102).

In the cell, abnormal protein aggregation and degradation of misfolded proteins by the UPS are closely interrelated. If proper refolding by chaperones fails, misfolded proteins are tagged with ubiquitin and deconstructed by the proteasome (103). Thus, impairment of one of the UPS components will also lead to abnormal protein accumulation. In turn, excess amounts of aggregated proteins could inhibit the UPS. Ultimately, both processes could potentiate each other in a vicious circle.

Essentially, both phenomena are involved in familial PD (see overview of PD genes above). In sporadic PD, oxidative stress may lead to abnormally oxidized proteins prone to misfolding. Actually, abnormal oxidation of proteins increases with age (104) and could lead to an overload of the UPS due to misfolded proteins.

### ***Mitochondrial dysfunction and oxidative stress***

Similar to protein aggregation and the UPS, mitochondrial dysfunction and oxidative stress are closely intertwined. Due to the production of free radicals like hydrogen peroxide and superoxid during respiration, the mitochondria are the major intracellular site of ROS generation. Conversely, oxidative damage of lipids, protein and DNA by ROS in turn can culminate in dysfunction of cellular organelles, including the mitochondrion and its electron transport chain (105).

Apart from familial PD genes associated to oxidative stress (see overview of PD genes above) and beyond the discovery of the complex I inhibitor MPTP as a toxin

inducing PD-identical symptoms and pathology, additional evidence for an involvement of mitochondrial dysfunction and oxidative stress in the pathogenesis of PD has been found. Analyses of postmortem PD brains revealed a heightened level of biochemical markers for oxidative stress (106, 107). Moreover, activity of complex I is decreased above average in PD patients, especially in the SN. In contrast, MSA patients, who also develop degeneration of the SN, do not show complex I defects, suggesting that its decrease in PD patients is not a secondary event following neuronal degeneration but could rather be causal (108). Other potential sources of oxidative stress include generation of ROS during dopamine metabolism or catalysis by free iron (which is increased in PD brains). Furthermore, dopaminergic neurons could be more vulnerable to oxidative stress because of compromised antioxidant mechanisms. For example, levels of glutathion, an important detoxifier of hydrogen peroxide, are reduced in the SNpc of PD patients, but are normal in other brain regions (109).

However, mutations directly affecting oxidative phosphorylation usually do not lead to parkinsonism. Thus, oxidative phosphorylation and ROS abnormalities do not seem to be the primary cause of PD (4).

## **2.2 PARK8: Leucine-rich repeat kinase 2 (LRRK2)**

Point mutations in the gene encoding leucine-rich repeat kinase 2 (LRRK2) are the most common cause for autosomal-dominant, late-onset PD (110, 111). Located at the PARK8 locus on chromosome 12 described in 2002 (112), successful positional cloning of LRRK2 was achieved in late 2004 (110, 111). Several unique findings argue for a highly important role of LRRK2 in the pathogenesis of parkinsonism and maybe even in upstream events leading to neurodegeneration.

### **2.2.1 Phenotype and neuropathology**

Clinically, PARK8 parkinsonism is indistinguishable from idiopathic PD. Patients mostly become affected in their 5<sup>th</sup> decade ('late-onset') and present with the well-known cardinal symptoms of tremor at rest, rigidity, bradykinesia and postural

instability. However, this uniformity in symptoms is not always reflected in histopathological findings. *LRRK2* neuropathology can be diverse and even vary within the same family. Besides the compulsory collective degeneration of dopaminergic neurons in the SNpc, neuropathological manifestations range from  $\alpha$ -synuclein positive Lewy bodies in the brainstem (classical PD) and more widespread Lewy bodies (Lewy Body Disease) to tau pathology reminiscent of progressive supranuclear palsy (113). Thus, *LRRK2* apparently is involved in both  $\alpha$ -synucleinopathy as well as tauopathy. Surprisingly, there are also patients showing neither  $\alpha$ -synuclein nor tau aberrations (110). However, most patients display classical Lewy body pathology.

### 2.2.2 Structure

The 51 exons of *LRRK2* encode a very large multi-domain protein with 2527 aa, adding up to a calculated molecular weight of ~286kD (Fig. 2-4A). *In silico* analyses predict several putative protein binding domains, located in the N-terminal half (Armadillo repeats, ankyrin repeats and leucine-rich repeats) and at the C-terminus (WD40 domain). These domains enframe the putative catalytic core consisting of a ROC (Ras of complex proteins), COR (C-terminal of ROC) and kinase domain (114). Only the region between the ankyrin and leucine-rich repeats (aa 800 – 1000, designated 'Mid') does not seem to have a known domain signature and is probably natively unfolded (A. Lupas, MPI for Developmental Biology, Tübingen, personal communication). The particular ROC-COR domain combination is the archetypal signature of the so-called ROCO protein family (see 2.3). Whereas the ROC domain shows sequence similarity to Ras/Rab-like small GTPases, the invariably following COR region does not resemble any known protein domain (115). The kinase domain reveals closest sequence homology to MAPKKKs of the MLK(mixed-lineage kinase)-type.

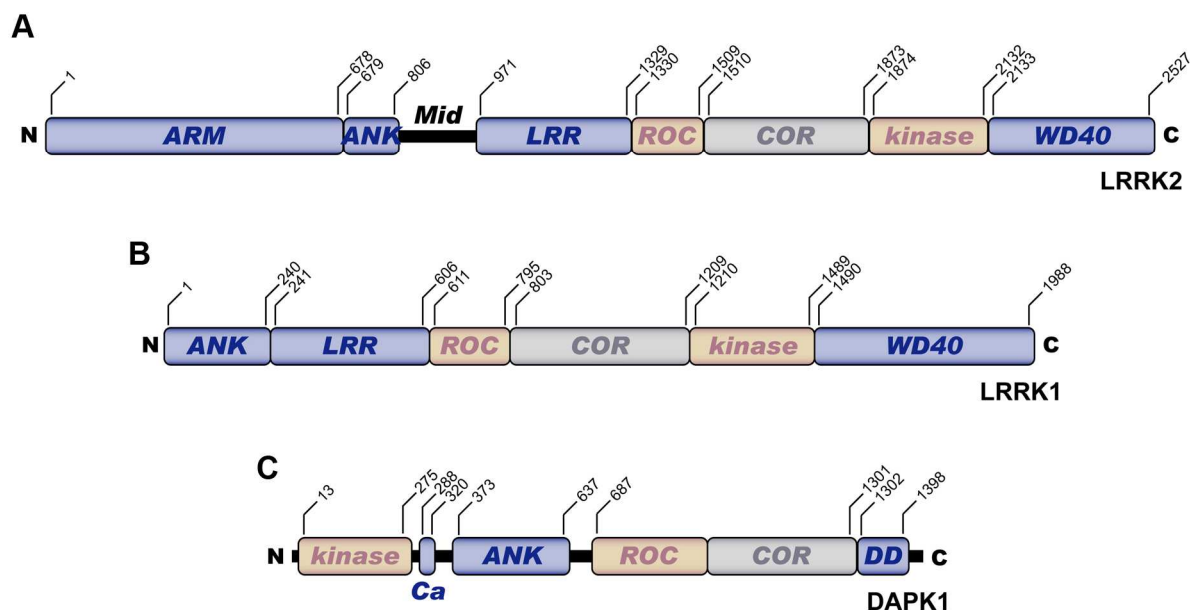


**Figure 2-4. Domain architecture of mammalian ROCO kinases.**

(A) Domain structure of LRRK2. The catalytic domain core consisting of a ROC/GTPase, COR and kinase domain is enframed by several putatively protein binding domains (colored in blue). The ARM domain was also described as a unique N-terminal LRRK2 repeat (116). (B) The LRRK1 domain structure shows a very similar composition to LRRK2. Apart from the ARM and MID domain, all domains from LRRK2 are also present in LRRK1, including the well-conserved ROC-COR-kinase core. (C) Domain structure of DAPK1. The more distant relationship to the LRRK proteins is reflected in a quite different domain architecture. The kinase domain is located N-terminally, and a death domain (DD) is following the ROCO domain tandem. *ARM*, armadillo; *ANK*, ankyrin; *LRR*, leucine-rich repeat; *ROC*, Ras of complex proteins; *COR*, C-terminal of ROC; *Ca*, Ca<sup>2+</sup>/Calmodulin regulatory domain; *DD*, death domain.

Information on LRRK2 crystal structure is scarce. Recently, the isolated ROC domain was described to exist as a unique ROC dimer, with parts of both monomers contributing to the dimer interface ('domain-swapping') (117). In contrast, crystal structures derived from the COR and ROCO fragments of the *Chlorobium tepidum* Roco protein suggest a dimerization via the C-terminal subdomain of the COR domain (118), challenging the accuracy of the domain-swapped ROC dimer. Obviously, more structural analyses complemented by functional assays will be needed for determining the crystal structure of human LRRK2. Nevertheless, LRRK2 dimerization is an emerging theme (see 2.2.5).

### **2.2.3 Expression and localization**

A multitude of studies analyzing LRRK2 mRNA and protein levels have demonstrated its ubiquitous expression pattern. Alongside robust expression throughout the human and rodent brain, LRRK2 is also expressed in various peripheral tissues including heart, lung, liver, and kidney (110, 111, 119-121). Actually, expression levels seem to be more prominent in peripheral tissues compared to brain (111). In the human and rodent brain, LRRK2 mRNA and protein expression is encountered particularly in the striatum (caudate and putamen), hippocampus, cortex and cerebellum, and could be detected in a variety of neuronal cell types. While data about expression in the SNpc is conflicting, there is wide consent about significant LRRK2 expression in dopaminoceptive areas (110, 111, 121-128).

On the subcellular level, LRRK2 has consistently been shown as a cytosolic protein, partly associated with cytoskeletal or membranous fractions (119-121, 129, 130). LRRK2 was detected at the outer mitochondrial membrane (119), and EM analyses suggest association to membranous/vesicular structures like ER or Golgi, yet no association to synaptic vesicles has been found (121). Furthermore, LRRK2 was proposed to be localized to lipid rafts, special cell membrane 'domains' with distinct composition and importance for signal transduction (131).

### **2.2.4 Mutations**

LRRK2 mutations are scattered throughout the whole gene sequence and occur at a high frequency in both familial and sporadic PD. Actually, mutation in LRRK2 is the most common known genetic cause of PD. To date, nearly 30 mutations have been identified (Fig. 2-5). Among these, seven variants show disease segregation and are thus thought to be definitely pathogenic (132). Interestingly, all pathogenic mutations are located in the C-terminal half of LRRK2. Special interest has been raised by the most common mutation G2019S, located in the LRRK2 kinase domain. It is accounting for 2 – 8% of hereditary and 0,6 – 1,6% of sporadic cases (133-138). In distinct ethnic populations, G2019S frequency is even higher and ranges from 11% in Portuguese and 20% in Ashkanezi Jewish to 40% in North African Arab PD populations (139-141). In contrast, this variant is much less common in asian populations (142, 143). Furthermore, penetrance for this mutation increases with age

(134, 140, 144). However, due to the large size of LRRK2, most genetic studies analyzing mutations focus on regions with known variants, particularly the G2019S mutation. Thus, these constricted screening approaches could reflect a biased representation of the occurrence of LRRK2 mutations in PD (132).

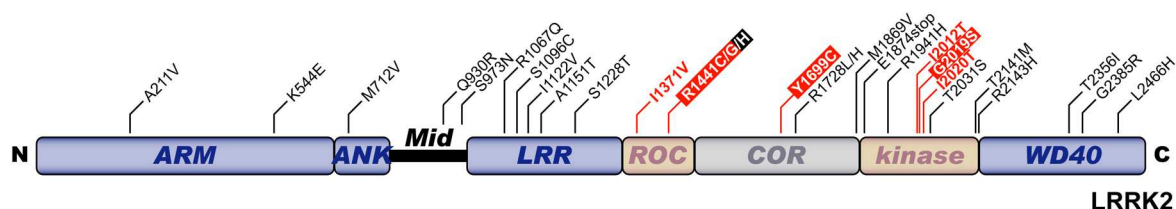


**Figure 2-5. Mutations in LRRK2.**

Nearly 30 aa substitutions in LRRK2 patients have been identified (132). Mutations confirmed to be pathogenic are highlighted in red, mutations used in this study are depicted invertedly. Note that pathogenic mutations cluster in the C-terminal half of the protein.

## 2.2.5 Putative functions and effects of mutations

Despite great efforts to elucidate its function in health and disease, the (patho)physiological role(s) of LRRK2 remain obscure. Nevertheless, there is a considerable amount of mostly *in vitro* data revealing hints of how LRRK2 might work.

### ***Kinase activity***

As expected from its kinase domain, LRRK2 *in vitro* functions as a serine/threonine kinase. Besides autophosphorylation, phosphorylation of the generic substrate MBP has been shown (119, 129, 145, 146). Recently, a kinase substrate screen identified the ERM (ezrin, radixin, moesin) proteins as more specific *in vitro* LRRK2 substrates (147), which now await confirmation in physiological settings. Biochemical studies analyzing the effects of PD associated mutations on kinase activity have yielded ambiguous results. Whereas G2019S modestly but concordantly augments kinase activity *in vitro* (119, 130, 145, 147), effects for other pathologic mutations are less clear. Another mutation in the kinase domain, I2020T, has been demonstrated to either increase or decrease kinase activity (129, 145, 147). Mutations in the ROC (R1441C, R1441G) and in the COR domain (Y1699C) were reported to increase activity, while other studies did not find any impact of these mutations (119, 130, 145,

147). Furthermore, mutations I1371V (ROC) and G2385R (WD40) do not appear to affect kinase activity (145), and I2012T (kinase domain) was reported to reduce activity (145, 147). The discrepancies between these studies are most probably due to differing experimental procedures and readouts (variable expression systems, purifying conditions, and *in vitro* substrates; full length LRRK2 vs. LRRK2 fragments) and clearly warrant ongoing analysis of effects of pathogenic mutations on LRRK2 kinase activity, preferably in more physiological settings.

### ***GTP binding and hydrolysis***

By sequence similarity, the LRRK2 ROC domain belongs to the Ras/GTPase superfamily (115), suggesting LRRK2 GTP binding and hydrolysis activity. Indeed, a multitude of studies has demonstrated binding of GTP to LRRK2 and the LRRK2 ROC fragment, respectively (145, 146, 148-150). However, definite proof for intrinsic LRRK2 GTPase activity is not at hand. Whereas LRRK2 purified from transgenic mouse brain demonstrated robust GTPase activity (148), studies analyzing cultured cells noticed only very low levels or no GTPase activity at all (148-150). Consequently, assessment of the effects of mutations on GTP binding and hydrolysis are not yet reliable. Several mutations have been proposed to increase GTP binding (R1441C, R1441G, I1371V, Y1699C) and ROC mutations R1441C and R1441G reportedly decrease GTPase activity (145, 148, 149).

In common cellular signal transduction pathways, GTPases frequently stimulate MAPKKKs by an intermolecular activation mechanism. In LRRK2, both GTPase and kinase activity are contained within a single protein, suggesting that the GTPase – kinase activation cascade could also run in an intramolecular mode. Actually, GTP binding to the ROC domain was found to stimulate LRRK2 kinase activity, and artificial mutations rendering LRRK2 GTP binding deficient consequently led to decreased LRRK2 kinase activity (145, 146, 150). Thus, the LRRK2 ROC domain is apparently able to activate the kinase domain by an unknown intramolecular mechanism. Hence, mutations outside the kinase domain still could affect kinase activity by perturbing GTP binding or influencing the hypothesized intramolecular kinase activation mechanism.



### ***Toxicity, pathways and binding partners***

In vitro expression of several LRRK2 mutant proteins (R1441C, Y1699C, G2019S and I2020T) reportedly led to toxicity in cultured cells, and some variants apparently resulted in formation of protein aggregates. The toxic effects of the LRRK2 mutants were found to be dependent on an intact kinase domain. Abolishing GTP binding (K1347A) led to a decrease in cell toxicity, supporting the hypothesis of an intramolecular kinase activation mechanism involving GTP binding via the ROC domain (130, 145, 146, 151, 152).

Despite its proposed function as a kinase of the MAPKKK-type, so far LRRK2 could not be assigned convincingly to one of the three major MAPK signal transduction pathways. One study noticed an upregulation of total c-Jun after LRRK2 overexpression in cell culture, but overall effects on signal transduction cascades described were independent from GTPase and kinase activity as well as from LRRK2 mutations (145). In differentiated SH-SY5Y cells, a MEK inhibitor apparently attenuated G2019S LRRK2-induced neurite shortening and neuritic autophagy, associating LRRK2 to the ERK pathway. Yet, phosphorylation of ERK upon overexpression of G2019S LRRK2 was not convincingly shown by this study (153). Likewise, data on putative LRRK2 binding partners – despite various predicted protein binding domains – is sparse. An *in vitro* interaction with Parkin (152) was never reproduced just as well as an in-depth analysis of various proposed candidate binding partners is still lacking (154). Recently, LRRK2 was demonstrated to be stabilized through binding to HSP90 (155) and proposed to interact with  $\alpha/\beta$ -tubulin (156).

### ***Dimerization***

Dimerization is a general feature of many protein kinases. However, evidence for LRRK2 dimerization is just emerging and putative LRRK dimerization is for the first time thoroughly scrutinized in the present study. Previously, co-immunoprecipitation of differentially tagged LRRK2 constructs co-expressed in cell culture (129) as well as the crystal structure of a LRRK2 ROC domain dimer (117) provided initial evidence for a possible dimerization of LRRK2. Recently, LRRK2 was demonstrated to exist predominantly as a dimer by gel filtration and blue native PAGE experiments. LRRK2 constructs with impaired kinase activity (K1906M, K1347A) seemingly tended to form higher-order oligomers, suggesting that the dimer could be the physiologically

active form of LRRK2 (157). However, discerning the functional relationship between kinase activity and dimerization remains demanding. Greggio and colleagues could not find evidence for transphosphorylation of kinase dead LRRK2 by wild type protein, thus drawing the conclusion that phosphorylation of LRRK2 is an intramolecular event (157). In contrast, a previous study noticed phosphorylation of a purified kinase dead COR-kinase fragment by a purified active kinase fragment, pointing at intermolecular phosphorylation (158). Beyond the exact mechanism of phosphorylation, the question of what comes first – phosphorylation or dimerization – is still to be solved.

### ***Putative (patho)physiological functions***

Only a few studies provide clues for LRRK2's putative (patho)physiological function. So far, the most prominent phenotype associated with mutations in LRRK2 is neuritic retraction observed in LRRK2 transfected cultured cells, pointing at an involvement of LRRK2 in growth cone dynamics. Additionally, a reduction in overall neurite branching was observed, whereas there was apparently no change of neuronal polarity, i.e. the ratio of axons to dendrites (151). Other studies found evidence for an involvement of autophagy and HSP90 (through maintaining stability of LRRK2) in the neurite remodelling process induced by mutant LRRK2, respectively (153, 155). Furthermore, analysis of *C. elegans* deletion mutants suggested a role for the worm LRRK2 homolog in regulating axonal-dendritic polarity of synaptic vesicle proteins (159). The few studies conducted in *D. melanogaster* have yielded conflicting results; whereas one report found induction of retinal and dopaminergic degeneration as well as impairment of fly locomotion by wild type and G2019S LRRK2 overexpression (160), another study could not detect significant effects in mutant flies lacking the whole LRRK2 homolog C-terminus including the kinase domain (161). Noteworthy, an evolutionary analysis of LRRK2 doubted the suitability of *C. elegans* and *D. melanogaster* homologs as models for LRRK2 function, as they are lacking an N-terminal repeat specific to LRRK2 (116).

Summing up, *in vivo* data for LRRK2 is scarce, yet evidence is emerging that links LRRK2 to the cytoskeleton and growth cone dynamics. The relevance of kinase activity for LRRK2 (patho)physiology is still not fully resolved, and *in vitro* and cell culture effects of kinase activity will have to await in-depth validation in *in vivo*

models. Additionally, kinase-independent, scaffold-like functions of LRRK2 can be anticipated. For instance, KSR (kinase suppressor of Ras) acts as an essential scaffold protein in the MEK/ERK pathway, mediating activation by binding all the participating kinases (reviewed in (162)). Similarly, LRRK2 could bring together the components of distinct signal transduction pathways, regulating their activation.

## 2.3 The ROCO protein family

Usually, members of the Ras/GTPase superfamily are small proteins devoid of additional protein domains (163). Recently, Bosgraaf and colleagues (115) identified several large proteins with complex domain architecture, containing a Ras/GTPase-like domain along with various additional protein domains. Besides the Ras/GTPase domain, which was termed ROC, all identified proteins shared a unique sequence stretch directly following the ROC domain, designated COR. Interestingly, despite extensive sequence database search, ROC and COR domains exclusively occurred in combination. Thus, these proteins have been grouped into a family designated ROCO, indicating that the ROC and COR domains might act as one functional unit. ROCO proteins have been detected in prokaryotes, *Dictyostelium*, plants and metazoa, but are absent in *Plasmodium* and yeast (115). Previously analyzed ROCO proteins play a role in cell proliferation, cell division, intracellular transport and cytoskeletal metabolism (115).

Besides LRRK2, three other mammalian ROCO proteins have been identified: LRRK1, DAPK1, and MFHAS1 (malignant fibrous histiocytomas-amplified sequences with leucine-rich tandem repeats 1), with LRRK1 being the closest LRRK2 relative (115). According to the few studies published, LRRK1 resembles LRRK2 in several aspects: LRRK1 shows (1) a very similar predicted domain architecture (Fig. 2-4B), is able (2) to undergo autophosphorylation, was demonstrated (3) as a GDP/GTP binding protein and seems to have a similar intrinsic GTP-dependent kinase activation mechanism, apparently is (4) widely expressed in brain and peripheral tissues, and (5) is a predominantly cytosolic protein (164). Nevertheless, PD-associated LRRK1 mutations have not been found so far, and a possible biological relationship to LRRK2 remains elusive (165).

DAPK1 is the third of the three mammalian ROCO proteins with a kinase domain. However, it is only distantly related to the LRRK ROCO kinases; correspondingly, its architecture is quite distinct, with the kinase domain located at the N-terminus (Fig. 2-4C). The barely recognized ROCO domain of DAPK1 has not been studied so far. Apart from being a ROCO protein, DAPK1 has been assigned to a group of closely related serine/threonine,  $\text{Ca}^{2+}$ /calmodulin-dependent kinases which are all associated to cell death. DAPK1 kinase activity is needed to sensitize the cell to various apoptotic signals and thus acts as a tumor suppressor. Beyond cell death, DAPK1 involvement in regulation of actin/cytoskeleton dynamics and vesicular fusion have been proposed. Moreover, *DAPK1* has been linked to AD and neuronal injury, hinting at a putative role in neurodegenerative processes (166-168).

## 2.4 Goals of this study

An involvement of LRRK2 in the pathogenesis of PD was revealed just before the beginning of this study. Accordingly, neither knowledge about LRRK2 function nor basic experimental assays were at hand. Thus, an important aim of this project was the establishment of elementary lab techniques and tools allowing for an investigation of putative LRRK2 functions. Initially, cloning of the full length gene had to be achieved, followed by establishment of transient transfection, Western blotting and immunoprecipitation, expectedly complicated by the tremendous size of LRRK2 (2527 aa). To circumvent these possible technical problems, *in silico* analyses of the primary aa sequence should reveal protein domain boundaries, allowing for an alternative and parallel investigation of single or combined LRRK2 domains. Furthermore, a polyclonal antibody specific for LRRK2 was generated and characterized.

Generally, protein kinases are known to be able to dimerize. Containing a kinase domain, LRRK2 could be suspected to self-interact. At the beginning of this study, only one co-immunoprecipitation of differentially tagged co-expressed full length LRRK2 was suggesting LRRK2 self-association (129). Thus, this project aimed at a thorough analysis of putative LRRK2 dimerization. Thereby, the main goals were (1) mapping of the dimerization domain, (2) examining the effect of familial PD mutations on dimerization and (3) investigating the functional relevance of dimerization.

Moreover, because of its close relation to LRRK2, LRRK1 should be analyzed for dimerization to reveal putative functional similarities among the LRRK proteins. Taken together, this study intended to advance the understanding of LRRK2 biology and biochemistry with a main focus on dimerization.



## 3 RESULTS

### 3.1 Characterization of the $\alpha$ Mid LRRK2 antibody

Specific antibodies are an indispensable tool for studying various aspects of a protein's function. At the beginning of this study, commercial antibodies for LRRK2 were not available. Hence, three peptide antibodies were generated. Additionally, an antiserum against a bigger protein stretch of LRRK2 was developed, as peptide antibodies often do not yield satisfying results. Cooperating with Prof. Andrei Lupas (MPI for Developmental Biology, Tübingen), a predictedly unfolded and exposed region of LRRK2 – termed Mid – encompassing aa 800 to 1000 was selected. Briefly, this region of LRRK2 was cloned into a pMAL vector containing the MBP coding sequence 5' of the multiple cloning site. Subsequently, the MBP-Mid fusion protein was expressed, purified and sent away for immunization (for details, see 5.6). A total of three consecutive antigen injections (one initial immunization and two boostings) were carried out, and the obtained antisera were tested by Western blot analysis of HEK 293T cell lysates containing overexpressed LRRK2 constructs.

Whereas none of the three peptide antibodies gave a specific immunoreactive signal (data not shown), all three LRRK2 Mid antisera detected a single immunoreactive band at ~ 280 kD in transiently transfected HEK 293T cells, corresponding to the expected molecular mass of LRRK2 (Fig. 3-1A). Boosting obviously increased sensitivity of the respective LRRK2 antiserum. Furthermore, an immunoreactive band at ~280 kD was noticed in non-transfected control cell lysates, apparently representing endogenous LRRK2 recognized by the antisera in a similar sensitivity-increasing manner. Noteworthy, none of the antisera showed further unspecific immunoreactive bands. As the Mid-Boost2 (MidB2) antiserum gave the strongest signals, all further experiments were conducted with this polyclonal antiserum. To prove specificity of the MidB2-antibody, the antiserum was pre-incubated with a molar excess of antigen (purified MBP-Mid). This led to a total disappearance of immunoreactivity, regardless if full length LRRK2 or the MidLRR fragment was present in the HEK 293T cell lysate (Fig 3-1B).

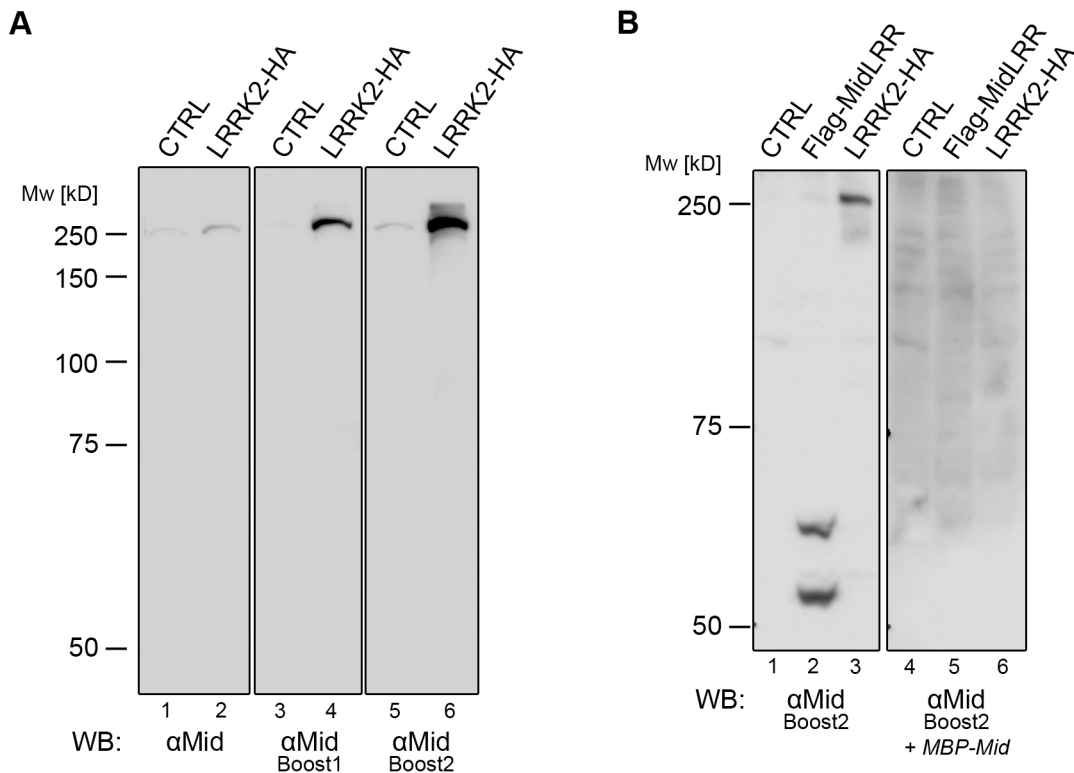


**Figure 3-1. Characterization of the αMid LRRK2 antibody.**

HEK 293T cells were not transfected (CTRL) or transiently transfected with LRRK2-HA or Flag-MidLRR, and cell lysates were subjected to SDS-PAGE/immunoblot. **(A)** All three LRRK2 antisera showed an immunoreactive signal at ~280 kD for transfected and non-transfected cell lysates. Signal intensity increased after boosting (consecutive immunizations). **(B)** Pre-incubation of MidB2 antiserum with a molar excess of antigen (MBP-Mid) led to a total disappearance of immunoreactivity (right panel).

To further demonstrate that the signal at around 280 kD is LRRK2, immunoprecipitation experiments with the MidB2 antibody coupled to protein G agarose were conducted. Enough protein to obtain a band visible on a coomassie gel was only pulled down through MidB2 from HEK 293T cells transiently transfected with LRRK2-HA (Fig 3-2). In contrast, no band in the range of LRRK2 could be detected when using pre-immune rabbit serum instead of MidB2 antibody or when IP was performed from non-transfected control cell lysates, indicating MidB2 to be specific for LRRK2. Essentially, MS-analysis unequivocally identified the obtained band as LRRK2 (Proteom Centrum, University of Tübingen). To sum up, the generated MidB2 antibody specifically detects endogenous and transfected LRRK2 protein on Western blot level and pulls down LRRK2 in immunoprecipitations.



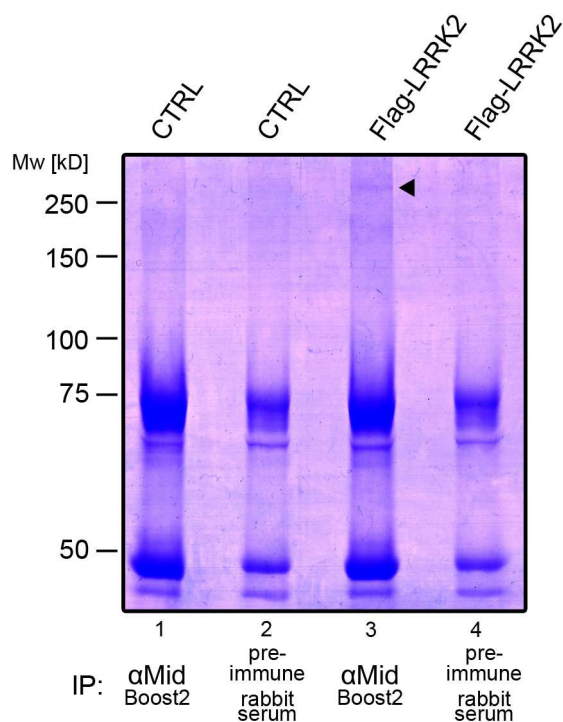


**Figure 3-2. The Mid LRRK2 antibody immunoprecipitates LRRK2 protein.**

HEK 293T cells were not transfected (CTRL) or transiently transfected with LRRK2-HA, and cell lysates were subjected to IP with MidB2-coupled protein G-agarose, followed by SDS-PAGE and coomassie staining. Mid LRRK2 antibody specifically immunoprecipitated a band at ~280 kD from transfected cell lysate (arrowhead). MS-analysis identified this band unequivocally as LRRK2.

### 3.2 LRRK2 homodimerizes via its ROCO domain

Many protein kinases are able to undergo dimerization or even oligomerization. Besides the well-known dimerization of receptor tyrosine kinases upon binding of ligand, also intracellular kinases have been found to dimerize. The serine/threonine kinases Raf-1 and MLK-3 (mixed lineage kinase-3), allocated to the same branch of the human kinome as LRRK2 (169), even require homodimerization for proper kinase activation (170, 171). Recently, co-immunoprecipitation of differentially tagged LRRK2 constructs co-expressed in cell culture (129), the crystal structure of a LRRK2 ROC domain dimer (117), and gel filtration / blue native PAGE experiments (157) provided initial evidence for a possible dimerization of LRRK2. Here, a comprehensive analysis of LRRK2 dimerization was conducted to advance the understanding of LRRK2 biochemistry.

The mere size of LRRK2 considerably complicates analysis of putative dimerization, as one or more of its many domains could be involved in self-interaction. To set a solid framework for subsequent in-depth analyses, the LRRK2 dimerization potential was first investigated in a yeast two-hybrid (Y2H) interaction study. Several predicted

LRRK2 single domains were cloned in the yeast vectors containing the coding sequence for the GAL4 activation (AD) and DNA binding domain (BD), respectively, and the fusion constructs were co-transformed into yeast in all possible combinations. Interestingly, a specific albeit weak interaction was exclusively observed between the LRRK2 ROC and COR domains fused to AD and BD, respectively (Fig 3-3A). A reciprocal AD-COR – BD-ROC interaction could not be detected. Checking fusion protein expression in yeast lysates on Western blots demonstrated proper expression of all fragments except BD-LRR, which showed decreased protein levels (Fig. 3-3B). Thus, the lack of growing yeast after fusion construct co-transformation does not reflect missing protein expression but rather indicates that there is no specific interaction between these fusion proteins in Y2H.

Using extended ROC fusion proteins, a very robust homomeric interaction of the ROCO domains was revealed. Moreover, heteromeric interactions between ROCO and LRRK2 fragments comprising ROC-COR-kinase (RCK) and the complete C-terminus including the WD40 repeats (RCKW) were detected (Fig. 3-3C). Reciprocal interactions were verified for all these combinations. However, homomeric interactions were not observed among domains larger than ROCO, possibly due to limitations of the Y2H method.

To overcome Y2H inherent restrictions and confirm the interaction results employing an independent method, a thorough co-IP analysis of LRRK2 dimerization in transiently co-transfected HEK 293T cells was performed. The homologous ROCO<sup>LRRK2</sup> interaction was validated, as HA-tagged ROCO<sup>LRRK2</sup> robustly co-immunoprecipitated along with MYC-tagged ROCO<sup>LRRK2</sup> (Fig. 3-3D). Missing precipitation of HA-ROCO<sup>LRRK2</sup> alone showed specificity of ROCO<sup>LRRK2</sup> homodimerization. The same results were obtained vice versa using HA-agarose (data not shown). Importantly, the MYC-ROCO<sup>LRRK2</sup> fragment was also co-immunoprecipitated with full length LRRK2-HA (Fig. 3-3E). In contrast to the Y2H interaction studies, a homomeric interaction of the large RCKW domains was detected in co-IP experiments, as evidenced by co-IP of HA-RCKW along with MYC-RCKW, whereas HA-RCKW alone was not precipitated by MYC-agarose (Fig. 3-3F). Finally, homodimerization of full length LRRK2 was shown by co-IP of MYC-LRRK2 with co-transfected LRRK2-HA (Fig. 3-3G).

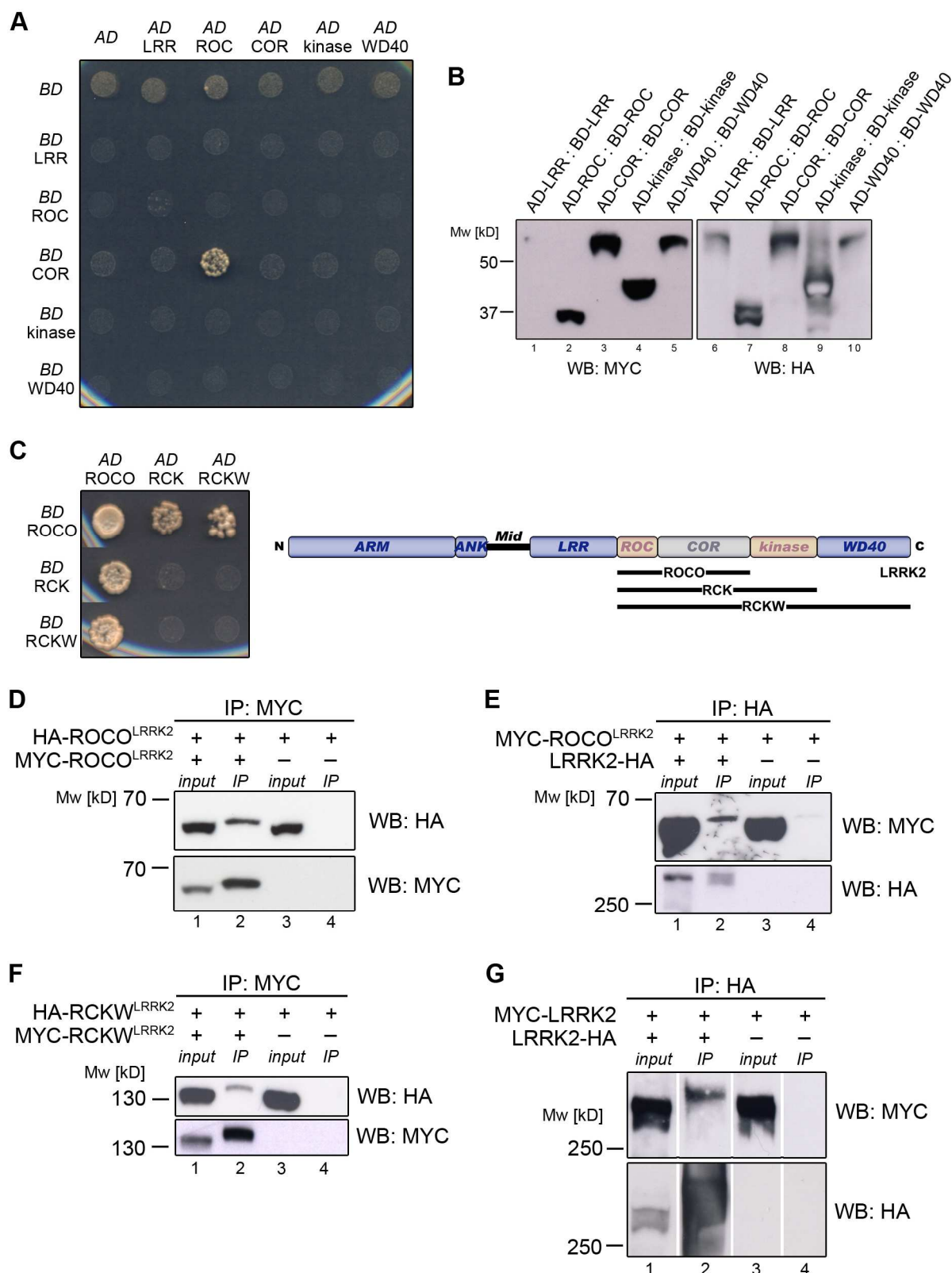


**Figure 3-3. LRRK2 homodimerizes via its ROCO domain.**

(A) Y2H interaction assay with single LRRK2 protein domains. Growth of yeast on selective media lacking Leu, Trp and His was only observed for yeast co-transformed with AD-ROC and BD-COR fusion proteins. (B) Expression levels of AD and BD fusion proteins in yeast strain AH109. Co-transformed fusion proteins were extracted from yeast and subjected to SDS-PAGE/immunoblot analysis. Probing with anti-MYC revealed immunoreactivity for BD fusion proteins (lanes 2 – 5), with only BD-LRR being expressed at considerably lower levels

(lane 1). Anti-HA detected immunoreactive signals for all AD fusion proteins (lanes 6 – 10), indicating proper expression of the constructs in yeast. Localization of the immunoreactive signals corresponds to the expected molecular weight of the fusion proteins. **(C)** Y2H interaction study using extended ROC domains as depicted in the LRRK2 domain sketch. Strong growth of yeast on selective media lacking Leu, Trp and His was detected for ROCO-ROCO, weaker interaction for ROCO-RCK and ROCO-RCKW, respectively, both for AD-BD and BD-AD fusion protein combinations. **(D-G)** HEK 293T cells were transiently co-transfected with HA- and MYC-tagged LRRK2 constructs. **(D)** HA-ROCO<sup>LRRK2</sup> was co-transfected with MYC-ROCO<sup>LRRK2</sup> (lanes 1-2) or alone (lanes 3-4). Input probings with anti-HA (upper panel) and anti-MYC (lower panel) revealed an immunoreactive signal at the expected ~65 kD for each transfected construct. MYC-agarose co-immunoprecipitated HA-ROCO<sup>LRRK2</sup> along with MYC-ROCO<sup>LRRK2</sup> (lane 2), but not in controls (lane 4). **(E)** Co-transfection of MYC-ROCO<sup>LRRK2</sup> and full length HA-LRRK2 (lanes 1-2) or single transfection of MYC-ROCO<sup>LRRK2</sup> (lanes 3-4). Probing input with anti-HA showed immunoreactivity at ~280 kD, indicative of full length HA-LRRK2 (lane 1). HA-agarose co-immunoprecipitated MYC-ROCO<sup>LRRK2</sup> only when HA-LRRK2 was co-transfected and immunoprecipitated (lanes 2 and 4). **(F)** MYC- and HA-RCKW<sup>LRRK2</sup> were co-transfected. HA-RCKW<sup>LRRK2</sup> was only co-immunoprecipitated during MYC-agarose when MYC-RCKW<sup>LRRK2</sup> was present (compare lane 2 to 4). **(G)** HA-agarose co-IP with both full length HA- and MYC-LRRK2. Anti-MYC immunoreactivity at ~280 kD represented full length MYC-LRRK2 (lanes 1 and 3, upper panel). MYC-LRRK2 was co-immunoprecipitated with HA-LRRK2 (lane 2) but did not bind unspecifically to HA-agarose (lane 4).

Although the initial Y2H studies suggested an exclusive involvement of the ROC and COR domain in LRRK2 dimerization, additional interactions among LRRK2 domains can not be excluded. To test the potential of other LRRK2 domains to assist dimerization, additional co-IP experiments were performed. FLAG-tagged ArmAnk (Armadillo-Ankyrin), MidLRR (Mid-leucine-rich repeat), LRR or WD40 domains were cotransfected with LRRK2-HA, and HEK 293T cell lysates were subjected to FLAG-IP. Whereas all domains were expressed and immunoprecipitated properly, none of them co-immunoprecipitated full length LRRK2 (Fig. 3-4).

In conclusion, LRRK2 has the potential to homodimerize, and this self-interaction is primarily mediated by the ROCO domain. Other LRRK2 domains were not found to be involved in dimerization, yet an additional minor role for other LRRK2 domains in assisting dimerization can not be excluded.

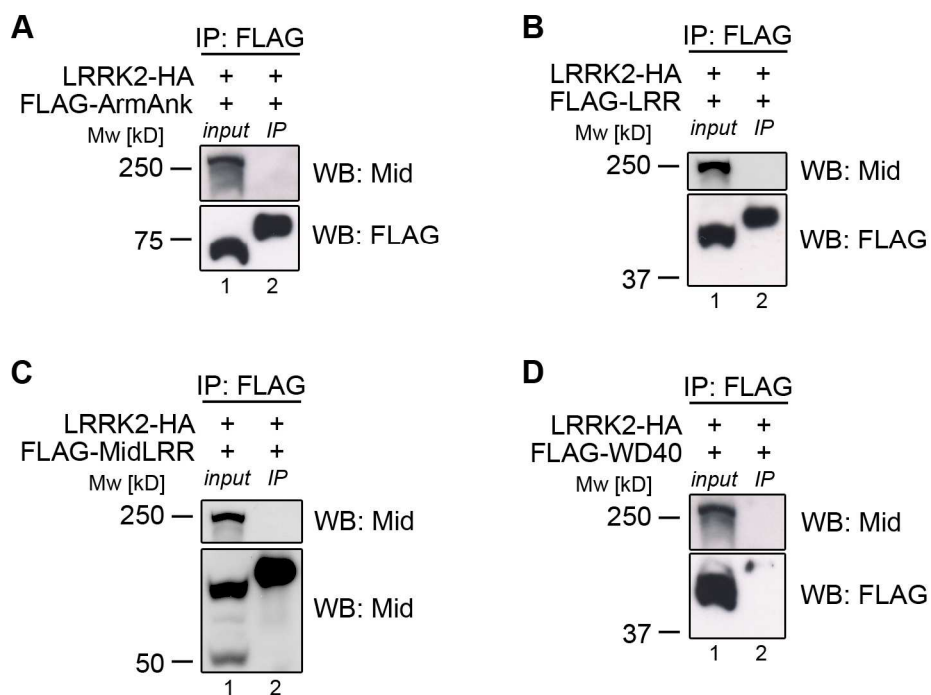


**Figure 3-4. LRRK2 does not interact with ArmAnk, MidLRR, LRR or WD40 domains in co-IP assays.**

(A-D) HEK 293T cells were transiently co-transfected with HA- and FLAG-tagged LRRK2 constructs. (A) Co-expression of HA-LRRK2 and FLAG-ArmAnk. Probing input with anti-FLAG reveals immunoreactivity at ~75 kD (lane 1), as expected for ArmAnk. Whereas FLAG-ArmAnk is immunoprecipitated by FLAG-agarose (lane 2, lower panel), there was no evidence of co-IP of full length HA-LRRK2 (lane 2, upper panel). (B-D) Analogous co-expression of HA-LRRK2 with FLAG-LRR (B), FLAG-MidLRR (C) and FLAG-WD40 (D), respectively. Anti-FLAG immunoreactivity was detected at the expected molecular weight of the respective fragment (~40 kD, ~65 kD, and ~40 kD). Whereas all FLAG constructs were immunoprecipitated by FLAG-agarose (lanes 2, lower panels), there was no evidence of co-IP of full length HA-LRRK2 (lanes 2, upper panels).

### 3.3 LRRK1 homodimerizes via its ROCO domain

LRRK1 is the closest homolog of LRRK2, showing not only a very similar domain architecture, but also similar basic biochemical properties like kinase activity and GTP binding (see 2.3). Strikingly, the ROCO domain core is quite conserved, sharing 40,9% consensus and 25,9% identity on aa level. Thus, LRRK1 was postulated to possess homodimerization potential similar to LRRK2. In an approach identical to the LRRK2 Y2H interaction study, predicted single LRRK1 protein domains were cloned into the yeast AD and BD vectors and co-transformed into yeast in all possible combinations. However, an interaction of the co-transformed ROC and COR fusion proteins was not detected. Moreover, no other specific interactions among co-

transformed fusion proteins were noticed (Fig. 3-5A). Growth of yeast colonies in some of the domain combinations was due to auto-activation of some fusion proteins. As all fusion proteins except BD-kinase were expressed properly as analyzed by Western blot of yeast lysates (Fig. 3-5B), the lack of yeast growth indicates that there is no specific interaction among the different fusion proteins in the Y2H system.

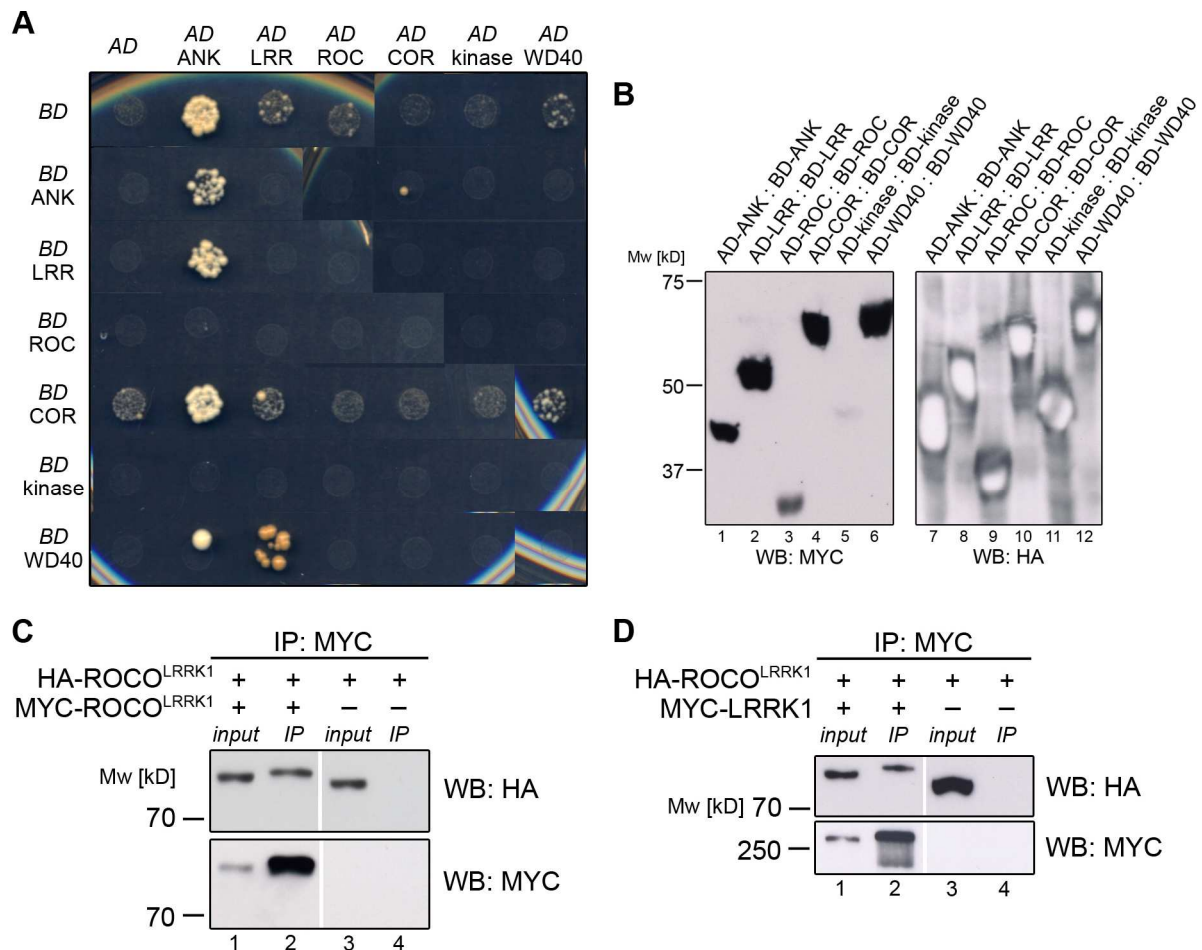


**Figure 3-5. LRRK1 homodimerizes via its ROCO domain.**

(A) Y2H interaction assay with single LRRK1 protein domains. Specific growth of yeast on selective media lacking Leu, Trp and His could not be detected for any domain combination, yet some fusionproteins showed autoactivation. (B) Expression levels of AD and BD fusion proteins in yeast strain AH109. Probing with anti-MYC revealed immunoreactivity for BD fusion proteins (lanes 1 – 6), with only BD-kinase being expressed at lower levels (lane 5). Anti-HA detected immunoreactive signals for all AD fusion proteins (lanes 7 – 12), indicating proper expression of the constructs in yeast. Localization of the immunoreactive signals corresponds to the expected molecular weight of the fusion proteins. (C+D) HEK 293T cells were transiently co-transfected with HA- and MYC-tagged LRRK1 constructs. (C) Co-transfection of HA-ROCO<sup>LRRK1</sup> and MYC-ROCO<sup>LRRK1</sup> or single transfection of HA-ROCO<sup>LRRK1</sup>. Input probing with anti-HA (upper panel) and anti-MYC (lower panel) detected immunoreactive signals at the expected ~75 kD for each transfected construct. Whereas HA-ROCO<sup>LRRK1</sup> did not bind unspecifically to MYC-agarose (lane 4), it was co-immunoprecipitated with MYC-ROCO<sup>LRRK1</sup> (lane 2). (D) Co-transfection of HA-ROCO<sup>LRRK1</sup> and full length MYC-LRRK1 (lanes 1-2) or single transfection of HA-ROCO<sup>LRRK1</sup> (lanes 3-4).

MYC-LRRK1 was detected as a ~250 kD immunoreactive band by anti-MYC probing (lane 1, lower panel). MYC-agarose co-immunoprecipitated HA-ROCO<sup>LRRK1</sup> along with MYC-LRRK1 (lane 2), whereas no precipitation of HA-ROCO<sup>LRRK1</sup> alone could be observed (lane 4).

Since the Y2H LRRK2 ROC – COR interaction was rather weak, co-IP experiments with ROCO<sup>LRRK1</sup> domains were performed despite the negative results from the LRRK1 Y2H interaction study. In experimental settings identical to LRRK2 co-IPs, HA-ROCO<sup>LRRK1</sup> specifically co-immunoprecipitated with MYC-ROCO<sup>LRRK1</sup>, while HA-ROCO<sup>LRRK1</sup> alone was not precipitated by MYC-agarose (Fig. 3-5C). Conversely, HA-agarose co-immunoprecipitated HA-ROCO<sup>LRRK1</sup> along with MYC-ROCO<sup>LRRK1</sup> (data not shown). Importantly, HA-ROCO<sup>LRRK1</sup> co-immunoprecipitated with full length MYC-LRRK1 (Fig. 3-5D), analogous to the observed ROCO<sup>LRRK2</sup>-LRRK2 interaction. Thus, LRRK1 also shows homodimerization potential, similarly mediated by its ROCO domain. Collectively, these data demonstrate homodimerization potential of the LRRK ROCO domains and suggest that the two LRRK proteins homodimerize by means of their respective ROCO domains.

### 3.4 LRRK2 and LRRK1 heterodimerize via their ROCO domains

Having shown that the ROCO domain is involved in both LRRK2 and LRRK1 homodimerization, an additional heterologous interaction between LRRK2 and LRRK1 was hypothesized. To explore putative heterodimerization, co-IP experiments with differentially tagged LRRK ROCO domains co-expressed in HEK 293T cells were performed. Indeed, HA-ROCO<sup>LRRK1</sup> was co-immunoprecipitated with MYC-ROCO<sup>LRRK2</sup> by MYC-agarose, as observed for ROCO homodimerization (Fig. 3-6A). Co-IP was specific, as HA-ROCO<sup>LRRK1</sup> was not precipitated when MYC-ROCO<sup>LRRK2</sup> was omitted. Heterologous ROCO co-IP was also successful in reciprocal HA-IP assays (data not shown). Additionally, interaction of co-expressed MYC-ROCO<sup>LRRK1</sup> and HA-ROCO<sup>LRRK2</sup> was verified by MYC- and HA-agarose co-IPs (data not shown). Moreover, MYC-ROCO<sup>LRRK1</sup> co-immunoprecipitated with full length LRRK2-HA (Fig. 3-6B) and conversely, HA-ROCO<sup>LRRK2</sup> was co-immunoprecipitated via full length MYC-LRRK1 (Fig. 3-6C). In both cases, ROCO fragments were only co-immunoprecipitated under presence of full length LRRK proteins, validating the specificity of the assay. Ultimately, co-IP of full length MYC-LRRK1 with full length

LRRK2-HA (Fig. 3-6D) was demonstrated, even though expression levels of full length LRRK2-HA were consistently reduced whenever co-transfecting full length MYC-LRRK1. In summary, these experiments demonstrate a potential interaction between both LRRK proteins, apparently mediated by the ROCO domains.

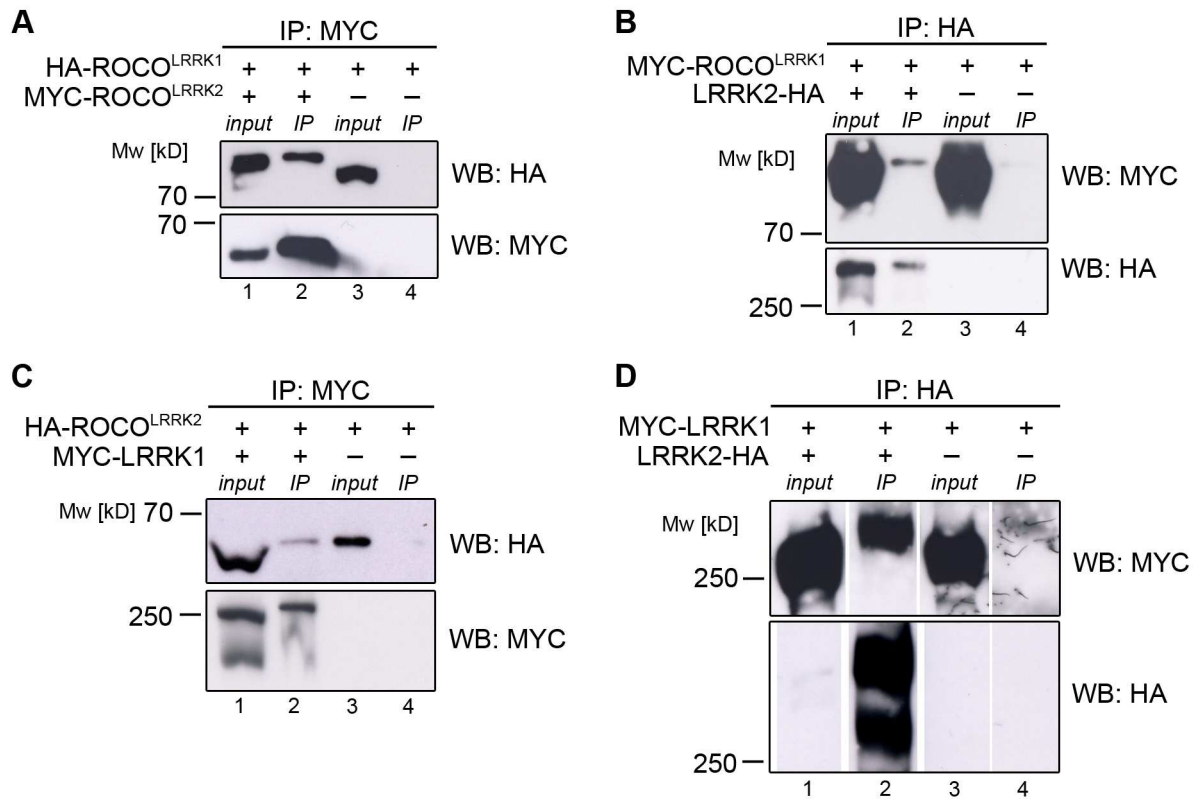


**Figure 3-6. LRRK2 and LRRK1 heterodimerize via their ROCO domain.**

(A-D) HEK 293T cells were transiently co-transfected with HA- and MYC-tagged LRRK constructs. (A) HA-ROCO<sup>LRRK1</sup> was co-immunoprecipitated with MYC-ROCO<sup>LRRK2</sup> (lane 2), whereas HA-ROCO<sup>LRRK1</sup> did not bind unspecifically to MYC-agarose (lane 4). (B) HA-agarose co-immunoprecipitated MYC-ROCO<sup>LRRK1</sup> along with HA-LRRK2 (lane 2), but not in controls (lane 4). (C) Conversely, MYC-agarose co-immunoprecipitated HA-ROCO<sup>LRRK2</sup> along with MYC-LRRK1 (lane 2), but not in controls (lane 4). (D) Co-transfected full length HA-LRRK2 and MYC-LRRK1 were co-immunoprecipitated by HA-agarose (lane 2), whereas single transfected MYC-LRRK1 did not bind unspecifically to HA-agarose (lane 4). Note that co-transfection with full length MYC-LRRK1 consistently led to low HA-LRRK2 expression levels (lane 1, lower panel).



### 3.5 DAPK1 demonstrates homodimerization capability and shows heterodimerization potential with LRRK ROCO kinases

DAPK1 is a well-known protein kinase just recently identified as belonging to the ROCO family (115). The more distant relationship of DAPK1 and LRRK proteins is reflected in a different domain architecture. In DAPK1, the kinase domain does not immediately follow the ROCO domain, but is separately located at the N-terminus (Fig. 3-7A). Moreover, the ROCO domains of DAPK1 and LRRK proteins differ substantially on aa level. Whereas the heterodimerizing ROCO domains of LRRK1 and LRRK2 share 40,9% similarity and 25,9% identity at the aa level, the ROCO domain of DAPK1 shares only 26,8% (22,9%) similarity and 15,0% (11,0%) identity with ROCO<sup>LRRK2</sup> (ROCO<sup>LRRK1</sup>). To investigate if the dimerization potential of the ROCO domain in the LRRK proteins can be extended to a more distantly related ROCO domain – and thus maybe is generalizable – dimerization of ROCO<sup>DAPK1</sup> was analyzed. Hence, the ROCO<sup>DAPK1</sup> fragment (as defined by Boosgraf et al. (115)) was cloned and transiently transfected into HEK 293T cells. Interestingly, co-IP experiments with differentially tagged ROCO<sup>DAPK1</sup> domains revealed homodimerization potential of DAPK1 analogous to LRRK2 and LRRK1 (Fig. 3-7B). ROCO<sup>DAPK1</sup> co-immunoprecipitation was specific, as there was no precipitation of HA-ROCO<sup>DAPK1</sup> when MYC-ROCO<sup>DAPK1</sup> was omitted. Moreover, HA-ROCO<sup>DAPK1</sup> also specifically co-immunoprecipitated with MYC-ROCO<sup>LRRK2</sup> as well as with MYC-ROCO<sup>LRRK1</sup>, albeit to a lesser degree compared to MYC-ROCO<sup>DAPK1</sup> (Fig. 3-7B). Unfortunately, co-IP assays employing co-expressed full length DAPK1 and LRRK proteins were hampered by unspecific precipitation of HA-DAPK1 via MYC-agarose (data not shown) and require further optimization. Nevertheless, these findings suggest that DAPK1 has the capability to homodimerize and shows potential for heterodimerization with the two LRRK ROCO kinases. Taken together, these data propose a general dimerization function for the mammalian ROCO domain.

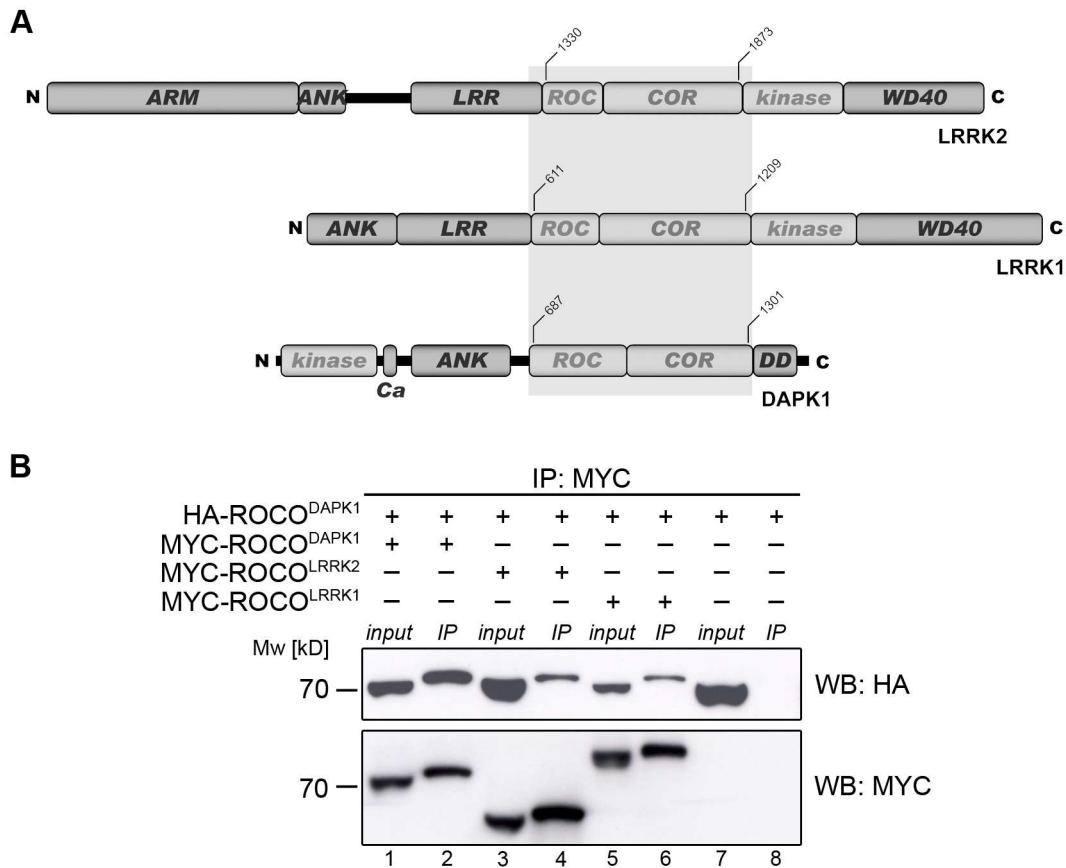


**Figure 3-7. DAPK1 shows potential for homo- and heterodimerization.**

(A) Domain alignment of the three mammalian ROCO kinases. The shared ROCO domain is highlighted in grey. (B) HEK 293T cells were transiently co-transfected with HA- and MYC-tagged DAPK1 and LRRK ROCO constructs, respectively. HA-ROCO<sup>DAPK1</sup> was co-immunoprecipitated with MYC-ROCO<sup>DAPK1</sup> (lane 2) as well as with MYC-ROCO<sup>LRRK2</sup> (lane 4) and MYC-ROCO<sup>LRRK1</sup> (lane 6), whereas HA-ROCO<sup>DAPK1</sup> did not bind unspecifically to MYC-agarose (lane 8). Note that the two LRRK ROCO fragments co-immunoprecipitated less amounts of HA-ROCO<sup>DAPK1</sup>.

### 3.6 The ROCO<sup>LRRK2</sup> homodimerization is independent of GTP

It has been shown that both LRRK2 and the LRRK2 ROC fragment bind GTP (145, 146, 148-150, 172). Consequently, the ROC-containing ROCO<sup>LRRK2</sup> fragment can also be expected to bind GTP, and such binding may influence ROCO<sup>LRRK2</sup> dimerization. Thus, it was tested if the observed interaction between the ROCO<sup>LRRK2</sup> domains is GTP-dependent. First, GTP binding of the ROCO<sup>LRRK2</sup> domain was demonstrated by affinity purification on immobilized GTP-sepharose beads (Fig. 3-8A). To prove specificity of the observed interaction, nucleotide competition experiments were conducted.

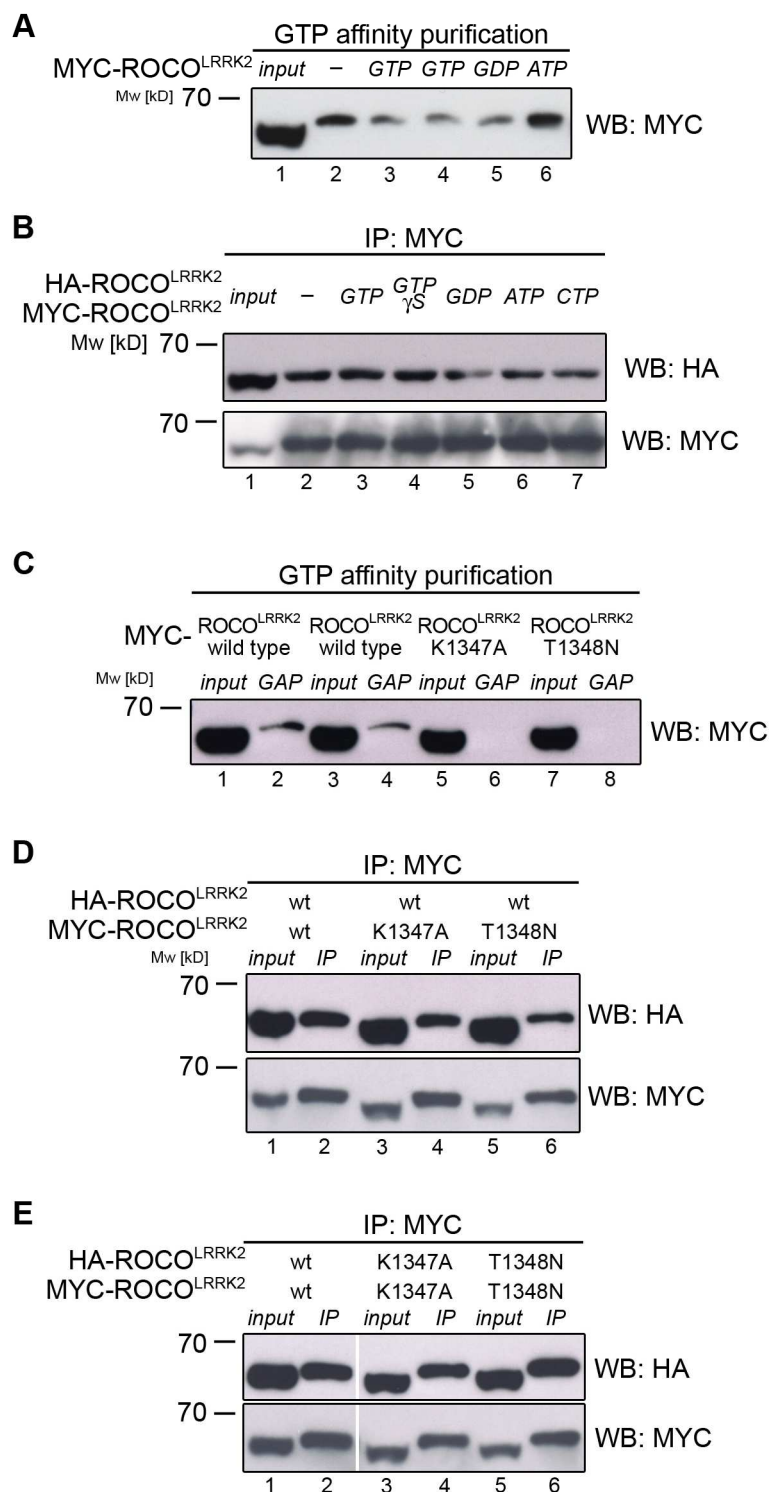


**Figure 3-8. The ROCO<sup>LRRK2</sup> homodimerization is independent of GTP.**

(A-E) ROCO<sup>LRRK2</sup> constructs were transiently (co-)transfected into HEK 293T cells as indicated. (A) MYC-ROCO<sup>LRRK2</sup> was precipitated by GTP-sepharose affinity purification (lane 2). Whereas excess amounts of ATP (final concentration: 2 mM) did not alter the amount of GTP-precipitated MYC-ROCO<sup>LRRK2</sup> (lane 6), adding GDP or GTP to a final concentration of 2 mM led to a decreased precipitation of MYC-ROCO<sup>LRRK2</sup> (lanes 3 - 5, lanes 3 and 4 are duplicates). (B) Experimental conditions from (A) applied to a ROCO<sup>LRRK2</sup> co-IP. Excess amounts of the indicated nucleotides (2 mM) had no impact on the amounts of HA-ROCO<sup>LRRK2</sup> co-immunoprecipitated with MYC-ROCO<sup>LRRK2</sup> by MYC-agarose (cf. lane 2 to lanes 3 - 7). (C) In contrast to wild type (lane 2 and 4), mutant K1347A or T1348N

ROCO<sup>LRRK2</sup> were not precipitated by GTP-sepharose affinity purification (lanes 6 and 8). (D) GTP binding deficient MYC-ROCO<sup>LRRK2</sup> mutants are co-immunoprecipitated along with wild type HA-ROCO<sup>LRRK2</sup> to the same extent as wild type MYC-ROCO<sup>LRRK2</sup> (compare lane 2 to lanes 4 and 6). (E) GTP binding deficient MYC-ROCO<sup>LRRK2</sup> mutants are co-immunoprecipitated along with their mutant GTP binding deficient HA-tagged counterpart identical to wild type ROCO<sup>LRRK2</sup> homodimerization (compare lane 2 to lanes 4 and 6).

Theoretically, excess amounts of GTP or GDP should compete with GTP-sepharose, resulting in diminished precipitation of a GTP-binding protein, whereas excess amounts of other nucleotides should have no impact. As expected, addition of excess GTP or GDP during affinity purification diminished binding of MYC-ROCO<sup>LRRK2</sup> to GTP-sepharose, whereas excess ATP had no effect. To investigate if the ROCO<sup>LRRK2</sup> homodimerization is influenced by GTP, nucleotide competition ROCO<sup>LRRK2</sup> co-IPs were performed. However, excess amounts of GTP or its non-hydrolyzable analog GTPγS did not affect ROCO<sup>LRRK2</sup> self-binding (Fig. 3-8B). Thus, ROCO<sup>LRRK2</sup> homodimerization is apparently not influenced by free GTP.

Of course, these findings can not exclude the necessity of a basal level of bound GTP for proper ROCO<sup>LRRK2</sup> self-interaction. To investigate GTP-dependence of ROCO<sup>LRRK2</sup> dimerization, ROCO<sup>LRRK2</sup> mutants K1347A and T1348N were generated. These mutations have been described to render LRRK2 GTP binding deficient (146, 150) and thus can be expected to abolish GTP binding also for the ROCO fragment. Actually, none of both ROCO<sup>LRRK2</sup> mutants was purified by GTP-sepharose, whereas wild type ROCO<sup>LRRK2</sup> bound to GTP-sepharose as above (Fig. 3-8C). Having proven the GTP binding deficiency of both ROCO<sup>LRRK2</sup> mutants, co-IP studies with mutant and wild type ROCO<sup>LRRK2</sup> fragments were performed. Interestingly, MYC-ROCO<sup>LRRK2</sup> K1347A and T1348N were co-immunoprecipitated along with wild type HA-ROCO<sup>LRRK2</sup> in the same manner as wild type MYC-ROCO<sup>LRRK2</sup> (Fig. 3-8D). Yet, these data does not exclude that GTP bound to one ROCO fragment is sufficient to induce dimerization. Therefore, co-IP assays from cell lysates co-transfected exclusively with GTP binding deficient ROCO<sup>LRRK2</sup> fragments were performed. Importantly, HA-tagged mutant ROCO<sup>LRRK2</sup> fragments were immunoprecipitated along with their corresponding MYC-tagged mutant counterpart in the same way as wild type ROCO<sup>LRRK2</sup> fragments (Fig. 3-8E). Taken together, these data provide evidence that the ROCO<sup>LRRK2</sup> homodimerization is independent of GTP.

### 3.7 Familial PD mutations in the ROCO<sup>LRRK2</sup> domain alter ROCO homo- and heterodimerization

The ROCO<sup>LRRK2</sup> domain contains missense mutations associated to autosomal dominant PD. Mutations considered to be pathogenic comprise R1441C/G in the ROC and Y1699C in the COR subdomain (132). Given ROCO as the core dimerization interface of LRRK1 and LRRK2, this study sought to investigate a possible influence of these mutations on LRRK homo- and heterodimerization. Initially, mutations R1441G/H (ROC) and Y1699C (COR) were cloned as AD/BD fusion proteins for Y2H interaction analyses. However, results were inconsistent, with some fusion proteins showing auto-activation (data not shown). Hence, the more robust ROCO<sup>LRRK2</sup> co-IP assay was used for analyzing a possible impact of mutations on ROCO<sup>LRRK2</sup> dimerization. To investigate effects on ROCO<sup>LRRK2</sup> homodimerization, co-expressed wild type MYC- and mutant (R1441C/G/H or Y1699C) HA-ROCO<sup>LRRK2</sup> were subjected to IP with MYC-agarose. Compared to wild type HA-ROCO, all four mutant HA-ROCO fragments co-immunoprecipitated to a lesser degree with wild type MYC-ROCO fragments (Fig. 3-9A). To test for the statistical significance of this observation, at least four independent experiments per mutation were analyzed by densitometry. Thus comparing ratios of mutant – wild type with wild type – wild type interaction, ROCO<sup>LRRK2</sup> homodimerization was found to be significantly weakened by all four tested substitutions (Fig. 3-9B). As mutations at both positions R1441 and Y1699 diminished ROCO<sup>LRRK2</sup> self-interaction, a double mutant ROCO<sup>LRRK2</sup>R1441C+Y1699C fragment was generated and tested for homodimerization in co-IPs. Double mutant ROCO<sup>LRRK2</sup> retained capability for homodimerization, as HA-ROCO<sup>LRRK2</sup>R1441C+Y1699C was specifically co-immunoprecipitated along with MYC-ROCO<sup>LRRK2</sup>R1441C+Y1699C in MYC-agarose IPs (Fig. 3-9C). A putative additive effect of both mutations subsequently resulting in an increased weakening of ROCO<sup>LRRK2</sup> homodimerization remains to be determined.

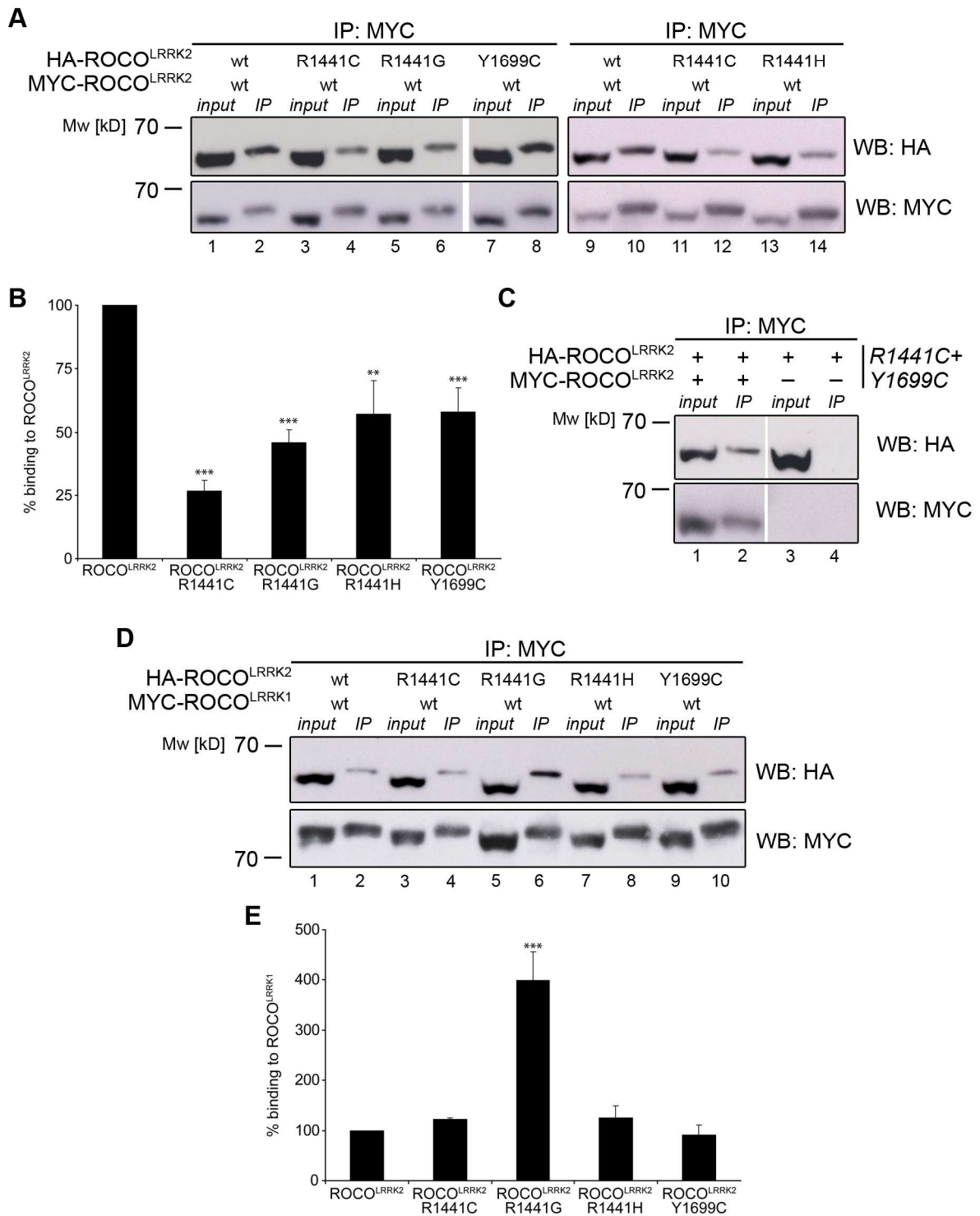


**Figure 3-9. Familial PD mutations in the ROCO<sup>LRRK2</sup> domain alter ROCO homo- and heterodimerization.**

(A) MYC-agarose co-IP from HEK 293T cell lysates co-transfected with wild type MYC- and mutant HA-ROCO<sup>LRRK2</sup> constructs. Compared to wild type HA-ROCO<sup>LRRK2</sup> (lane 2 and 10), HA-ROCO<sup>LRRK2</sup> mutants R1441C/G/H (lanes 4+12/6/14) and Y1699C (lane 8) show decreased binding to wild type MYC-ROCO<sup>LRRK2</sup>. (B) Quantification of (A) by densitometrical analysis. Binding of wild type HA-ROCO<sup>LRRK2</sup> to wild type MYC-ROCO<sup>LRRK2</sup> was set to 100%. At least four experiments for each mutation were analyzed and proven to be statistically significant by one-way ANOVA with Student-Newman-Keuls post-test. (C) Co-expression of HA- and MYC-ROCO<sup>LRRK2</sup> double mutants R1441C+Y1699C in HEK 293T cells. Double mutant HA-ROCO<sup>LRRK2</sup> was co-immunoprecipitated along with double mutant MYC-

ROCO<sup>LRRK2</sup> (lane 2), whereas double mutant HA-ROCO<sup>LRRK2</sup> alone was not immunoprecipitated by MYC-agarose (lane 4). **(D)** MYC-agarose co-IP from HEK 293T cell lysates co-transfected with wild type MYC-ROCO<sup>LRRK1</sup> and wild type or mutant HA-ROCO<sup>LRRK2</sup> constructs. Compared to wild type HA-ROCO<sup>LRRK2</sup> (lane 2), HA-ROCO<sup>LRRK2</sup> mutant R1441G (lane 6) showed increased binding to wild type MYC-ROCO<sup>LRRK1</sup>. The remainder of HA-mutants co-immunoprecipitated with MYC-ROCO<sup>LRRK1</sup> identical to wild type HA-ROCO<sup>LRRK2</sup> (lanes 4, 8, 10). **(E)** Quantification of **(D)** by densitometrical analysis. Binding of wild type HA-ROCO<sup>LRRK2</sup> to wild type MYC-ROCO<sup>LRRK1</sup> was set to 100%. Each column represents quantification from at least three independent experiments, and the increase of ROCO<sup>LRRK2</sup>R1441G in binding to ROCO<sup>LRRK1</sup> was found to be significant by one-way ANOVA with Student-Newman-Keuls post-test. \*\*  $p < 0.01$ , \*\*\*  $p < 0.001$ ; error bars represent SEM.

To assess effects of the mutations on heterodimerization of the LRRK ROCO fragments, analogous co-IP approaches employing co-expressed MYC-ROCO<sup>LRRK1</sup> and wild type or mutant HA-ROCO<sup>LRRK2</sup> were conducted. Whereas ROCO mutants R1441C/H and Y1699C co-immunoprecipitated along with ROCO<sup>LRRK1</sup> identical to wild type ROCO<sup>LRRK2</sup>, interestingly ROCO mutant R1441G was co-immunoprecipitated considerably stronger (Fig. 3-9D). Again, this effect showed statistical significance as determined by densitometric analysis of at least three independent experiments (Fig. 3-9E). In conclusion, these data suggest a weakened homodimerization potential for familial LRRK2 mutations in the ROCO domain, whereas the R1441G mutation could exert its deleterious actions also by enhanced binding to LRRK1.

### **3.8 The ROCO<sup>LRRK2</sup> fragment exerts an inhibitory effect on LRRK2 kinase activity**

It is well known that many protein kinases have to undergo dimerization to become catalytically active and fulfill their tasks in cellular signal transduction pathways. By analogy, LRRK2 self-interaction may be critically involved in LRRK2 kinase function. Consequently, perturbing dimerization would interfere with kinase activity. By binding to the core LRRK2 dimerization region, ROCO<sup>LRRK2</sup> fragments could convey such disturbance of dimerization and subsequently inhibit kinase activity.

To test this hypothesis, LRRK2 autophosphorylation activity under presence of ROCO<sup>LRRK2</sup> fragments was measured. First, LRRK2 *in vitro* autophosphorylation was confirmed in immune complex kinase assays, and augmented levels for the G2019S mutation and diminished levels for the kinase dead K1906M mutation were found,

respectively (Fig. 3-10A), as consistently reported in the literature (119, 130, 145, 147). Interestingly, co-expression of ROCO<sup>LRRK2</sup> led to decreased autophosphorylation of both wild type and G2019S LRRK2 (Fig. 3-10A). Under these conditions of reduced kinase activity, MYC-ROCO<sup>LRRK2</sup> strongly bound to the full length kinases, as evidenced by co-IP. To test the statistical significance of the kinase inhibiting effect, at least five independent experiments were quantified by densitometry and autophosphorylation levels were normalized to the immunoprecipitated amount of LRRK2 construct. Most importantly, kinase activity of both wild type and G2019S LRRK2 was found to be significantly reduced (Fig. 3-10B).

Since the ROCO<sup>LRRK1</sup> fragment interacted with full length LRRK2 in co-IP assays, a similar kinase inhibiting effect could be postulated. Thus, the LRRK2 kinase inhibiting potential of ROCO<sup>LRRK1</sup> was attempted to be examined by co-transfection of MYC-ROCO<sup>LRRK1</sup> with full length LRRK2-HA (wild type or G2019S) and subsequent determination of LRRK2 autophosphorylation levels. Surprisingly, whenever co-transfecting MYC-ROCO<sup>LRRK1</sup>, LRRK2 or G2019S HA-constructs could not be immunoprecipitated successfully on coomassie level (Fig. 3-10A), reminiscent of the lower expression levels of LRRK2-HA after co-transfection with MYC-LRRK1 (Fig. 3-6D). Accordingly, co-IP of MYC-ROCO<sup>LRRK1</sup> is rather ineffective as evidenced by faint signals on immunoblots (Fig. 3-10A). Co-IP is working despite of missing coomassie LRRK2 bands, because apparently a basal level of LRRK2 protein expression is retained and weak immunoreactive signals are visible on immunoblots (data not shown). Given the insufficient IP of wild type or G2019S LRRK2, the impact of ROCO<sup>LRRK1</sup> on LRRK2/G2019S autophosphorylation activity can not be assessed in this setting. Thus, a functional relevance of the LRRK2-LRRK1 interaction remains elusive.

Several studies analyzing LRRK2 kinase activity have demonstrated that the minimal kinase-active LRRK2 construct requires the ROC, COR and kinase domain as well as the full intact C-terminus (including the WD40 domain) (147, 157). Concordantly, the RCKW<sup>LRRK2</sup> fragment used in this study also showed autophosphorylation activity in *in vitro* immune complex kinase assays (Fig. 3-10A). As the RCKW<sup>LRRK2</sup> fragment showed self-association in co-IP experiments, an interaction with full length LRRK2 could be expected. Based on this assumption, it was hypothesized that the supply of an active kinase domain by RCKW<sup>LRRK2</sup> could inverse the kinase inhibiting effect



when co-expressed instead of ROCO<sup>LRRK2</sup>. As expected, co-expressed RCKW<sup>LRRK2</sup> co-immunoprecipitated along with LRRK2-HA or G2019S-HA. However, presence of RCKW<sup>LRRK2</sup> quenched wild type and G2019S LRRK2 kinase activity equal to ROCO<sup>LRRK2</sup> (Fig. 3-10A). A rescue of LRRK2 autophosphorylation levels was not observed.

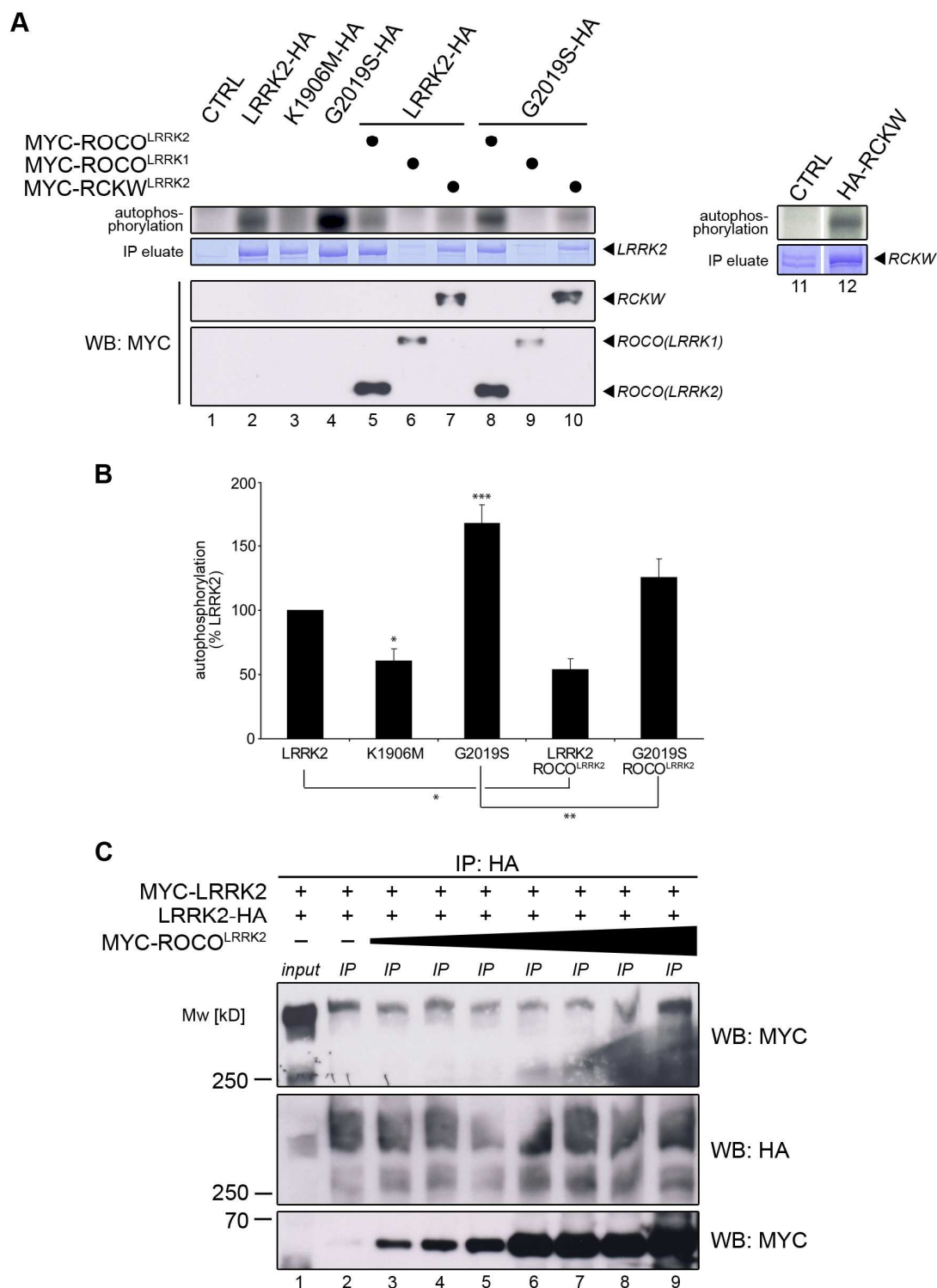


**Figure 3-10.** The ROCO<sup>LRRK2</sup> fragment exerts an inhibitory effect on LRRK2 kinase activity.

**(A)** As evidenced by autoradiography (upper panel), LRRK2 underwent autophosphorylation (lane 2) with decreased levels for the kinase dead K1906M (lane 3) and increased levels for the G2019S mutation (lane 4). Co-transfection of MYC-ROCO<sup>LRRK2</sup> led to diminished autophosphorylation levels for both wild type (lane 5) and G2019S (lane 8) LRRK2 constructs. Likewise, co-transfection of MYC-RCWK<sup>LRRK2</sup> decreased LRRK2 wild type and G2019S autophosphorylation levels (lane 7 and 10, respectively). Single-transfected HA-RCKW fragment showed autophosphorylation (lane 12). Co-expression of MYC-ROCO<sup>LRRK1</sup> led to an almost complete disappearance of LRRK2 proteins in the IP eluate (lane 6 and 9, respectively). The second highest panel shows Coomassie blue staining of immunoprecipitated full length LRRK2 constructs. Lower panels demonstrate anti-MYC immunoreactivity of co-immunoprecipitated MYC-ROCO<sup>LRRK2</sup> (lanes 5 and 8), MYC-RCKW<sup>LRRK2</sup> (lanes 7 and 10) and MYC-ROCO<sup>LRRK1</sup> (lanes 6 and 9) with full length wild type and G2019S HA-LRRK2 by HA-agarose, respectively. **(B)** Quantification of autophosphorylation levels from (A) normalized to the amount of the respective immunoprecipitated LRRK2 construct. At least five independent experiments were densitometrically analyzed. Autophosphorylation levels of wild type LRRK2 were set to 100%. K1906M and G2019S were compared to wild type LRRK2, and differences were found to be statistical significant by one-way ANOVA with Student-Newman-Keuls post test. Autophosphorylation levels after co-transfection of MYC-ROCO<sup>LRRK2</sup> were compared to autophosphorylation levels of the respective single transfected LRRK2 or G2019S, and were statistically significant applying one-way ANOVA with Student-Newman-Keuls post test. \*  $p < 0.05$ , \*\*  $p < 0.01$ , \*\*\*  $p < 0.001$ ; error bars represent SEM. **(C)** HEK 293T lysates co-transfected with HA-LRRK2 and MYC-LRRK2 were mixed with increasing amounts of lysates from cells single-transfected with MYC-ROCO<sup>LRRK2</sup> and subjected to co-IP with HA-agarose. MYC-LRRK2 (upper panel) was co-immunoprecipitated along with HA-LRRK2 (middle panel) by HA-agarose. In parallel, MYC-ROCO<sup>LRRK2</sup> (lower panel) was co-immunoprecipitated in a concentration-dependent manner via HA-LRRK2. Full length LRRK2 co-IP was not found to be altered by the addition of ROCO<sup>LRRK2</sup>.

To explore the putative kinase inhibiting mechanism of ROCO<sup>LRRK2</sup>, the dimer disrupting potential of the ROCO<sup>LRRK2</sup> fragment was investigated. Therefore, increasing amounts of cell lysate containing transfected MYC-ROCO<sup>LRRK2</sup> were added to cell lysate containing co-transfected MYC- and HA-LRRK2, followed by coIP assays with HA-agarose. Even though MYC-ROCO<sup>LRRK2</sup> was co-immunoprecipitated along with LRRK2-HA in a concentration-dependent manner, changes in the amount of co-immunoprecipitated MYC-LRRK2 were not evident under these conditions (Fig. 3-10C). Thus, a dimer disrupting potential of the ROCO<sup>LRRK2</sup> fragment could not be verified here.

### 3.9 Influence of familial and artificial mutations in the ROCO<sup>LRRK2</sup> fragment on the LRRK2 kinase inhibiting effect

In ROCO<sup>LRRK2</sup> homodimerization assays, familial PD mutations in the ROC (R1441C/G/H) or COR (Y1699C) domain resulted in a weakening of the self-interaction (Fig. 3-9A+B). Transferring these observations to the ROCO<sup>LRRK2</sup> kinase inhibiting effect, a reduction of the kinase inhibition by mutant ROCO<sup>LRRK2</sup> fragments can be anticipated. To test this assumption, effects of mutant ROCO<sup>LRRK2</sup> fragments R1441C and Y1699C on LRRK2 autophosphorylation activity were analyzed in comparison to wild type ROCO<sup>LRRK2</sup>. Indeed, LRRK2 kinase inhibition was reduced in the presence of mutant ROCO<sup>LRRK2</sup> fragments (Fig. 3-11A+C). Moreover, compared to wild type ROCO<sup>LRRK2</sup>, mutant ROCO<sup>LRRK2</sup> fragments co-immunoprecipitated to a lesser degree with LRRK2-HA, confirming the results obtained by homodimerization experiments with ROCO<sup>LRRK2</sup> fragments. Densitometrical analysis of three independent experiments demonstrated the reduced inhibition of LRRK2 kinase activity by ROCO<sup>LRRK2</sup> R1441C as statistically significant, whereas the trend of reduced kinase inhibition by ROCO<sup>LRRK2</sup> Y1699C was not statistically significant (Fig. 3-11B). Furthermore, the double mutant ROCO<sup>LRRK2</sup> R1441C+Y1699C fragment lead to a reduction of LRRK2 autophosphorylation inhibition similar to the ROCO<sup>LRRK2</sup> fragments with a single mutation (Fig. 3-11C). Surprisingly, the situation was partly different with G2019S LRRK2. Whereas mutant ROCO<sup>LRRK2</sup> fragments similarly were co-immunoprecipitated to a lesser degree, inhibition of G2019S autophosphorylation apparently was not reduced accordingly (Fig. 3-11A). Thus, wild type LRRK2 and G2019S may be regulated differently.

Besides disrupting or disturbing LRRK2 dimerization, ROCO<sup>LRRK2</sup> could consume co-factors needed for LRRK2 kinase activation and thus confer kinase inhibition indirectly. Reportedly, binding of GTP by the LRRK2 ROC domain is essential for LRRK2 kinase activity (145, 146, 150). Hence, ROCO<sup>LRRK2</sup> – which is also able to bind GTP – could deplete the pool of freely available GTP and secondly lead to LRRK2 kinase inhibition. To ascertain this putative mechanism, GTP binding deficient ROCO<sup>LRRK2</sup> mutants K1347A or T1348N were co-expressed with full length LRRK2-HA, followed by measurement of LRRK2 autophosphorylation levels by *in vitro* kinase assays as above. Importantly, co-expression of both ROCO<sup>LRRK2</sup> mutants inhibited LRRK2 autophosphorylation to the same extent as wild type ROCO<sup>LRRK2</sup>

(Fig. 3-11C). Moreover, mutant  $\text{ROCO}^{\text{LRRK2}}$  fragments were also co-immunoprecipitated along with full length LRRK2-HA equal to their wild type counterpart, validating the findings from co-IPs employing wild type and K1347A or T1348N  $\text{ROCO}^{\text{LRRK2}}$ .

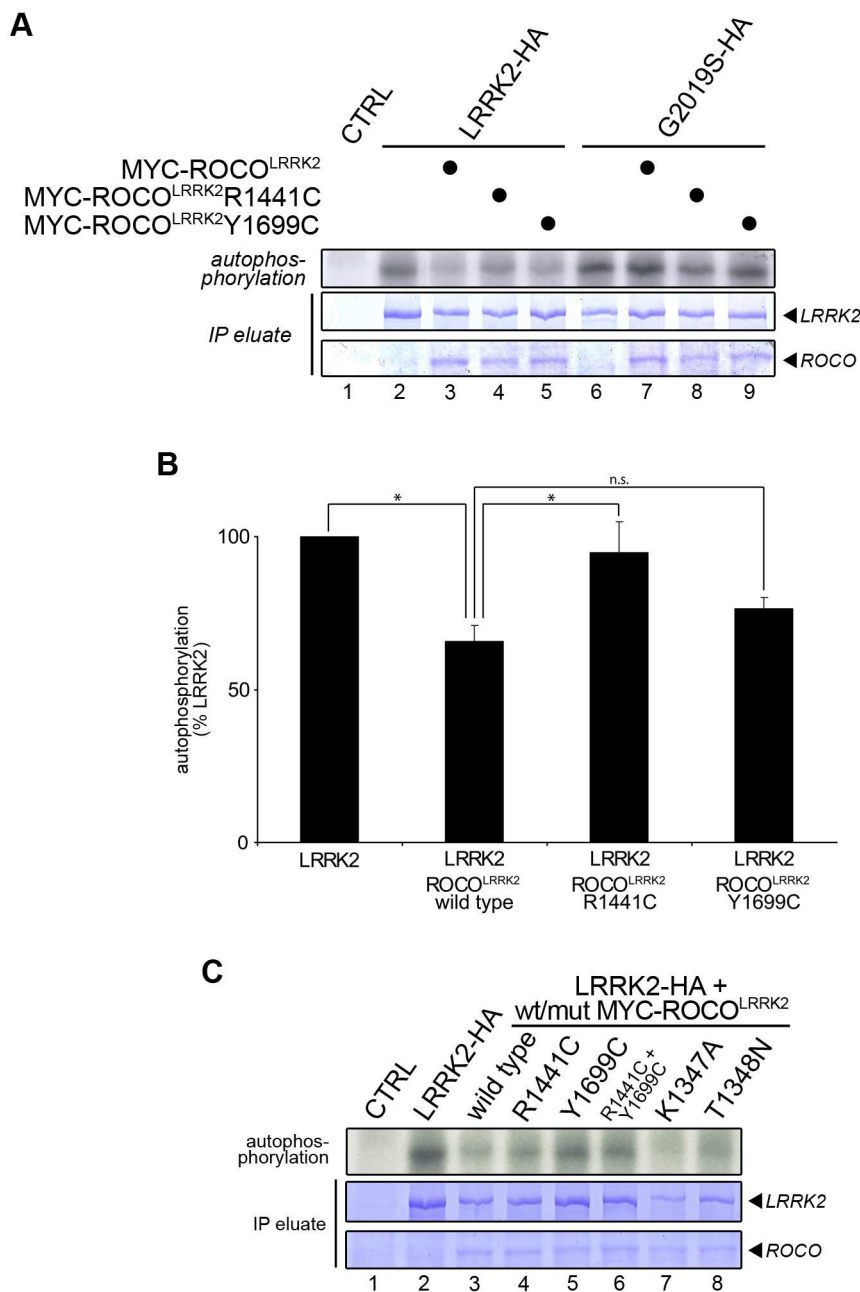


**Figure 3-11. Effects of familial and artificial mutations in the  $\text{ROCO}^{\text{LRRK2}}$  fragment on LRRK2 kinase activity.**

Upper panels depict LRRK2 autophosphorylation levels, middle and lower panels show Coomassie blue staining of immunoprecipitated full length LRRK2 and ROCO constructs, respectively. (A) Co-transfection of  $\text{MYC-ROCO}^{\text{LRRK2}}$  R1441C and Y1699C with full length LRRK2-HA showed a reduced inhibitory effect on autophosphorylation (upper panel, lanes 4 and 5) compared to co-expressed wild type  $\text{MYC-ROCO}^{\text{LRRK2}}$  (lane 3). Compared to wild type  $\text{MYC-ROCO}^{\text{LRRK2}}$ , mutant  $\text{MYC-ROCO}$  fragments co-immunoprecipitated to a lesser degree with LRRK2 as evidenced by Coomassie blue staining (lower panel, lanes 4 and 5). Co-

transfecting mutant MYC-ROCO<sup>LRRK2</sup> constructs with G2019S LRRK2 did not result in a consistent reduction of the inhibitory effect on autophosphorylation (upper panel, lanes 8 and 9). Similar to wild type LRRK2, mutant ROCO fragments co-immunoprecipitated to a lesser extent with G2019S LRRK2 (lower panel, lanes 8 and 9). **(B)** Quantification of autophosphorylation levels from (A) normalized to the amount of the respective immunoprecipitated LRRK2 construct. Three independent experiments were densitometrically analyzed. Autophosphorylation levels of wild type LRRK2 were set to 100%. Compared to co-expressed wild type fragment, co-expressed ROCO<sup>LRRK2</sup> R1441C leads to a statistically significant reduction of kinase inhibition by one-way ANOVA with Student-Newman-Keuls post test. \*  $p < 0.05$ , n.s., not significant; error bars represent SEM. **(C)** Wild type or mutant MYC-ROCO<sup>LRRK2</sup> fragments were co-expressed with LRRK2-HA in HEK 293T cells as indicated. Whereas GTP binding deficient ROCO mutants showed an inhibitory effect on LRRK2 autophosphorylation identical to wild type ROCO (upper panel, compare lanes 7 and 8 to lane 3), familial mutations in ROCO fragments led to a reduction in LRRK2 autophosphorylation inhibition (lanes 4 and 5), including the ROCO double mutant R1441C+Y1699C (lane 6).

In summary, these data demonstrate a prominent kinase inhibiting potential of the ROCO<sup>LRRK2</sup> fragment, both on normal and pathological LRRK2. ROCO<sup>LRRK2</sup> fragments with familial PD mutations showed a diminished potential to inhibit LRRK2 autophosphorylation, consistent with their reduced ability to dimerize. GTP binding deficient ROCO<sup>LRRK2</sup> mutants showed wild type-like potential of inhibition, concordant with their normal ability to dimerize. Thus, the kinase inhibiting effect is exerted most probably directly through binding of the ROCO<sup>LRRK2</sup> fragment to the ROCO domain of full length LRRK2, suggesting a functional link between LRRK2 self-interaction and kinase activity.



## 4 DISCUSSION

Even though dimerization is a common theme among protein kinases, a thorough investigation of LRRK2 dimerization is currently lacking. So far, only few approaches to elucidate LRRK2 dimerization have been undertaken, showing co-immunoprecipitations of differentially tagged LRRK2 constructs, the crystal structure of a LRRK2 ROC domain dimer, and predominance of LRRK2 dimer species by gel filtration experiments (117, 129, 157).

The present study undertook a systematic approach to analyze LRRK2 dimerization and mapped the dimerization domain. Based on a thorough analysis by Y2H and co-IP studies, the ROCO domain was revealed as core interface for LRRK2 homodimerization. Likewise, homodimerization of LRRK1, the closest LRRK2 relative, was identified. Furthermore, experimental evidence argues for a LRRK2-LRRK1 heterodimerization via the ROCO domains, suggesting LRRK1 as a new LRRK2 binding partner. Moreover, DAPK1 showed homo- as well as heterodimerization potential, suggesting a regulatory interplay between the mammalian ROCO kinases LRRK2, LRRK1 and DAPK1. In addition, familial PD mutations in the ROCO domain were found to significantly influence ROCO homo- and heterodimerization. Most importantly, an inhibitory effect of the ROCO<sup>LRRK2</sup> fragment on LRRK2 kinase activity was detected. This inhibitory effect was apparently dependent on binding strength of the ROCO<sup>LRRK2</sup> fragment, as mutant ROCO fragments showing weakened self-association accordingly demonstrated reduced kinase inhibiting potential.

### 4.1 The ROCO<sup>LRRK2</sup> domain directs LRRK2 dimerization

Several pieces of experimental evidence obtained in this study unequivocally map the core LRRK2 dimerization interface to the ROCO<sup>LRRK2</sup> domain: (1) a very robust interaction of the ROCO<sup>LRRK2</sup> domain with itself but also with full length LRRK2 was found in different interaction assays; (2) interactions among single LRRK2 domains other than ROC and COR could not be detected in Y2H, just as ArmAnk, MidLRR, LRR and WD40 domains failed to co-immunoprecipitate full length LRRK2 in

extensive co-IP approaches; and (3) familial LRRK2 mutations in the ROC as well as in the COR domain significantly decreased ROCO<sup>LRRK2</sup> homodimerization.

Nevertheless, putative additional interactions between LRRK2 domains maintaining or assisting dimerization cannot be excluded. Interestingly, LRRK2 already contains another protein domain known to be involved in dimerization, the LRRs. For instance, this domain is responsible for dimerization of the extracellular matrix protein decorin (173). Intriguingly, alignment of the LRR domains of decorin and LRRK2 reveals that key residues directing decorin dimerization correspond to LRRK2 aa that are mutated in familial PD cases (S1096C and S1228T). Thus, LRRK2 dimerization via the LRRs – maybe even affected by the mentioned mutations – was basically conceivable. However, the multitude of interaction experiments presented here could not detect evidence for an involvement of the LRR domain in self-interaction and pinpoints ROCO<sup>LRRK2</sup> as the core LRRK2 dimerization interface.

These results are only partly conforming with recent reports describing co-crystallization of ROC fragments as a dimer (117) and co-IP of FLAG-ROC and FLAG-WD40 with MYC-ROC, respectively (157). Despite robust expression levels of the individual ROC and WD40 fusion proteins in the Y2H interaction study, a homomeric ROC-ROC or heteromeric ROC-WD40 interaction was not detected. Thus, the interactions of individual ROC domains may be weak or transient. In addition, varying results with single domains could be due to different domain boundaries, leading to variable expression levels, which in turn may influence interaction assays. Concordantly, the interaction of the ROC domain with COR observed in the present Y2H analysis was also reported by others (117, 118). However, co-IP experiments with differentially tagged ROC and COR domains failed because of poor protein expression in HEK 293T cells (data not shown).

In contrast, extended ROC domains showed an overall increased tendency for self-association in this as well as in other studies (117, 118, 157), suggesting that the ROC domain alone is not sufficient to mediate LRRK2 dimerization. Testing ROCO, ROC-COR-kinase and ROC-COR-kinase-WD40 constructs in Y2H and/or co-IP experiments, the ROCO fragment was found to be the minimal configuration sufficient for proper self-association. Remarkably, the ROC and COR domains have been found to only exist as a combined ROCO domain in proteins and consequently, a distinct function for the ROCO domain as a whole has been suspected (115).



Concordantly, this study supports the view that ROCO may operate as one inseparable functional unit.

Very recently, the ROCO domain crystal structure of the Roco protein from *C. tepidum* was reported (118). Essentially, this is the first structure of an entire ROCO domain, and although its bacterial origin handicaps comparison with mammalian ROCO domains, some general lessons for ROCO domain features may be learned. In contrast to the domain-swapped ROC dimer suggested recently (117), *C. tepidum* ROCO primarily dimerizes via the C-terminal subdomain of COR, as evidenced by COR and ROCO crystals. In addition, one ROC domain contacts the COR domains of both monomers. Whereas the latter finding perfectly fits the Y2H-based ROC-COR interaction detected in this study, a COR-COR interaction was not observed here. However, the crystalized bacterial ROCO fragment contained a mutation in the COR domain which abolishes dimerization of the isolated COR fragment, yet surprisingly does not prevent ROCO dimerization. Hence, consistent with the findings presented here, the ROC domain apparently has an important role in dimerization. In further concordance with this study, a stabilization of the ROC domain was observed when extended with COR (118). Taken together, evidence converges on the ROCO domain tandem as the minimal necessary unit for dimerization.

Frequently, identification of the essential dimerization domain is verified by deleting the determined region and analyzing the deletion constructs for dimerization potential. Lack of deletion construct dimerization consequently confirms the dimerization domain mapping. To further validate the ROCO domain as the core dimerization device, LRRK2 deletion constructs lacking the ROCO segment were generated. However, the deletion proteins were hardly expressed in HEK 293T cells, preventing assessment of their dimerization potential (data not shown). Thus, deletion construct analysis will require further improvement of experimental conditions.

## 4.2 Predicted model of the ROCO<sup>LRRK2</sup> self-interaction

In the initial Y2H interaction study with single LRRK2 domains, an interaction, albeit weak, was exclusively observed for ROC and COR. This finding opens up two different qualities of possible interaction, namely an intra- or intermolecular

interaction. The strong interaction of the combined ROCO fragment in Y2H as well as in co-IP studies clearly points at predominance of an intermolecular interaction. Moreover, the ROCO fragment also bound to full length protein, similarly preferring intermolecular binding. Taken together, these data indicate a putative antiparallel interaction of the ROCO domains, with ROC binding COR and vice versa. To further investigate this assumption, a split-Venus bimolecular fluorescence complementation (BiFC) system was initiated. Venus is a derivative of GFP, and these fluorescent proteins can be splitted at distinct aa residues, thereby losing their fluorescence emitting properties. Fluorescence is restored when the protein fragments are brought into close spacial proximity, a condition which can be achieved by fusing the GFP/Venus fragments to proteins which interact (174, 175). Thus, fusion constructs of various ROCO – split-Venus combinations were cloned and assessed for complementation of fluorescence. Unfortunately, already the non-fused Venus fragments showed a considerable rate of (background) fluorescence emission, apparently interacting unspecifically. Hence, experimental optimization will be required to investigate the orientation of the ROCO interaction by this sophisticated method.

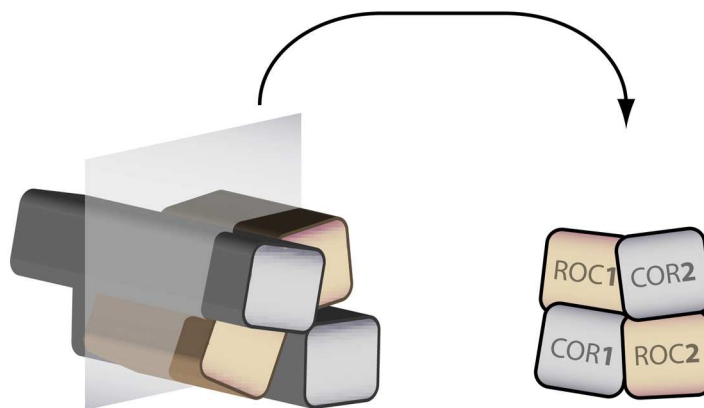


**Figure 4-1. Predicted model of the ROCO<sup>LRRK2</sup> interaction.**

Currently available data on ROCO interaction suggests multiple contacts maintaining the ROCO dimer. Proposed interactions comprise ROC-ROC, COR-COR and ROC-COR contacts. The latter could occur in an intra- as well as intermolecular manner.

The detailed mode of interaction between mammalian ROCO fragments will remain obscure until structural data is at hand. Previously solved structures of a LRRK2 ROC fragment and a bacterial ROCO fragment were highly differing (117, 118) and thus hardly allow for general deductions concerning ROCO<sup>LRRK2</sup> conformation. Data obtained in this study ignites speculation about a compact and strong ROCO

structure maintained by multiple interactions between ROC and COR subdomains, both in an intra- and intermolecular manner (Fig. 4-1). Interestingly, this model simultaneously allows furthermore for the reported ROC-ROC and COR-COR interactions, thus unifying currently available data on LRRK2 self-interaction.

### **4.3 LRRK1 homodimerization and LRRK2/LRRK1 heterodimerization**

LRRK1 is the closest relative of LRRK2 and shows a very similar predicted domain architecture with a particularly well-conserved ROCO domain core. Thus, LRRK1 homodimerization similar to LRRK2 was conceivable. Unexpectedly, a Y2H interaction study with single LRRK1 domains did not reveal any significant interaction, despite proper expression of the fusion proteins in yeast. Thus, the ROC-COR interaction found among LRRK2 domains could not be confirmed for LRRK1 domains. However, the Y2H-based LRRK2 ROC-COR interaction was not very strong, indicating that an analogous interaction of LRRK1 ROC-COR domains may be too weak to be detected. Indeed, the LRRK1 ROCO domains dimerized analogous to the robust ROCO<sup>LRRK2</sup> self-interaction in co-IP assays. Thus, identical to ROCO<sup>LRRK2</sup>, extending the ROC domain with COR led to a robust self-interaction. Furthermore, ROCO<sup>LRRK1</sup> also bound to full length LRRK1, suggesting a homodimerization of LRRK1 mediated by the ROCO domains, just as observed for LRRK2. Formally, an interaction of differentially tagged full length LRRK1 proteins has yet to be shown.

Given homodimerization of LRRK1 and LRRK2, in each case mediated by the respective ROCO domains, a ROCO-directed heterodimerization of both kinases has been an imaginable consequence. Indeed, co-IPs of ROCO fragments and full length LRRKs demonstrated a potential for LRRK heterodimerization. Such potential is also known for other closely related kinases. For instance, heterodimerization has been shown for the Raf and MLK serine/threonine kinases (176-179), which are moreover assigned to the same kinase family as LRRK1 and LRRK2. As both LRRK proteins are localized in the cytosol (119, 129, 130, 152, 164), there are no spatial restrictions for a functional interaction. Furthermore, LRRK2 and LRRK1 appear to be coordinately regulated and co-expressed in restricted areas of the brain (180, 181).

Deciphering the functional relevance of LRRK heterodimerization is now clearly warranted. Interestingly, LRRK2 expression levels were observed to be considerably diminished whenever LRRK1 or ROCO<sup>LRRK1</sup> was co-transfected. This trend was also noticed in HEK 293 cells stably expressing wild type LRRK2 (data not shown). Thus, LRRK1 could initiate or accelerate LRRK2 breakdown on RNA or protein level, most probably by means of its ROCO domain. Certainly, this interesting preliminary finding has to be explored with further in-depth analyses (see 4.8).

#### **4.4 Putative functions of the mammalian ROCO domain**

Having identified the ROCO domain as mediator of LRRK homo- and heterodimerization, a general role for the mammalian ROCO domain in dimerization was conceivable. Since the discovery of ROCO as a new self-contained protein domain, a ROCO domain was also spotted in DAPK1, a well-known Ser/Thr protein kinase involved in cell death and cancer as well as in neuronal injury and degeneration (168). Despite the low level of homology between LRRK and DAPK1 ROCO domains, co-IP studies not only revealed ROCO<sup>DAPK1</sup> homodimerization capability, but also potential for ROCO<sup>DAPK1</sup> heterodimerization with both LRRK ROCO fragments. Hence, speculation about a functional regulatory interplay among all three mammalian ROCO kinases is justified. Most importantly, this study proposes for the first time a distinct function for the ROCO domain as a whole, suggesting structural entity to be reflected in functional unity. Like leucine zippers, ROCO domains could mediate dimerization in general. The very recently reported dimerization of the ROCO fragment from the Roco protein of *C. tepidum* clearly supports this hypothesis (118). An investigation of the even more distantly related ROCO domain of MFHAS1 (which does not contain a kinase domain) could further validate a general dimerization function for the mammalian ROCO domain. Collectively, this study supports the view of ROCO as one inseparable structural and functional entity, composed of a ROC and COR subdomain.

Apart from a distinct role for the ROCO domain tandem, both ROC and COR subdomains probably have functions on their own. Similar to full length LRRK2, the isolated LRRK2 ROC fragment was shown to have GTP binding and hydrolysis ability (148-150, 172), and GTP binding was demonstrated for LRRK1 (164). Both

GTP binding and hydrolysis have not been analyzed for ROC<sup>DAPK1</sup> so far. Furthermore, binding of tubulin by the ROC<sup>LRRK2</sup> fragment was proposed recently (156). Interestingly, the DAPK1 region binding to the cytoskeleton overlaps with the ROC part of the ROCO<sup>DAPK1</sup> domain (168). Thus, there could be additional functional features shared by ROC and ROCO domains of different ROCO family members. Putative functions of the COR domain remain obscure. It could be a linker domain, functionally connecting the ROC and kinase domain, thus playing an important role for the hypothesized GTP-dependent kinase activation of LRRK2. Very recently, COR was demonstrated to be apparently responsible for dimerization in a crystalized bacterial ROCO fragment (118). More speculative, COR could function as a GEF (guanosine nucleotide exchange factor) or GAP (GTPase activating protein) assisting ROC GTPase function. Actually, similar configurations are known for other non-mammalian ROCO proteins (115, 182) and would have interesting consequences, rendering LRRK2 even independent from GEF or GAP co-factors normally needed for proper GTPase function. However, the hereby sketched virtually anarchic intramolecular LRRK2 self-activation through a COR – ROC – kinase activation cascade will have to withstand scientific examination. The fast GTP dissociation rate measured in a bacterial ROCO fragment rather suggests independence of ROC from GEFs (118). Certainly, many additional functions for the ROCO domain and its ROC and COR constituents are imaginable.

#### **4.5 Influence of artificial and familial PD mutations on LRRK dimerization**

Mutations in LRRK2 might impact on dimerization. Particularly, familial PD mutations in the ROCO core dimerization interface could interfere with normal dimerization, either leading to a weakened or strengthened interaction. Ultimately, altered LRRK2 dimerization could be a mechanism of how familial mutations in LRRK2 cause PD. Analyzing familial ROCO mutations R1441C/G/H (ROC domain) and Y1699C (COR domain), a significantly weakened homodimerization of ROCO<sup>LRRK2</sup> fragments was detected. These results are in agreement with data from a recent study, which showed decreased interaction of R1441C ROC with LRRK2 in pull down assays and predicted a disruption of the ROC dimer whenever the arginine at position 1441

would be replaced by any residue with a shorter side chain (117). Moreover, predictions from a bacterial ROCO fragment crystal structure similarly suggest familial PD mutations I1371V, R1441C/G/H and Y1699C to weaken ROCO self-interaction (118). Importantly, the finding that mutations in both the ROC and COR subdomain decreased ROCO<sup>LRRK2</sup> self-interaction supports the assumption that the whole ROCO domain is necessary for proper dimerization. In addition, compared to wild type, mutant ROCO<sup>LRRK2</sup> fragments R1441C and Y1699C showed diminished binding to full length LRRK2. Nevertheless, these results have to be confirmed by interaction assays using exclusively full length LRRK2 constructs containing the respective mutations, as additional influences of other LRRK2 domains on self-interaction can not be ruled out.

Data about the influence of familial mutations outside the ROCO domain on LRRK2 dimerization is scarce. One report analyzing the I2020T mutation in the kinase domain found that this mutation apparently had no impact on dimerization (129). Actually, currently available evidence (including this study) excludes an involvement of the kinase domain in dimerization (117, 157). Whether other mutations outside the ROCO domain could influence dimerization will have to be investigated, but does not seem too likely given ROCO as the core dimerization interface.

Additional influence on LRRK2 dimerization could be exerted by GTP. Binding of this nucleotide supposedly is important for proper LRRK2 kinase activity, and the same could hold true for dimerization. Full length LRRK2 and the LRRK2 ROC fragment have been shown to bind GTP, and this study demonstrated GTP binding also for the ROCO<sup>LRRK2</sup> fragment. Here, excess amounts of guanyl nucleotides (including the non-hydrolyzable GTP $\gamma$ S) did not influence ROCO<sup>LRRK2</sup> homodimerization. Concordantly, mutant ROCO<sup>LRRK2</sup> fragments unable to bind GTP (K1347A or T1348N) still self-interacted like wild type. While GTP independence has to be confirmed for full length LRRK2 dimerization, these results suggest that binding of GTP is not necessary for LRRK2 dimerization. In agreement, a recent report showed that the GTP-binding deficient K1347A mutation did not have an impact on the ROC-LRRK2 interaction in GST-ROC pull-down assays (117).

Remarkably, ROCO fragments containing familial PD mutations R1441C/G/H and Y1699C showed differences in ROCO homo- and heterodimerization, respectively. In contrast to weakened self-interaction for all tested mutant ROCO<sup>LRRK2</sup> fragments, ROCO R1441G mutant bound significantly stronger to ROCO<sup>LRRK1</sup>. Surprisingly, the

remainder of ROCO mutants did not show any changes in ROCO<sup>LRRK1</sup> binding. Thus, mechanisms for LRRK homo- and heterodimerization may be different, albeit using the ROCO interaction surface. Certainly, differences between LRRK homo- and heterodimerization will have to be validated with full length proteins, and functional assays will be needed to assess the biological relevance of LRRK heterodimerization.

#### 4.6 ROCO<sup>LRRK2</sup> exerts an inhibitory effect on LRRK2 kinase activity

This study demonstrated that the ROCO<sup>LRRK2</sup> fragment binds to full length LRRK2 and exerts a significant inhibitory effect on both wild type and G2019S LRRK2 autophosphorylation. Mutant ROCO<sup>LRRK2</sup> fragments R1441C and Y1699C showed a decreased inhibition of LRRK2 autophosphorylation, consistent with their weaker potential for homodimerization. Thus, the direct binding of ROCO fragments to full length LRRK2 confers kinase inhibition, and this effect is accordingly influenced by PD associated mutations diminishing homodimerization. Hence, it can be hypothesized that proper dimerization is necessary for LRRK2 kinase activity. This is in concordance with a recent report showing that kinase inactive LRRK2 mutants do not form dimeric protein species (183). Moreover, intracellular kinases related to LRRK2 can be activated by dimerization. Raf-1 has been shown to become active after coumermycin-induced dimerization (171), and MLK-3 requires dimerization via tandem leucine zippers for proper activation (170).

Assuming that LRRK2 dimerization is important for kinase activity, substitution of ROCO<sup>LRRK2</sup> with the larger kinase-active RCKW<sup>LRRK2</sup> fragment was supposed to mimic normal dimerization by bringing together the two kinase domains and thus possibly reversing kinase inhibition. Surprisingly, co-expression of RCKW<sup>LRRK2</sup> inhibited wild type and G2019S autophosphorylation comparable to ROCO<sup>LRRK2</sup>. Thus, there was apparently no *trans*-autophosphorylation in the LRRK2-RCKW<sup>LRRK2</sup> complex in this setting. Concordantly, a recent report identified LRRK2 autophosphorylation to occur in *cis* rather than in *trans* (157), a mechanism previously proposed also for LRRK1 (164). Interestingly, missing autophosphorylation in the heterogenic LRRK2-RCKW<sup>LRRK2</sup> complex suggests that

homogenic dimerization (i.e., two full length LRRK2 proteins or two RCKW fragments) is a prerequisite for proper *cis*-autophosphorylation (Fig. 4-2)

Given the homology in LRRK domain architecture and dimerization behaviour, there was the obvious question of a similar kinase inhibiting effect by ROCO fragments on LRRK1. However, LRRK1 autophosphorylation could not be detected by kinase assays performed under LRRK2 conditions (data not shown), thus measuring LRRK1 kinase activity under presence of  $\text{ROCO}^{\text{LRRK1}}$  and  $\text{ROCO}^{\text{LRRK2}}$  will require further improvement.

Due to the artificial nature of *in vitro* kinase assays, obtained functional information must be taken with care. Clearly, a confirmation of the observed effects in cell-based settings is desirable. So far, there is no approved physiological kinase substrate of LRRK2, but the ERM proteins may be good candidates (147). However, measuring ERM phosphorylation by Western blot analysis of HEK 293T cell lysates containing (co-)expressed LRRK2 and ROCO constructs did not produce consistent results (data not shown), and thus requires further experimental optimization. Additionally, alternative *in vivo* analyses of the *in vitro* LRRK2 kinase inhibiting effect will have to be designed and established (see 4.8).

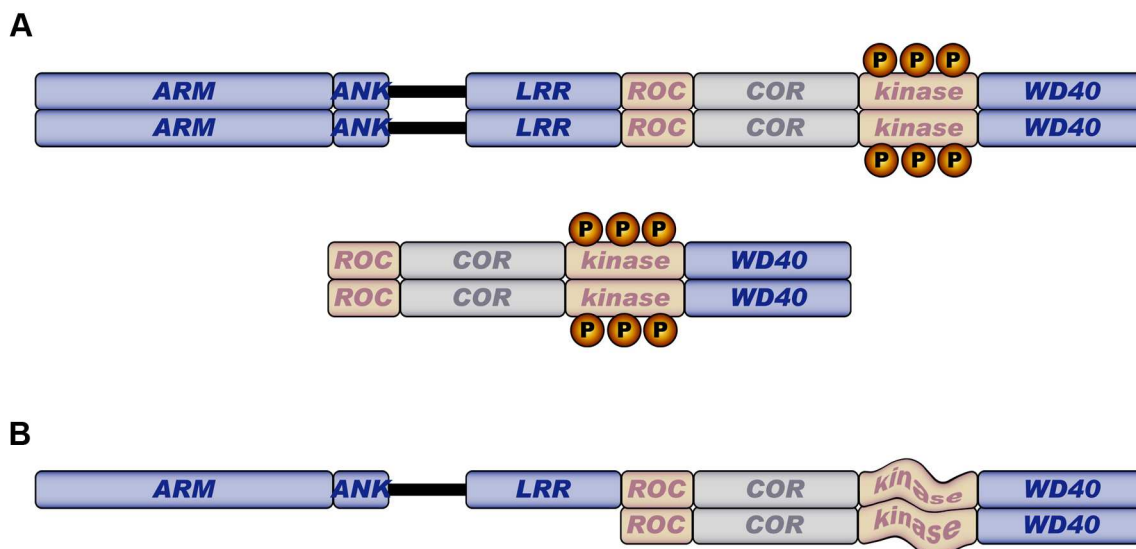


**Figure 4-2. Homogenic dimerization is a prerequisite for LRRK2 kinase activity.**

(A) Homogenic dimerization between full length LRRK2 or RCKW monomers allows for autophosphorylation (indicated by the phosphate groups at the kinase domain), most probably by accurately arranging the respective monomers. LRRK2 autophosphorylation is most likely an intramolecular event. (B) Heterogenic dimerization between full length LRRK2 and the RCKW construct prevents autophosphorylation (indicated by a distorted kinase domain) by an as yet unknown mechanism. Possibly, LRRK2 molecules of different length can not be arranged to a functional dimeric conformation.



#### 4.7 Predicted model of the ROCO<sup>LRRK2</sup>-mediated LRRK2 kinase inhibition

This study highlights an unprecedented, exciting possibility of inhibiting LRRK2 kinase activity. Even if the precise molecular mechanism of ROCO-mediated kinase inhibition remains elusive, it does not seem to involve direct binding to the kinase domain, as an interaction of the ROC or the COR domain with the kinase domain could not be detected here and elsewhere (117). Concordantly, whereas the majority of kinase inhibitors directly target the catalytical core of the kinase, allosteric inhibition is also a known mechanism (184, 185).

Mechanistically, LRRK2 kinase inhibition by co-expressed ROCO could either be direct or indirect. The latter would be exerted due to consumption of essential kinase-inducing co-factors by the ROCO fragment, consequently leading to a lack of activation for the LRRK2 kinase domain. One co-factor apparently necessary for LRRK2 kinase activation is GTP, as GTP binding-deficient LRRK2 mutants showed decreased kinase activity and addition of the non-hydrolyzable GTPγS stimulated the kinase (145, 146, 150, 172). Thus, GTP binding by ROCO could cause indirect LRRK2 kinase inhibition by depleting the pool of available GTP. However, GTP binding deficient ROCO<sup>LRRK2</sup> mutants inhibited LRRK2 autophosphorylation similar to wild type fragments, thus excluding kinase inhibition due to depletion of GTP. Naturally, this does not eliminate the consumption of other co-factors by ROCO. However, a major influence of putative co-factors on kinase activity in *in vitro* kinase assays is rather negligible because of several washing and purification steps. Thus, an indirect kinase inhibition mechanism due to consumption of co-factors by the ROCO fragment is largely unlikely.

Consistently, the data presented in this study suggest that the kinase inhibiting effect is crucially depending on direct binding of the ROCO<sup>LRRK2</sup> fragment to the ROCO domain of full length LRRK2, as weaker binding of mutant ROCO fragments resulted in diminished kinase inhibition. However, there are still different possibilities for kinase inhibition by direct binding (Fig. 4-3). Interestingly, ROCO<sup>LRRK2</sup> fragments seemingly do not disrupt LRRK2 dimers, as the addition of increasing amounts of ROCO<sup>LRRK2</sup> fragment had no impact on LRRK2 co-IPs. However, the added ROCO<sup>LRRK2</sup> fragment was simultaneously co-immunoprecipitated via LRRK2 in a

concentration-dependent manner, indicating that ROCO<sup>LRRK2</sup> fragments could perturb proper LRRK2 dimerization by inserting (Fig. 4-3A) or attaching (Fig. 4-3B). This scenario of a partial disturbance of dimerization resembles the action of thioredoxin on ASK1 (apoptosis signal-regulating kinase 1). Thioredoxin was found to prevent N-terminal homophilic interaction of ASK1 when bound to its N-terminal binding site, whereas overall ASK1 dimerization was not influenced (186).

Assuming monomeric LRRK2 as the active species, the ROCO<sup>LRRK2</sup> fragment could inhibit kinase activity by binding to the ROCO domain, subsequently distorting the conformation of the kinase domain (Fig. 4-3C).

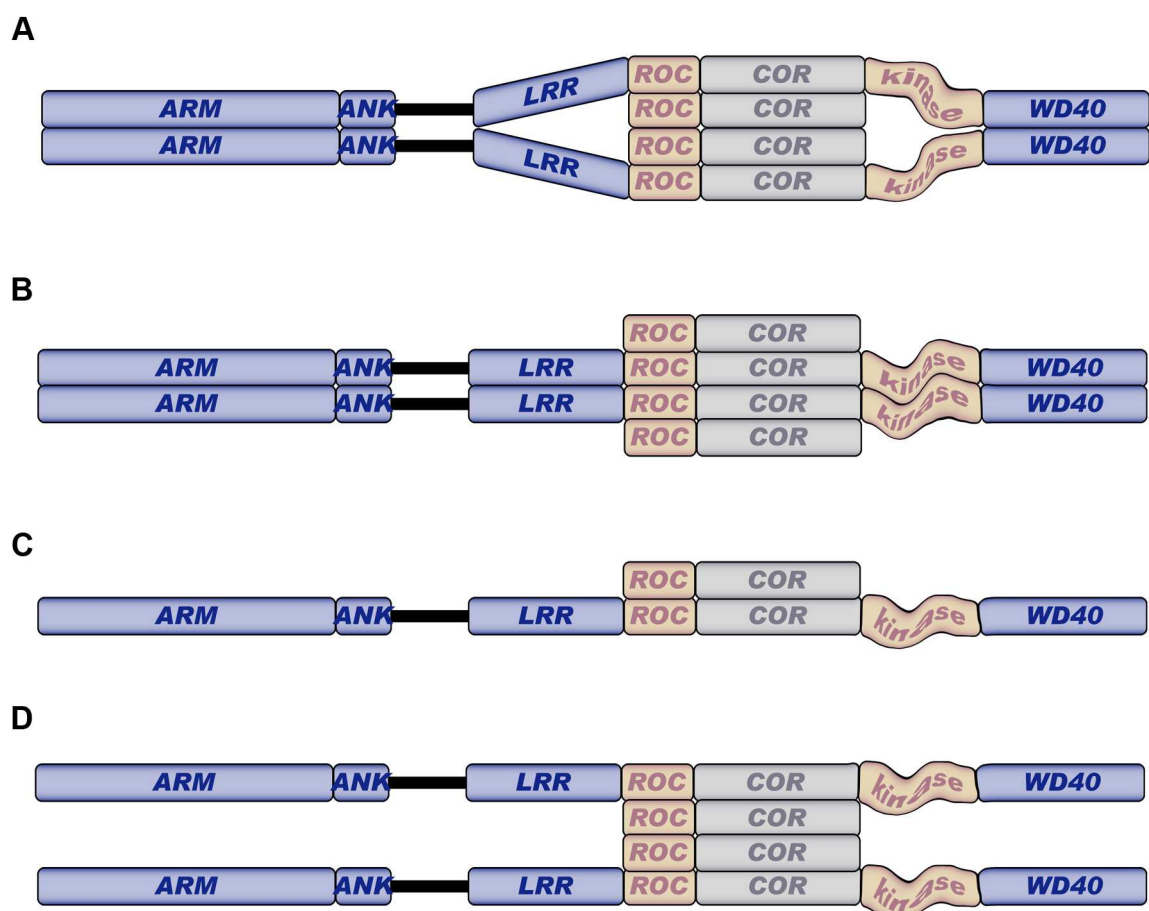


**Figure 4-3. Possible mechanisms of the ROCO<sup>LRRK2</sup> mediated inhibitory effect on LRRK2 kinase activity.**

LRRK2 kinase impairment is depicted by graphical distortion of the kinase domain. (A+B) Assuming LRRK2 dimerization to be the necessary conformation for proper kinase activity, ROCO<sup>LRRK2</sup> may perturb proper LRRK2 dimerization and consequently inhibit kinase activity by inserting in between (A) or attaching to (B) the LRRK2 dimer. (C) Supposing monomeric LRRK2 as the kinase active species, binding of ROCO<sup>LRRK2</sup> fragment to the ROCO domain of LRRK2 could induce a conformational change rendering the kinase inactive. (D) The findings presented in this study suggest a model where ROCO<sup>LRRK2</sup> fragments act as spacers separating the halves of the LRRK2 dimer. Thus, a functional dimer conformation is abrogated, subsequently leading to inhibition of the LRRK2 kinase domain.

Ultimately, all evidence gathered in this study converges to a model where ROCO<sup>LRRK2</sup> forms a complex with LRRK2 and acts as a 'spacer' separating the two LRRK2 monomers, thus functionally inhibiting the dimer and accordingly also kinase activity (Fig. 4-3D). A partial disturbance of dimerization as known for ASK1 is rather unlikely, as interactions among LRRK2 domains other than ROCO could not be detected.

Whatever the exact mechanism, the artificial ROCO<sup>LRRK2</sup> fragment could serve as a template for new allosteric drug design in PD by virtue of its LRRK2 kinase inhibiting effect. Once reduced to their minimal functional size and proven in cell-based functional assays, ROCO-like dimerization/kinase inhibitors might have important implications for the treatment of PD.

## 4.8 Outlook

Based on the results of this study, a multitude of future experiments is at hand. Certainly, exploring the therapeutic potential of ROCO<sup>LRRK2</sup> mediated kinase inhibition will be the most exciting direction of research. However, consisting of roughly 550 aa, ROCO<sup>LRRK2</sup> is too large for direct pharmacological applications. Thus, a considerable reduction in ROCO<sup>LRRK2</sup> size without loss of its inhibitory potential has to be achieved. Indeed, there is evidence that small peptide or protein domains derived from full length polypeptides can still exert biological function(s). Due to their supposed superior clinical properties over currently used biomolecules like antibodies in terms of blood clearance, diffusion and tissue penetration, these small agents are considered as putative therapeutics in an emerging field called chemical genetics or peptide therapeutics (187). Actually, a recent report described TNFR-1-dependent DAPK1 degradation in cell culture induced through an yet unknown mechanism by a DAPK1 miniprotein (188). Interestingly, while this 110 aa miniprotein is considerably smaller than ROCO<sup>LRRK2</sup>, it is a fragment from the middle of the DAPK1 ROCO domain. Given that ROCO<sup>DAPK1</sup> is the DAPK1 core dimerization interface, the DAPK1 miniprotein could exert its action through prevention or disturbance of DAPK1 dimerization. Consequently, smaller ROCO fragments could be generally able to still

perturb dimerization of ROCO kinases, suggesting a possibility to reduce the size of ROCO-based LRRK2 antagonists.

Naturally, an ideal LRRK2 kinase inhibitor on ROCO-basis should have no side effects on related protein kinases. However, heterodimerization potential between ROCO domains of LRRK2, LRRK1 and DAPK1 confirmed in this study foreshadows that ROCO-like kinase inhibitors could show problems of selectivity. Thus, future experiments analyzing a therapeutical relevance of ROCO-like kinase inhibitors will have to turn their attention to selectivity issues.

Regardless of a desirable size reduction, the ROCO-mediated kinase inhibiting effect will have to be validated in additional experimental settings. Concerning *in vitro* studies, kinase assays should be extended beyond measurement of autophosphorylation to analyze ROCO-mediated inhibition effects on phosphorylation of ERM proteins (so far the only established *in vitro* LRRK2 substrate (147)). To investigate if the kinase inhibiting effect is dependent on ROCO dose, ROCO fragments or miniproteins will have to be isolated and purified from expression systems like *E. coli*. Subsequently, these recombinant proteins can be used to titrate the strength of the kinase inhibiting effect. However, previous attempts to isolate and purify ROCO fragments failed due to poor expression and/or solubility, suggesting that finding the appropriate domain boundaries will be crucial for a successful production of recombinant protein.

Moreover, confirmation of ROCO-mediated LRRK2 kinase inhibition in more physiological *in vivo* systems is needed. Currently, cell culture phenotypes induced by pathogenic and/or overexpressed LRRK2 comprise neurite shortening, protein aggregation and cell toxicity. Generally, cells (neuronal-like or rodent primary neurons) analyzed in these systems are hardly transfectable, thus cell lines stably expressing LRRK2 constructs will have to be generated. Co-expression of ROCO fragments or miniproteins in sufficient quantity could be achieved by viral transduction. Once these experimental setting are established, an expected rescue of the respective phenotype by co-expression of ROCO fragments can be assessed.

This study found evidence for an interaction potential among all three ROCO kinases, suggesting that the ROCO domain could be a domain with general dimerization function. To further clarify this question, analysis of the MFHAS1 dimerization potential is indicated. MFHAS1, the last of the four known mammalian ROCO proteins, is only very distantly related to the ROCO kinases, as it does not

have a kinase domain at all. Thus, it will be very interesting to see if its ROCO domain nevertheless is capable of directing dimerization, and if there is heterodimerization potential with the ROCO kinases. Furthermore, it will be important to ascertain if other ROCO features are also shared among proteins of the ROCO family. For instance, GTP binding has been demonstrated for the LRRKs, but not for DAPK1 and MFHAS1. Similarly, binding to the cytoskeleton will have to be assessed for LRRK1 and MFHAS1. These studies should reveal if structural similarity is reflected in shared functions.

Although this study identified ROCO as the core dimerization interface, a further finemapping of the exact dimerization region is indispensable. Deletion constructs lacking the ROCO, ROC or COR domain will elucidate which regions are absolutely necessary for dimerization and kinase activity. To obtain structural information, the ROCO<sup>LRRK2</sup> fragment will have to be purified in sufficient amounts. Once structural information is available, residues identified to be important for dimerization will be artificially mutated, and effects on dimerization and kinase activity can be evaluated.

To study a possible functional relationship among the ROCO kinases, kinase assays will have to be established for LRRK1 and DAPK1. Subsequently, quenching of kinase activity by ROCO fragments can be assessed in all possible combinations. Moreover, the specificity of the respective ROCO domain can be investigated by cloning ROCO domain chimeras, which are accordingly to be tested in functional assays. Ultimately, these experiments should help to put together the puzzle of a putative regulatory interplay between ROCO kinases, which could have important impact on the understanding of neurodegeneration in general.



## 5 MATERIALS AND METHODS

### 5.1 Chemicals

chemical	manufacturer
1,4-Dithiothreitol (DTT)	Roth
2-propanol	Merck
40% Acrylamid/Bis solution 19:1	Biorad
Acetic acid (glacial) 100%	Merck
Adenine hemisulphate	Sigma
Agar	Fluka
Ammonium persulfate (APS)	Sigma
Ampicillin	Sigma
Amylose resin	NEB
Bacto peptone (Y2H)	Beckton Dickinson
Bacto-Agar (Y2H)	Becton Dickinson
Bovine Serum Albumin (BSA)	Roth
Bromphenol blue sodium salt (BPB)	Merck
Complete® protease inhibitor cocktail	Roche
Coomassie brilliant blue R-250	AppliChem
Dimethylsulfoxide (DMSO)	Sigma
DMEM (Dulbecco's minimal essential medium)	Biochrom
DNA 1 kb ladder	NEB/Fermentas
DNA 100 bp ladder	NEB/Fermentas
DNA T4 Ligase (1U/μl), DNA T4 Ligase buffer (10x)	Fermentas
EDTA	Sigma
Ethanol	Merck
Ethidium bromide (1% in water)	Merck
Fetal bovine serum gold	PAA
FuGENE 6 transfection reagent	Roche
Glycerol	AppliChem
Glycine	Roth
GTP-sepharose	Jena Biosciences
HA-, MYC-, FLAG-EZview agarose	Sigma
Hepes	Sigma
Hydrochloric acid (HCL)	Merck
Immobilon Western HRP substrate	Millipore

Immun-Star HRP substrate	Biorad
Kanamycin	Sigma
kinase buffer 10x	Cell Signaling
Licium acetate dihydrate (LiAc)	Sigma
Methanol	Merck
N,N,N',N'-Tetramethylethylenediamine (TEMED)	Merck
Nitrogen base, dropout media	Formedium
Non fat milk powder	Sucofin (Edeka)
Nucleotides (ATP, CTP, GTP, GDP, GTP $\gamma$ S)	Sigma
One Shot® TOP10Electrocomp™ <i>E. coli</i>	Invitrogen
Optimem	Gibco
$\gamma$ - <sup>32</sup> P-ATP	GE healthcare/ Hartmann Analytic
Polyethylene glycol (PEG)	Sigma
Ponceau S Staining Solution	Sigma
Potassium chloride (KCL)	Merck
Potassium dihydrogen phosphate (KH <sub>2</sub> PO <sub>4</sub> )	Merck
Precision Plus Protein Standard, prestained	Biorad/Fermentas
Protein G-agarose	Roche/Upstate
Restriction endonucleases and buffers	Roche/Fermentas
Shrink alkaline phosphatase (SAP), SAP buffer (10x)	Fermentas
Sodium azide (NaN <sub>3</sub> )	Sigma
Sodium chloride (NaCl)	Merck
Sodium dodecyl sulfate (SDS)	Sigma
Sodium hydroxide (NaOH)	Merck
Sodium phosphate dibasic heptahydrate (Na <sub>2</sub> HPO <sub>4</sub> ·7 H <sub>2</sub> O)	Merck
Sodium pyrophosphate tetrabasic decahydrate (NaPP)	Sigma
TaKaRa <i>Ex Taq</i> DNA polymerase (+ 10x buffer, dNTPs)	Lonza
<i>Taq</i> DNA polymerase (+ 10x buffer, dNTPs)	Qiagen
Trichloroacetic acid solution, 6.1 N (TCA)	Sigma
Triton X-100	AppliChem
TRIZMA® Base (Tris base)	Sigma
Trypsin-EDTA (10x)	Gibco
Tryptone/Peptone	Roth
Tween® 20	Merck
Yeast extract	Sigma/AppliChem
$\beta$ -Mercaptoethanol	Roth

---



## 5.2 Solutions and buffers

### 5.2.1 Molecular biology

#### *Ampicillin stock solution*

100 mg/ml in H<sub>2</sub>O bidest. Aliquots were stored at –20°C.

#### *Kanamycin stock solution*

30 mg/ml in H<sub>2</sub>O bidest. Aliquots were stored at –20°C.

#### *LB medium*

10 g Tryptone, 5 g Bacto-Yeast extract, and 8 g NaCl were dissolved in 1000 ml H<sub>2</sub>O and sterilized by autoclaving. Ampicillin (100 µg/ml) or Kanamycin (30 µg/ml) was added after cooling down to approximately 50°C. LB containing antibiotic was stored at 4°C.

#### *LB agar plates*

10 g Bacto-Tryptone, 5 g Yeast extract, 8 g NaCl, and 16 g Bacto-Agar were dissolved in 1000 ml H<sub>2</sub>O and sterilized by autoclaving. Ampicillin (100 µg/ml) or Kanamycin (30 µg/ml) was added after cooling down to approximately 50°C. Plates were stored at 4°C.

#### *10x DNA gel loading buffer*

250 mg bromphenol blue, 33 ml 150 mM Tris base (pH 7.6), 60 ml glycerol, 7 ml H<sub>2</sub>O bidest. Stored at 4°C.

#### *Tris-borate buffer (TBE) 10x*

108 g Tris, 55 g Boric acid in 900 ml H<sub>2</sub>O bidest. 40 ml 0.5 M Na<sub>2</sub>EDTA (pH 8.0) was added and volume adjusted to 1 liter with H<sub>2</sub>O bidest.

#### *1% (w/v) Agarose gel*

1 g agarose was dissolved in 100 ml 1x TBE by microwave heating. 2.0 µl of ethidium bromide (1% in water solution) were added after cooling to ~50°C .

### **5.2.2 Yeast two-hybrid (Y2H)**

#### *YPAD medium*

5 g yeast extract, 10 g peptone, and 50 mg adenine hemisulphate were dissolved in 450 ml H<sub>2</sub>O bidest. After autoclaving, 50 ml 20% glucose was added.

#### *-Leu-Trp yeast selective medium*

6.9 g nitrobase, and 0.64 g -Leu-Trp dropout medium were dissolved in 900 ml H<sub>2</sub>O bidest. After autoclaving, 100 ml 20% glucose was added.

#### *LiT*

100 mM LiAc, 10 mM Tris pH 7.4

#### *PEG/LiT*

3 ml 1M LiAc, 0.3 ml 1M Tris pH 7.4, fill up to 30 ml with 50% PEG (in water)

#### *Yeast selective agar plates*

17 g agar were dissolved in 500 ml H<sub>2</sub>O bidest and autoclaved. 6.9 g nitrobase, and selective dropout medium (0.64 g -Leu-Trp or 0.62 g -His-Leu-Trp) were dissolved in 400 ml H<sub>2</sub>O bidest, adjusted to pH 5.6, and autoclaved. 500 ml autotplaved agar solution and 100 ml 20% glucose were added to 400 ml medium solution. Plates were stored at 4°C.

#### *HU buffer (yeast protein extraction)*

8 M Urea, 5 % SDS, 200 mM Tris pH 6.8, 1 mM EDTA, BPB, and 1.5 % DTT

### **5.2.3 Protein biochemistry**

#### *SDS-PAGE stacking gel buffer*

0.5 M Tris base, pH 6.8 and 0.4% SDS.

#### *SDS-PAGE resolving gel buffer*

1.5 M Tris base, pH 8.8 and 0.4% SDS.

*10x SDS-PAGE running buffer*

30.3 g Tris base, 145 g glycine, 10 g SDS in 1 liter H<sub>2</sub>O bidest.

*4x SDS-PAGE sample buffer (4x Laemmli buffer)*

2.5 ml 1 M Tris base (pH 6.8), 2.0 ml 20% SDS, 4.0 ml glycerol, 1.0 ml β-mercaptoethanol, 250 mg bromphenol blue, adjusted to 10 ml volume with H<sub>2</sub>O bidest. Aliquots were stored at -20°C.

*1x Transfer buffer*

3.03 g Tris base, 14.5 g glycine, 200 ml methanol, adjusted to 1 liter volume with H<sub>2</sub>O bidest.

*10x TBS - Tris buffered saline*

302.85 g Tris, 438.3 g NaCl in 4 liter H<sub>2</sub>O. pH was adjusted to 7.5 with 1 M HCl and volume was filled to 5 liter with H<sub>2</sub>O. Stable at 4°C for three months.

*1x TBS-T - Tris buffered saline/0.1% Tween 20*

Dissolving of 1.0 ml Tween 20 in 1 liter 1x TBS.

*10% Blocking solution*

Dissolving of 50 g non fat milk powder in 500 ml 1x TBS-T.

*Western Blot stripping solution*

7.57 g Tris base (pH 7.7), 20 g SDS, 6.98 ml β-mercaptoethanol, adjusted to 1 liter volume with H<sub>2</sub>O bidest.

*Primary antibody solution*

Dissolving 1 g BSA and 1 g NaN<sub>3</sub> in 100 ml TBS-T. Stored at 4°C.

*Column buffer*

20 mM HEPES pH 7.4, 200 mM NaCl, 1 mM EDTA

*MBP elution buffer*

10 mM maltose in column buffer

*Coomassie staining solution*

0.5 g Coomassie blue R250, 92 ml acetic acid (glacial), 454 ml methanol, and 454 ml H<sub>2</sub>O bidest (total volume 1000 ml).

*Coomassie destaining solution*

50 ml acetic acid (glacial), 250 ml methanol, and 700 ml H<sub>2</sub>O bidest (total volume 1000 ml).

## 5.2.4 Cell biology

*10x PBS - Phosphate buffered saline*

80 g NaCl, 2 g KCl, 26.8 g Na<sub>2</sub>HPO<sub>4</sub>-7 H<sub>2</sub>O and 2.4 g KH<sub>2</sub>PO<sub>4</sub> in 800 ml H<sub>2</sub>O. pH was adjusted to 7.4 with HCl and volume filled to 1 liter with H<sub>2</sub>O.

*HEK 293T cell freezing medium*

40 ml DMEM medium, 40 ml fetal bovine serum and 20 ml DMSO were mixed, sterile filtrated using a 0.22 µm filter, and stored at 4°C .

*Cell lysis buffer*

150 mM NaCl, 1% TritonX-100, 50 mM Tris base (pH 7.4), 1 mM EDTA, and 10 mM Na-pyrrophosphate in H<sub>2</sub>O bidest. 1x Complete® protease inhibitor cocktail (Roche) was added freshly.

## 5.3 Vectors and oligonucleotides

*vector backbones*

vector	tag(s)	manufacturer
pcDNA3	5' FLAG, 5' MYC	Invitrogen
pMAL	5' MBP	NEB
pCMV	5' HA, 5' MYC	Clontech
pGBKT7	5' MYC	Clontech
pGADT7	5' HA	Clontech

---

*plasmid constructs*

<b>construct</b>	<b>source</b>
pCI-LRRK2-HA	Giorgio Rovelli, Novartis Pharma AG, Basel, Schweiz
pCI-LRRK2[G2019S]-HA	Giorgio Rovelli, Novartis Pharma AG, Basel, Schweiz
pCI-LRRK2[K1906M]-HA	Giorgio Rovelli, Novartis Pharma AG, Basel, Schweiz
pCI-LRRK2[R1441C]-HA	Giorgio Rovelli, Novartis Pharma AG, Basel, Schweiz
pCI-LRRK2[R1441G]-HA	Giorgio Rovelli, Novartis Pharma AG, Basel, Schweiz
pCI-LRRK2[R1441H]-HA	Giorgio Rovelli, Novartis Pharma AG, Basel, Schweiz
pCI-LRRK2[Y1699C]-HA	Giorgio Rovelli, Novartis Pharma AG, Basel, Schweiz
pCMV-2xMYC-LRRK2[K1347A]	Mark Cookson, NIH, Bethesda, Maryland, USA
pCMV-3xFLAG-LRRK2[T1348N]	Takeshi Iwatsubo, University of Tokyo, Tokyo, Japan
pCMV-2xMYC-LRRK1	Bertram Weiss, Schering AG, Berlin
pcDNA3-HA-DAPK1	Adi Kimchi, Weizmann Institute of Science, Rehovot, Israel

*oligonucleotides*

Sequences of oligonucleotides are available on request.

## 5.4 Antibodies

<b>1° antibody</b>	<b>source</b>	<b>dilution (WB)</b>	<b>manufacturer</b>
anti-HA	rat monoclonal	1:1.000 – 1:30.000	Roche
anti-MYC 9E10	mouse monoclonal ascites	1:5.000 – 1:60.000	Developmental Studies Hybridoma Bank, University of Iowa
anti-FLAG M2	mouse monoclonal	1:1.000 – 1:5.000	Sigma
anti-Mid(LRRK2)	rabbit polyclonal	1:1.000 – 1:50.000	self-produced

2° antibody	source	dilution (WB)	manufacturer
anti-rat-HRP	rabbit polyclonal	1:5.000 – 1:40.000	Dako
anti-mouse-HRP	sheep polyclonal	1:10.000 – 1:60.000	GE healthcare
anti-rabbit-HRP	donkey polyclonal	1:10.000 – 1:30.000	GE healthcare

## 5.5 Molecular cloning

### 5.5.1 PCR, agarose gel electrophoresis and extraction of DNA

All cDNA sequences to be subcloned were amplified by PCR according to the manufacturer's protocol with primers bearing the appropriate restriction sites. Analytical PCR was done with *Taq* DNA polymerase, whereas preparative PCR was performed with TaKaRa *ExTaq* DNA polymerase because of its proof-reading ability. To further prevent unwanted mutations in the amplified sequences, the number of PCR cycles was reduced to 10 rounds of amplification. PCR products were separated on 1% agarose gels, visualized via detection of incorporated ethidium bromide by UV illumination, excised and purified by QIAquick gel extraction kit (Qiagen).

### 5.5.2 Enzymatic digestion of DNA fragments and plasmid DNA

The amount of a restriction enzyme needed to digest DNA were calculated according to the following equation:

$$\frac{\text{DNA assayed for enzyme (bp)} \cdot 2 \text{ (security)}}{\text{target DNA (bp)} \cdot \text{restriction sites in DNA assayed for enzyme}} = U \text{ (1 cut in 1 } \mu\text{g DNA in 1 h)}$$

Digests were performed in a total volume of 50  $\mu$ l. For DNA fragments, removal of salts and nucleotides was achieved with QIAquick PCR purification kit (Qiagen). Digested vectors were purified by gel extraction and dephosphorylated (1  $\mu$ l SAP per ~ 450 ng DNA, 10 min at 37°C). Afterwards, SAP was heat inactivated (15 min at 65°C).

### 5.5.3 Ligation of digested DNA fragments and transformation of DNA by electroporation

50 ng digested and dephosphorylated vector was used per ligation reaction. Amounts of digested DNA fragments needed for ligation were calculated according to the following equation:

$$\text{x-fold molar excess} \cdot \frac{\text{insert (bp)}}{\text{vector (bp)}} \cdot \text{amount of vector used (ng)} = \text{amount of insert needed}$$

Inserts were added in a three- or ten-fold molar excess. Ligations were incubated at RT for 2 h.

Subsequently, 4  $\mu$ l (5  $\mu$ l) of a ligation reaction (10 ng [1  $\mu$ l] of a plasmid for retransformation) were added to 40  $\mu$ l (50  $\mu$ l) of electrocompetent cells on ice and mixed by gently tapping the reaction tube. Samples were pipetted into pre-cooled 0.2 cm cuvettes and pulsed with 2.0 kV using a MicroPulser<sup>TM</sup> device (BioRad). 1 ml LB medium without antibiotics was immediately added to pulsed *E. coli* and transferred to 1 ml reaction tubes. After incubation for 1 h at 37°C and 300 rpm, 50-300  $\mu$ l of bacteria were spread on LB agar plates including the appropriate selective antibiotic and grown overnight at 37°C.

### 5.5.4 Production of electrocompetent cells

Fresh colonies from One Shot<sup>®</sup> TOP10 Competent Cells (Invitrogen) were produced by streaking out bacteria from cell stocks onto an LB-ampicillin agar plate and growing them overnight at 37°C. One single colony was used to inoculate 50 ml of fresh LB-ampicillin medium and again grown overnight at 37°C and 200 rpm. The next day, the culture was diluted 1:100 in two flasks with 1 liter LB-ampicillin medium and incubated at 37°C with 200 rpm until an OD<sub>600</sub> of 0.5 was reached. All further steps were done on ice or 4°C (centrifugations) and only cold equipment and solutions were used. Cells were centrifuged in four 500 ml bottles for 30 min at 4000 rpm (75006445 rotor, Sorvall-Heraeus). The supernatant was discarded and each cell pellet was resuspended in 10 ml sterile 10% glycerol, pooled to two 500 ml bottles, filled up to 400 ml sterile 10% glycerol and centrifuged for 30 min at 4000

rpm (75006445 rotor, Sorvall-Heraeus). The supernatant was again discarded, the two remaining pellets resuspended in 10 ml sterile 10% glycerol and combined into one bottle. After centrifugation as above, the pellet was resuspended in 10 ml sterile 10 % glycerol and transferred to a 50 ml conical tube. Volume was adjusted to 50 ml and the cell suspension was centrifuged again as above. The resulting cell pellet was resuspended in 1-1.5 ml sterile 10 % glycerol and 40  $\mu$ l (50  $\mu$ l) aliquots were prepared. Aliquots were shock-frozen in liquid nitrogen and stored at  $-80^{\circ}\text{C}$ .

### **5.5.5 Amplification, purification and validation of plasmid DNA**

A single colony from a selective plate was picked to inoculate 5-7 ml (MiniPrep) or 35-50 ml (MidiPrep) LB medium containing the appropriate selective antibiotic. Incubation was carried out for ~16 hours at  $37^{\circ}\text{C}$  with vigorous shaking (~200 rpm). For MaxiPrep, a MiniPrep overnight culture was diluted ~1:100 in selective LB medium and grown at  $37^{\circ}\text{C}$  for ~16 hours with vigorous shaking. For LRRK2 full length plasmids, both incubation time and medium volume had to be increased considerably to yield sufficient amounts of plasmid. Bacterial cells were harvested by centrifugation at 12000 x g for 1 min at RT (MiniPrep) or 6000 x g for 15 min at  $4^{\circ}\text{C}$  (MidiPrep, MaxiPrep). Purification steps were conducted with Mini, Midi or MaxiPrep kits (Qiagen) according to the manufacturer's instructions. Air-dried DNA pellets were redissolved in EB-buffer (MiniPrep: 30  $\mu$ l, MidiPrep: 150 – 350  $\mu$ l, MaxiPrep: 250 – 1000  $\mu$ l) and DNA concentration was measured by a NanoDrop<sup>®</sup> ND-1000 device (Peachlab). The entire coding sequences of all constructs were verified by DNA sequencing, and the integrity of vectors was validated by restriction analysis.

For long-term storage of constructed plasmids, bacterial glycerol stocks were generated. Briefly, 1 ml overnight bacterial culture was centrifuged (5 min, 2000 x g, RT). The pellet was resuspended in 800  $\mu$ l LB medium without antibiotics and mixed with 200  $\mu$ l 99,5% glycerol. Glycerol stocks were stored at  $-80^{\circ}\text{C}$ .



## 5.5.6 Cloned constructs

*LRRK2*

construct	pMAL	pCMV		pcDNA3		pGBKT7	pGDAT7
		HA	MYC	FLAG	MYC		
Mid	•			•		•	•
LRR				•		•	•
ROC		•	•			•	•
ROC R1441G						•	•
ROC R1441H						•	•
COR		•	•			•	•
COR Y1699C						•	•
kinase						•	•
WD40				•		•	•
ArmAnk				•			
MidLRR				•			
ROCO		•	•			•	•
ROCO R1441C		•	•				
ROCO R1441G		•	•				
ROCO R1441H		•	•				
ROCO Y1699C		•	•				
ROCO R1441C+Y1699C		•	•				
ROCO K1347A		•	•				
ROCO T1348N		•	•				
VN155-ROCO			•				
VC155-ROCO		•					
ROCO-VN155			•				
ROCO-VC155		•					
RCK						•	•
RCKW		•	•			•	•
ΔROCO		•	•				
LRRK2 (full length)	•			•	•		

*LRRK1*

construct	pCMV		pGBKT7	pGDAT7
	HA	MYC		
Ank			•	•
LRR			•	•
ROC			•	•
COR			•	•
kinase			•	•
WD40			•	•
ROCO	•	•		
VN155-ROCO		•		
VC155-ROCO	•			
ROCO-VN155		•		
ROCO-VC155	•			

LRRK2/LRRK1 sequence alignments were done with the AlignX software (Vector NTI, Invitrogen).

*DAPK1*

construct	pCMV	
	HA	MYC
ROCO	•	•

The DAPK1 ROCO domain was cloned as defined by Bosgraaf et al. (115).

## 5.6 MBP-Mid fusion protein expression and purification

The pMAL™ Protein Fusion and Purification System (NEB) provides a method for expressing and purifying a protein of interest. The protein encoding gene is inserted

into a pMAL vector downstream from the *malE* gene of *E. coli*, which encodes maltose-binding protein (MBP), resulting in expression of an MBP fusion protein.

The LRRK2 Mid fragment was subcloned into the pMAL-c2X vector as described above. Subsequently, the plasmid containing the MBP-Mid fusion gene was transformed into *E. coli* BL21-CodonPlus<sup>®</sup> Competent cells (Stratagene) as described above. The next day, 1 liter LB-Ampicillin (supplemented with 10 ml 20 % Glucose) was inoculated with ~3 ml of an overnight culture of cells containing the fusion plasmid. When the culture had reached an OD<sub>600</sub> of 0.5, expression of the recombinant protein was induced with IPTG (final concentration 0.3 mM). After 3 h additional incubation at 37°C and 200 rpm, bacterial cells were harvested (4000 x g, 20 min, 4°C), resuspended in 50 ml column buffer, and frozen in two aliquots à 25 ml overnight at -20°C. The next day, the two aliquots were thawed in a ice-water bath and bacterial cells of each aliquot were broken open by sonication for 240 sec in 10 x 1 sec pulses with 75 % power (Sonopuls, Bandelin). Tubes were kept on ice during sonication to prevent heating of the samples. After centrifugation (9000 x g, 30 min, 4°C), the supernatant (crude extract) was saved, and one aliquot was shock-frozen in liquid nitrogen for long-term storage at -80°C. The other aliquot was subjected to batch binding overnight at 4°C and 5 rpm (wheel, Model 79000, Labor-Brand). Thereby, 5 ml of the amylose resin were washed two times (40 ml column buffer, 5700 x g, 2 min, 4°C) and the 25 ml crude extract were added. The next day, the sample was again washed with 40 ml pre-chilled column buffer, resuspended in 15 ml pre-chilled column buffer and decanted into a Poly-Prep<sup>®</sup> chromatography column (0,8 x 4 cm, Bio-Rad). All following steps were performed at 4°C. The column was washed two times with 60 ml pre-chilled column buffer by gravity flow and eluted with MBP elution buffer. Ten fractions à 1 ml were collected and aliquots analyzed by SDS-PAGE and commassie staining and Western blotting, respectively. The remainder of the fractions were shock-frozen in liquid nitrogen. Fractions containing the fusion protein were thawed, pooled and dialysed into 1 x PBS overnight at 4°C with gentle stirring. Fusion protein concentration was determined by Bicinchoninic Acid Assay kit (BCA, Pierce), according to the manufacturer's instructions. Fusion protein in 1 x PBS was used for immunization of rabbits (Invitrogen EvoQuest).

## 5.7 Y2H interaction study

Y2H interaction studies were performed with the Matchmaker GAL4 two-hybrid system 3 (Clontech). Yeast strain AH109 was co-transformed with pGADT7 and pGBKT7 plasmids containing LRRK2 single or elongated/combined domains, respectively. Briefly, strain AH109 was grown overnight in YPAD full medium to an  $OD_{600}$  of 0,5 – 1,5 and pelleted by centrifugation (3 min, 1200 x g). After discarding the supernatant, aliquots of 100  $\mu$ l were transferred to 1,5 ml tubes and 10  $\mu$ l salmon sperm DNA (10 mg/ml), plasmid DNA (1 $\mu$ g), and 500  $\mu$ l PEG/LiT were added. After careful vortexing and incubation for 15 min at RT, 50  $\mu$ l DMSO were added. Subsequently, yeast was transformed by heat shock for 15 min at 42°C. After being centrifuged (30 sec, 800 x g), yeast pellets were resolved in 100  $\mu$ l ddH<sub>2</sub>O and plated on selective medium lacking Leu and Trp. After incubation at 30°C for 2 days, grown yeast colonies (positive transformants) were taken into liquid culture, grown overnight and equal amounts ( $OD_{600} = 0,25$ ) were spotted onto agar plates containing selective medium lacking Leu, Trp and His. Growing of yeast colonies was assessed after a minimum of 3 days.

To assay for expression of fusion proteins in yeast, yeast proteins were extracted and analyzed by SDS-PAGE/Western blotting. Briefly, yeast was grown in liquid culture to an  $OD_{600} \leq 1$  (starter culture:  $OD_{600} = 0,25$ ). Subsequently, 5 OD cells were harvested (5 min, 6000 x g, 4°C), and cell pellets were resuspended in 1 ml cold H<sub>2</sub>O bidest. This cell suspension was supplemented with 150  $\mu$ l 1,85 M NaOH/7,5 %  $\beta$ -Mercaptoethanol and incubated on ice for 15 min. Addition of 150  $\mu$ l 55 % TCA was followed by another 10 min of incubation on ice. Afterwards, cells were pelleted (10 min, 12000 x g, 4°C) and the supernatant discarded. After a second short centrifugation step, remaining supernatant was discarded and the pellet was resolved in 100  $\mu$ l HU buffer. 15  $\mu$ l of yeast protein extract were analyzed by SDS-PAGE/Western blotting.

## **5.8 Cell culture, transfection, cell harvest and cell lysis**

HEK 293T cells (189) were cultured in DMEM supplemented with 10% FBS at 37°C and 5% CO<sub>2</sub>. Transient expression was performed by transfecting plasmids with FuGENE6 (Roche) according to the manufacturer's protocol for 24 or 48h. Briefly, for one 10 cm plate and a transfection ratio of 3:1, 582 µl Optimem were mixed with 18 µl FuGENE6 and incubated for 5 min at RT. Subsequently, 6 µg DNA were added and the transfection complex was incubated for 45 min at RT.

Cells were harvested by scraping in cold PBS, washed three times in cold PBS and lysed in cell lysis buffer for 30 min on ice (375 µl cell lysis buffer per cell pellet from one 10 cm plate). After pelleting cell debris for 15 min at 20.000 x g at 4°C, protein amount in the supernatant (total cell lysate) was determined by quantification with BCA kit according to the manufacturer's instructions.

## **5.9 Immunoprecipitation, GTP-sepharose affinity purification and nucleotide competition assays**

Total cell lysate amounts ranging from 150 to 1000 µg were incubated in a total volume of 500 µl lysis buffer with 40 or 50 µl FLAG-, HA- or MYC-agarose or 50 µl protein G-agarose and 5 µl anti-MidB2 at 4°C for 3h or overnight. Following three washing steps (500 µl lysis buffer, 5 min, 4°C), beads were eluted with 40 or 50 µl 1x or 2x Laemmli buffer for 5 min at 95°C. For GTP binding studies, cell lysates were incubated with 50 µl GTP-sepharose for 2 h at 4°C. For nucleotide competition assays, the second hour of incubation with GTP-sepharose or MYC-agarose was carried out in the presence of 2 mM GDP, GTP, its non-hydrolysable analog GTPγS, or control nucleotides. Subsequently, beads were eluted in 50 µl 1x Laemmli buffer as described above. The same protocol was used for nucleotide competition during co-immunoprecipitation with MYC-agarose.

## **5.10 SDS-PAGE, Coomassie staining, Western blotting and densitometry**

Samples were prepared in Laemmli sample buffer and - without prior heating - separated on 1.5 mm polyacrylamide gels ranging from 4 to 6 %. Migration of proteins through the stacking gel was conducted with 20 mA per gel, separation in the resolving gel was achieved with a constant voltage of 150 V. Coomassie staining was performed for 40 min at RT with gentle shaking. Transfer of separated proteins onto PVDF membranes (75 mA per 9x7,5 cm membrane, semi-dry blotting) and subsequent membrane blocking (10% milk powder in T-BST), washing (T-BST) and antibody probing was done according to standard protocols. Primary antibody was diluted in primary antibody solution, secondary antibody was diluted in 5% milk powder in T-BST. Immunoreactive signals were detected by chemiluminescence (Immun-Star HRP substrate or Immobilon Western HRP substrate). Notably, blotting time for full length LRRK proteins was increased to at least 2,5 h. Stripping of membranes was done by incubation in WB stripping buffer for 30 min at 56°C, followed by three washing steps with TBS-T.

Densitometric analyses of coomassie and Western blotting signals were conducted with ImageJ software (Rasband, W.S., ImageJ, U. S. National Institutes of Health, Bethesda, Maryland, USA, <http://rsb.info.nih.gov/ij/>, 1997-2007.).

## **5.11 *In vitro* kinase assay**

24 hours after transfection, 375  $\mu$ l (350  $\mu$ g) cell lysate were filled to a total volume of 500  $\mu$ l with lysis buffer and incubated with 50  $\mu$ l HA-agarose overnight at 4°C. After three washing steps with lysis buffer (5 min, 4°C) and one washing step with kinase buffer, immune complexes were resuspended in 50  $\mu$ l kinase buffer supplemented with 1  $\mu$ l ATP (10 mM) and 1  $\mu$ l [ $\gamma$ -<sup>32</sup>P] ATP (10  $\mu$ Ci) and incubated for 30 minutes at 30°C. Supernatants were discarded, and beads were eluted 2 times with 50  $\mu$ l 2x Laemmli buffer. Eluates were pooled and separated by SDS-PAGE, followed by Coomassie blue staining and Western blot, respectively. Incorporated [ $\gamma$ -<sup>32</sup>P] ATP was detected by autoradiography, and quantified by densitometry as described above.

## 6 REFERENCES

1. Parkinson, J. (1817) An Essay on the Shaking Palsy. In Sherwood, N., and Jones, (ed.), London.
2. Calne, D.B. (1989) Is "Parkinson's disease" one disease? *J Neurol Neurosurg Psychiatry*, **Suppl**, 18-21.
3. Calne, D.B. (2000) Parkinson's disease is not one disease. *Parkinsonism Relat Disord*, **7**, 3-7.
4. Dauer, W. and Przedborski, S. (2003) Parkinson's disease: mechanisms and models. *Neuron*, **39**, 889-909.
5. Klein, C. and Lohmann-Hedrich, K. (2007) Impact of recent genetic findings in Parkinson's disease. *Curr Opin Neurol*, **20**, 453-64.
6. Calne, D.B. and Stoessl, A.J. (1986) Early parkinsonism. *Clin Neuropharmacol*, **9 Suppl 2**, S3-8.
7. Findley, L.J. and Gresty, M.A. (1981) Tremor. *Br J Hosp Med*, **26**, 16-32.
8. Marttila, R.J. and Rinne, U.K. (1977) Disability and progression in Parkinson's disease. *Acta Neurol Scand*, **56**, 159-69.
9. Galasko, D., Kwo-on-Yuen, P.F., Klauber, M.R. and Thal, L.J. (1990) Neurological findings in Alzheimer's disease and normal aging. *Arch Neurol*, **47**, 625-7.
10. Jenkyn, L.R., Reeves, A.G., Warren, T., Whiting, R.K., Clayton, R.J., Moore, W.W., Rizzo, A., Tuzun, I.M., Bonnett, J.C. and Culpepper, B.W. (1985) Neurologic signs in senescence. *Arch Neurol*, **42**, 1154-7.
11. Teräväinen, H. and Calne, D.B. (1983) Motor system in normal aging and Parkinson's disease. In Terry, R. (ed.), *The Neurology of Aging*. F.A. Davis, Philadelphia, pp. 85-109.
12. Pal, P.K., Samii, A. and Calne, D.B. (2002) Cardinal Features of Early Parkinson's Disease. In Weiner, W.J. (ed.), *Parkinson's disease diagnosis and clinical management*. Demos Medical Publishing, New York.
13. Thomas, B. and Beal, M.F. (2007) Parkinson's disease. *Hum Mol Genet*, **16 Spec No. 2**, R183-94.
14. de Rijk, M.C., Tzourio, C., Breteler, M.M., Dartigues, J.F., Amaducci, L., Lopez-Pousa, S., Manubens-Bertran, J.M., Alperovitch, A. and Rocca, W.A. (1997) Prevalence of parkinsonism and Parkinson's disease in Europe: the EUROPARKINSON Collaborative Study. European Community Concerted Action on the Epidemiology of Parkinson's disease. *J Neurol Neurosurg Psychiatry*, **62**, 10-5.
15. Mosewich, R.K., Rajput, A.H., Shuaib, A., Rozdilsky, B. and Ang, L. (1994) Pulmonary embolism: an under-recognized yet frequent cause of death in parkinsonism. *Mov Disord*, **9**, 350-2.
16. Rajput, M.L. and Rajput, A.H. (2002) Epidemiology of Parkinsonism. In Weiner, W.J. (ed.), *Parkinson's disease diagnosis and clinical management*. Demos Medical Publishing, New York.
17. (1992) The cost of disorders of the brain. National Foundation For Brain Research, Washington, D.C.

18. (1998) The average per-patient costs of Parkinson's Disease. In Associates, J.R., (ed.). John Robbins Associates, New York.
19. Dodel, R.C., Singer, M., Kohne-Volland, R., Szucs, T., Rathay, B., Scholz, E. and Oertel, W.H. (1998) The economic impact of Parkinson's disease. An estimation based on a 3-month prospective analysis. *Pharmacoeconomics*, **14**, 299-312.
20. Poirier, L.J. and Sourkes, T.L. (1965) Influence of the Substantia Nigra on the Catecholamine Content of the Striatum. *Brain*, **88**, 181-92.
21. Fearnley, J.M. and Lees, A.J. (1991) Ageing and Parkinson's disease: substantia nigra regional selectivity. *Brain*, **114 ( Pt 5)**, 2283-301.
22. Braak, H., Del Tredici, K., Rub, U., de Vos, R.A., Jansen Steur, E.N. and Braak, E. (2003) Staging of brain pathology related to sporadic Parkinson's disease. *Neurobiol Aging*, **24**, 197-211.
23. Marsden, C.D. (1983) Neuromelanin and Parkinson's disease. *J Neural Transm Suppl*, **19**, 121-41.
24. Spillantini, M.G., Crowther, R.A., Jakes, R., Hasegawa, M. and Goedert, M. (1998) alpha-Synuclein in filamentous inclusions of Lewy bodies from Parkinson's disease and dementia with lewy bodies. *Proc Natl Acad Sci U S A*, **95**, 6469-73.
25. Forno, L.S. (1996) Neuropathology of Parkinson's disease. *J Neuropathol Exp Neurol*, **55**, 259-72.
26. Hornykiewicz, O. and Kish, S.J. (1987) Biochemical pathophysiology of Parkinson's disease. *Adv Neurol*, **45**, 19-34.
27. Dexter, D.T., Carayon, A., Javoy-Agid, F., Agid, Y., Wells, F.R., Daniel, S.E., Lees, A.J., Jenner, P. and Marsden, C.D. (1991) Alterations in the levels of iron, ferritin and other trace metals in Parkinson's disease and other neurodegenerative diseases affecting the basal ganglia. *Brain*, **114 ( Pt 4)**, 1953-75.
28. Olanow, C.W. and Tatton, W.G. (1999) Etiology and pathogenesis of Parkinson's disease. *Annu Rev Neurosci*, **22**, 123-44.
29. Hernan, M.A., Takkouche, B., Caamano-Isorna, F. and Gestal-Otero, J.J. (2002) A meta-analysis of coffee drinking, cigarette smoking, and the risk of Parkinson's disease. *Ann Neurol*, **52**, 276-84.
30. Langston, J.W., Ballard, P., Tetrud, J.W. and Irwin, I. (1983) Chronic Parkinsonism in humans due to a product of meperidine-analog synthesis. *Science*, **219**, 979-80.
31. Markey, S.P., Johannessen, J.N., Chiueh, C.C., Burns, R.S. and Herkenham, M.A. (1984) Intraneuronal generation of a pyridinium metabolite may cause drug-induced parkinsonism. *Nature*, **311**, 464-7.
32. Javitch, J.A., D'Amato, R.J., Strittmatter, S.M. and Snyder, S.H. (1985) Parkinsonism-inducing neurotoxin, N-methyl-4-phenyl-1,2,3,6 - tetrahydropyridine: uptake of the metabolite N-methyl-4-phenylpyridine by dopamine neurons explains selective toxicity. *Proc Natl Acad Sci U S A*, **82**, 2173-7.
33. Chiba, K., Trevor, A.J. and Castagnoli, N., Jr. (1985) Active uptake of MPP+, a metabolite of MPTP, by brain synaptosomes. *Biochem Biophys Res Commun*, **128**, 1228-32.
34. Ramsay, R.R. and Singer, T.P. (1986) Energy-dependent uptake of N-methyl-4-phenylpyridinium, the neurotoxic metabolite of 1-methyl-4-phenyl-1,2,3,6-tetrahydropyridine, by mitochondria. *J Biol Chem*, **261**, 7585-7.



35. Nicklas, W.J., Vyas, I. and Heikkila, R.E. (1985) Inhibition of NADH-linked oxidation in brain mitochondria by 1-methyl-4-phenyl-pyridine, a metabolite of the neurotoxin, 1-methyl-4-phenyl-1,2,5,6-tetrahydropyridine. *Life Sci*, **36**, 2503-8.
36. Duvoisin, R.C., Eldridge, R., Williams, A., Nutt, J. and Calne, D. (1981) Twin study of Parkinson disease. *Neurology*, **31**, 77-80.
37. Marttila, R.J., Kaprio, J., Koskenvuo, M. and Rinne, U.K. (1988) Parkinson's disease in a nationwide twin cohort. *Neurology*, **38**, 1217-9.
38. Ward, C.D., Duvoisin, R.C., Ince, S.E., Nutt, J.D., Eldridge, R. and Calne, D.B. (1983) Parkinson's disease in 65 pairs of twins and in a set of quadruplets. *Neurology*, **33**, 815-24.
39. Vieregge, P., Schiffke, K.A., Friedrich, H.J., Muller, B. and Ludin, H.P. (1992) Parkinson's disease in twins. *Neurology*, **42**, 1453-61.
40. Vieregge, P., Hagenah, J., Heberlein, I., Klein, C. and Ludin, H.P. (1999) Parkinson's disease in twins: a follow-up study. *Neurology*, **53**, 566-72.
41. Tanner, C.M., Ottman, R., Goldman, S.M., Ellenberg, J., Chan, P., Mayeux, R. and Langston, J.W. (1999) Parkinson disease in twins: an etiologic study. *Jama*, **281**, 341-6.
42. Piccini, P., Burn, D.J., Ceravolo, R., Maraganore, D. and Brooks, D.J. (1999) The role of inheritance in sporadic Parkinson's disease: evidence from a longitudinal study of dopaminergic function in twins. *Ann Neurol*, **45**, 577-82.
43. Polymeropoulos, M.H., Lavedan, C., Leroy, E., Ide, S.E., Dehejia, A., Dutra, A., Pike, B., Root, H., Rubenstein, J., Boyer, R. *et al.* (1997) Mutation in the alpha-synuclein gene identified in families with Parkinson's disease. *Science*, **276**, 2045-7.
44. Kruger, R., Kuhn, W., Muller, T., Woitalla, D., Graeber, M., Kosel, S., Przuntek, H., Epplen, J.T., Schols, L. and Riess, O. (1998) Ala30Pro mutation in the gene encoding alpha-synuclein in Parkinson's disease. *Nat Genet*, **18**, 106-8.
45. Singleton, A.B., Farrer, M., Johnson, J., Singleton, A., Hague, S., Kachergus, J., Hulihan, M., Peuralinna, T., Dutra, A., Nussbaum, R. *et al.* (2003) alpha-Synuclein locus triplication causes Parkinson's disease. *Science*, **302**, 841.
46. Zarranz, J.J., Alegre, J., Gomez-Esteban, J.C., Lezcano, E., Ros, R., Ampuero, I., Vidal, L., Hoenicka, J., Rodriguez, O., Amares, B. *et al.* (2004) The new mutation, E46K, of alpha-synuclein causes Parkinson and Lewy body dementia. *Ann Neurol*, **55**, 164-73.
47. Savitt, J.M., Dawson, V.L. and Dawson, T.M. (2006) Diagnosis and treatment of Parkinson disease: molecules to medicine. *J Clin Invest*, **116**, 1744-54.
48. Nishioka, K., Hayashi, S., Farrer, M.J., Singleton, A.B., Yoshino, H., Imai, H., Kitami, T., Sato, K., Kuroda, R., Tomiyama, H. *et al.* (2006) Clinical heterogeneity of alpha-synuclein gene duplication in Parkinson's disease. *Ann Neurol*, **59**, 298-309.
49. Eriksen, J.L., Przedborski, S. and Petrucelli, L. (2005) Gene dosage and pathogenesis of Parkinson's disease. *Trends Mol Med*, **11**, 91-6.
50. Abeliovich, A., Schmitz, Y., Farinas, I., Choi-Lundberg, D., Ho, W.H., Castillo, P.E., Shinsky, N., Verdugo, J.M., Armanini, M., Ryan, A. *et al.* (2000) Mice lacking alpha-synuclein display functional deficits in the nigrostriatal dopamine system. *Neuron*, **25**, 239-52.
51. Yavich, L., Jakala, P. and Tanila, H. (2006) Abnormal compartmentalization of norepinephrine in mouse dentate gyrus in alpha-synuclein knockout and A30P transgenic mice. *J Neurochem*, **99**, 724-32.

52. Yavich, L., Tanila, H., Vepsalainen, S. and Jakala, P. (2004) Role of alpha-synuclein in presynaptic dopamine recruitment. *J Neurosci*, **24**, 11165-70.
53. Periquet, M., Fulga, T., Myllykangas, L., Schlossmacher, M.G. and Feany, M.B. (2007) Aggregated alpha-synuclein mediates dopaminergic neurotoxicity in vivo. *J Neurosci*, **27**, 3338-46.
54. Tofaris, G.K., Garcia Reitböck, P., Humby, T., Lambourne, S.L., O'Connell, M., Ghetti, B., Gossage, H., Emson, P.C., Wilkinson, L.S., Goedert, M. *et al.* (2006) Pathological changes in dopaminergic nerve cells of the substantia nigra and olfactory bulb in mice transgenic for truncated human alpha-synuclein(1-120): implications for Lewy body disorders. *J Neurosci*, **26**, 3942-50.
55. Anderson, J.P., Walker, D.E., Goldstein, J.M., de Laat, R., Banducci, K., Caccavello, R.J., Barbour, R., Huang, J., Kling, K., Lee, M. *et al.* (2006) Phosphorylation of Ser-129 is the dominant pathological modification of alpha-synuclein in familial and sporadic Lewy body disease. *J Biol Chem*, **281**, 29739-52.
56. Rochet, J.C., Outeiro, T.F., Conway, K.A., Ding, T.T., Volles, M.J., Lashuel, H.A., Bieganski, R.M., Lindquist, S.L. and Lansbury, P.T. (2004) Interactions among alpha-synuclein, dopamine, and biomembranes: some clues for understanding neurodegeneration in Parkinson's disease. *J Mol Neurosci*, **23**, 23-34.
57. Lucking, C.B., Durr, A., Bonifati, V., Vaughan, J., De Michele, G., Gasser, T., Harhangi, B.S., Meco, G., Deneffe, P., Wood, N.W. *et al.* (2000) Association between early-onset Parkinson's disease and mutations in the parkin gene. *N Engl J Med*, **342**, 1560-7.
58. Kitada, T., Asakawa, S., Hattori, N., Matsumine, H., Yamamura, Y., Minoshima, S., Yokochi, M., Mizuno, Y. and Shimizu, N. (1998) Mutations in the parkin gene cause autosomal recessive juvenile parkinsonism. *Nature*, **392**, 605-8.
59. Sasaki, S., Shirata, A., Yamane, K. and Iwata, M. (2004) Parkin-positive autosomal recessive juvenile Parkinsonism with alpha-synuclein-positive inclusions. *Neurology*, **63**, 678-82.
60. Mori, H., Kondo, T., Yokochi, M., Matsumine, H., Nakagawa-Hattori, Y., Miyake, T., Suda, K. and Mizuno, Y. (1998) Pathologic and biochemical studies of juvenile parkinsonism linked to chromosome 6q. *Neurology*, **51**, 890-2.
61. Farrer, M., Chan, P., Chen, R., Tan, L., Lincoln, S., Hernandez, D., Forno, L., Gwinn-Hardy, K., Petrucelli, L., Hussey, J. *et al.* (2001) Lewy bodies and parkinsonism in families with parkin mutations. *Ann Neurol*, **50**, 293-300.
62. Khan, N.L., Scherfler, C., Graham, E., Bhatia, K.P., Quinn, N., Lees, A.J., Brooks, D.J., Wood, N.W. and Piccini, P. (2005) Dopaminergic dysfunction in unrelated, asymptomatic carriers of a single parkin mutation. *Neurology*, **64**, 134-6.
63. Oliveira, S.A., Scott, W.K., Martin, E.R., Nance, M.A., Watts, R.L., Hubble, J.P., Koller, W.C., Pahwa, R., Stern, M.B., Hiner, B.C. *et al.* (2003) Parkin mutations and susceptibility alleles in late-onset Parkinson's disease. *Ann Neurol*, **53**, 624-9.
64. Shimura, H., Hattori, N., Kubo, S., Mizuno, Y., Asakawa, S., Minoshima, S., Shimizu, N., Iwai, K., Chiba, T., Tanaka, K. *et al.* (2000) Familial Parkinson disease gene product, parkin, is a ubiquitin-protein ligase. *Nat Genet*, **25**, 302-5.

65. Zhang, Y., Gao, J., Chung, K.K., Huang, H., Dawson, V.L. and Dawson, T.M. (2000) Parkin functions as an E2-dependent ubiquitin- protein ligase and promotes the degradation of the synaptic vesicle-associated protein, CDCrel-1. *Proc Natl Acad Sci U S A*, **97**, 13354-9.
66. Ko, H.S., von Coelln, R., Sriram, S.R., Kim, S.W., Chung, K.K., Pletnikova, O., Troncoso, J., Johnson, B., Saffary, R., Goh, E.L. *et al.* (2005) Accumulation of the authentic parkin substrate aminoacyl-tRNA synthetase cofactor, p38/JTV-1, leads to catecholaminergic cell death. *J Neurosci*, **25**, 7968-78.
67. Ko, H.S., Kim, S.W., Sriram, S.R., Dawson, V.L. and Dawson, T.M. (2006) Identification of far upstream element-binding protein-1 as an authentic Parkin substrate. *J Biol Chem*, **281**, 16193-6.
68. Feany, M.B. and Pallanck, L.J. (2003) Parkin: a multipurpose neuroprotective agent? *Neuron*, **38**, 13-6.
69. Henn, I.H., Bouman, L., Schlehe, J.S., Schlierf, A., Schramm, J.E., Wegener, E., Nakaso, K., Culmsee, C., Berninger, B., Krappmann, D. *et al.* (2007) Parkin mediates neuroprotection through activation of I $\kappa$ B kinase/nuclear factor-kappaB signaling. *J Neurosci*, **27**, 1868-78.
70. Hasegawa, T., Treis, A., Patenge, N., Fiesel, F.C., Springer, W. and Kahle, P.J. (2008) Parkin protects against tyrosinase-mediated dopamine neurotoxicity by suppressing stress-activated protein kinase pathways. *J Neurochem*, **105**, 1700-15.
71. Clark, I.E., Dodson, M.W., Jiang, C., Cao, J.H., Huh, J.R., Seol, J.H., Yoo, S.J., Hay, B.A. and Guo, M. (2006) Drosophila pink1 is required for mitochondrial function and interacts genetically with parkin. *Nature*, **441**, 1162-6.
72. Park, J., Lee, S.B., Lee, S., Kim, Y., Song, S., Kim, S., Bae, E., Kim, J., Shong, M., Kim, J.M. *et al.* (2006) Mitochondrial dysfunction in Drosophila PINK1 mutants is complemented by parkin. *Nature*, **441**, 1157-61.
73. Yang, Y., Gehrke, S., Imai, Y., Huang, Z., Ouyang, Y., Wang, J.W., Yang, L., Beal, M.F., Vogel, H. and Lu, B. (2006) Mitochondrial pathology and muscle and dopaminergic neuron degeneration caused by inactivation of Drosophila Pink1 is rescued by Parkin. *Proc Natl Acad Sci U S A*, **103**, 10793-8.
74. Moore, D.J., West, A.B., Dawson, V.L. and Dawson, T.M. (2005) Molecular pathophysiology of Parkinson's disease. *Annu Rev Neurosci*, **28**, 57-87.
75. Sang, T.K., Chang, H.Y., Lawless, G.M., Ratnaparkhi, A., Mee, L., Ackerson, L.C., Maidment, N.T., Krantz, D.E. and Jackson, G.R. (2007) A Drosophila model of mutant human parkin-induced toxicity demonstrates selective loss of dopaminergic neurons and dependence on cellular dopamine. *J Neurosci*, **27**, 981-92.
76. Hedrich, K., Djarmati, A., Schafer, N., Hering, R., Wellenbrock, C., Weiss, P.H., Hilker, R., Vieregge, P., Ozelius, L.J., Heutink, P. *et al.* (2004) DJ-1 (PARK7) mutations are less frequent than Parkin (PARK2) mutations in early-onset Parkinson disease. *Neurology*, **62**, 389-94.
77. Bonifati, V., Rizzu, P., van Baren, M.J., Schaap, O., Breedveld, G.J., Krieger, E., Dekker, M.C., Squitieri, F., Ibanez, P., Joesse, M. *et al.* (2003) Mutations in the DJ-1 gene associated with autosomal recessive early-onset parkinsonism. *Science*, **299**, 256-9.
78. Bandopadhyay, R., Kingsbury, A.E., Cookson, M.R., Reid, A.R., Evans, I.M., Hope, A.D., Pittman, A.M., Lashley, T., Canet-Aviles, R., Miller, D.W. *et al.* (2004) The expression of DJ-1 (PARK7) in normal human CNS and idiopathic Parkinson's disease. *Brain*, **127**, 420-30.

79. Canet-Aviles, R.M., Wilson, M.A., Miller, D.W., Ahmad, R., McLendon, C., Bandyopadhyay, S., Baptista, M.J., Ringe, D., Petsko, G.A. and Cookson, M.R. (2004) The Parkinson's disease protein DJ-1 is neuroprotective due to cysteine-sulfinic acid-driven mitochondrial localization. *Proc Natl Acad Sci U S A*, **101**, 9103-8.
80. Neumann, M., Muller, V., Gorner, K., Kretzschmar, H.A., Haass, C. and Kahle, P.J. (2004) Pathological properties of the Parkinson's disease-associated protein DJ-1 in alpha-synucleinopathies and tauopathies: relevance for multiple system atrophy and Pick's disease. *Acta Neuropathol*, **107**, 489-96.
81. Clements, C.M., McNally, R.S., Conti, B.J., Mak, T.W. and Ting, J.P. (2006) DJ-1, a cancer- and Parkinson's disease-associated protein, stabilizes the antioxidant transcriptional master regulator Nrf2. *Proc Natl Acad Sci U S A*, **103**, 15091-6.
82. Inden, M., Taira, T., Kitamura, Y., Yanagida, T., Tsuchiya, D., Takata, K., Yanagisawa, D., Nishimura, K., Taniguchi, T., Kiso, Y. *et al.* (2006) PARK7 DJ-1 protects against degeneration of nigral dopaminergic neurons in Parkinson's disease rat model. *Neurobiol Dis*, **24**, 144-58.
83. Paterna, J.C., Leng, A., Weber, E., Feldon, J. and Bueler, H. (2007) DJ-1 and Parkin modulate dopamine-dependent behavior and inhibit MPTP-induced nigral dopamine neuron loss in mice. *Mol Ther*, **15**, 698-704.
84. Taira, T., Saito, Y., Niki, T., Iguchi-Ariga, S.M., Takahashi, K. and Ariga, H. (2004) DJ-1 has a role in antioxidative stress to prevent cell death. *EMBO Rep*, **5**, 213-8.
85. Moore, D.J., Zhang, L., Troncoso, J., Lee, M.K., Hattori, N., Mizuno, Y., Dawson, T.M. and Dawson, V.L. (2005) Association of DJ-1 and parkin mediated by pathogenic DJ-1 mutations and oxidative stress. *Hum Mol Genet*, **14**, 71-84.
86. Shendelman, S., Jonason, A., Martinat, C., Leete, T. and Abeliovich, A. (2004) DJ-1 is a redox-dependent molecular chaperone that inhibits alpha-synuclein aggregate formation. *PLoS Biol*, **2**, e362.
87. Zhou, W., Zhu, M., Wilson, M.A., Petsko, G.A. and Fink, A.L. (2006) The oxidation state of DJ-1 regulates its chaperone activity toward alpha-synuclein. *J Mol Biol*, **356**, 1036-48.
88. Abou-Sleiman, P.M., Muqit, M.M. and Wood, N.W. (2006) Expanding insights of mitochondrial dysfunction in Parkinson's disease. *Nat Rev Neurosci*, **7**, 207-19.
89. Valente, E.M., Abou-Sleiman, P.M., Caputo, V., Muqit, M.M., Harvey, K., Gispert, S., Ali, Z., Del Turco, D., Bentivoglio, A.R., Healy, D.G. *et al.* (2004) Hereditary early-onset Parkinson's disease caused by mutations in PINK1. *Science*, **304**, 1158-60.
90. Klein, C., Djarmati, A., Hedrich, K., Schafer, N., Scaglione, C., Marchese, R., Kock, N., Schule, B., Hiller, A., Lohnau, T. *et al.* (2005) PINK1, Parkin, and DJ-1 mutations in Italian patients with early-onset parkinsonism. *Eur J Hum Genet*, **13**, 1086-93.
91. Li, Y., Tomiyama, H., Sato, K., Hatano, Y., Yoshino, H., Atsumi, M., Kitaguchi, M., Sasaki, S., Kawaguchi, S., Miyajima, H. *et al.* (2005) Clinicogenetic study of PINK1 mutations in autosomal recessive early-onset parkinsonism. *Neurology*, **64**, 1955-7.
92. Ibanez, P., Lesage, S., Lohmann, E., Thobois, S., De Michele, G., Borg, M., Agid, Y., Durr, A. and Brice, A. (2006) Mutational analysis of the PINK1 gene in early-onset parkinsonism in Europe and North Africa. *Brain*, **129**, 686-94.

93. Tan, E.K., Yew, K., Chua, E., Puvan, K., Shen, H., Lee, E., Puong, K.Y., Zhao, Y., Pavanni, R., Wong, M.C. *et al.* (2006) PINK1 mutations in sporadic early-onset Parkinson's disease. *Mov Disord*, **21**, 789-93.
94. Gandhi, S., Muqit, M.M., Stanyer, L., Healy, D.G., Abou-Sleiman, P.M., Hargreaves, I., Heales, S., Ganguly, M., Parsons, L., Lees, A.J. *et al.* (2006) PINK1 protein in normal human brain and Parkinson's disease. *Brain*, **129**, 1720-31.
95. Leutenegger, A.L., Salih, M.A., Ibanez, P., Mukhtar, M.M., Lesage, S., Arabi, A., Lohmann, E., Durr, A., Ahmed, A.E. and Brice, A. (2006) Juvenile-onset Parkinsonism as a result of the first mutation in the adenosine triphosphate orientation domain of PINK1. *Arch Neurol*, **63**, 1257-61.
96. Beilina, A., Van Der Brug, M., Ahmad, R., Kesavapany, S., Miller, D.W., Petsko, G.A. and Cookson, M.R. (2005) Mutations in PTEN-induced putative kinase 1 associated with recessive parkinsonism have differential effects on protein stability. *Proc Natl Acad Sci U S A*, **102**, 5703-8.
97. Murakami, T., Moriwaki, Y., Kawarabayashi, T., Nagai, M., Ohta, Y., Deguchi, K., Kurata, T., Morimoto, N., Takehisa, Y., Matsubara, E. *et al.* (2007) PINK1, a gene product of PARK6, accumulates in alpha-synucleinopathy brains. *J Neurol Neurosurg Psychiatry*, **78**, 653-4.
98. Muqit, M.M., Abou-Sleiman, P.M., Saurin, A.T., Harvey, K., Gandhi, S., Deas, E., Eaton, S., Payne Smith, M.D., Venner, K., Matilla, A. *et al.* (2006) Altered cleavage and localization of PINK1 to aggresomes in the presence of proteasomal stress. *J Neurochem*, **98**, 156-69.
99. Warrick, J.M., Chan, H.Y., Gray-Board, G.L., Chai, Y., Paulson, H.L. and Bonini, N.M. (1999) Suppression of polyglutamine-mediated neurodegeneration in *Drosophila* by the molecular chaperone HSP70. *Nat Genet*, **23**, 425-8.
100. Cummings, C.J., Reinstein, E., Sun, Y., Antalfy, B., Jiang, Y., Ciechanover, A., Orr, H.T., Beaudet, A.L. and Zoghbi, H.Y. (1999) Mutation of the E6-AP ubiquitin ligase reduces nuclear inclusion frequency while accelerating polyglutamine-induced pathology in SCA1 mice. *Neuron*, **24**, 879-92.
101. Cummings, C.J., Sun, Y., Opal, P., Antalfy, B., Mestril, R., Orr, H.T., Dillmann, W.H. and Zoghbi, H.Y. (2001) Over-expression of inducible HSP70 chaperone suppresses neuropathology and improves motor function in SCA1 mice. *Hum Mol Genet*, **10**, 1511-8.
102. Auluck, P.K., Chan, H.Y., Trojanowski, J.Q., Lee, V.M. and Bonini, N.M. (2002) Chaperone suppression of alpha-synuclein toxicity in a *Drosophila* model for Parkinson's disease. *Science*, **295**, 865-8.
103. Pickart, C.M. (2001) Mechanisms underlying ubiquitination. *Annu Rev Biochem*, **70**, 503-33.
104. Beckman, K.B. and Ames, B.N. (1998) The free radical theory of aging matures. *Physiol Rev*, **78**, 547-81.
105. Cohen, G. (2000) Oxidative stress, mitochondrial respiration, and Parkinson's disease. *Ann N Y Acad Sci*, **899**, 112-20.
106. Dexter, D.T., Carter, C.J., Wells, F.R., Javoy-Agid, F., Agid, Y., Lees, A., Jenner, P. and Marsden, C.D. (1989) Basal lipid peroxidation in substantia nigra is increased in Parkinson's disease. *J Neurochem*, **52**, 381-9.
107. Dexter, D.T., Holley, A.E., Flitter, W.D., Slater, T.F., Wells, F.R., Daniel, S.E., Lees, A.J., Jenner, P. and Marsden, C.D. (1994) Increased levels of lipid hydroperoxides in the parkinsonian substantia nigra: an HPLC and ESR study. *Mov Disord*, **9**, 92-7.

108. Schapira, A.H., Mann, V.M., Cooper, J.M., Dexter, D., Daniel, S.E., Jenner, P., Clark, J.B. and Marsden, C.D. (1990) Anatomic and disease specificity of NADH CoQ1 reductase (complex I) deficiency in Parkinson's disease. *J Neurochem*, **55**, 2142-5.
109. Sian, J., Dexter, D.T., Lees, A.J., Daniel, S., Agid, Y., Javoy-Agid, F., Jenner, P. and Marsden, C.D. (1994) Alterations in glutathione levels in Parkinson's disease and other neurodegenerative disorders affecting basal ganglia. *Ann Neurol*, **36**, 348-55.
110. Zimprich, A., Biskup, S., Leitner, P., Lichtner, P., Farrer, M., Lincoln, S., Kachergus, J., Hulihan, M., Uitti, R.J., Calne, D.B. *et al.* (2004) Mutations in LRRK2 cause autosomal-dominant parkinsonism with pleomorphic pathology. *Neuron*, **44**, 601-7.
111. Paisan-Ruiz, C., Jain, S., Evans, E.W., Gilks, W.P., Simon, J., van der Brug, M., Lopez de Munain, A., Aparicio, S., Gil, A.M., Khan, N. *et al.* (2004) Cloning of the gene containing mutations that cause PARK8-linked Parkinson's disease. *Neuron*, **44**, 595-600.
112. Funayama, M., Hasegawa, K., Kowa, H., Saito, M., Tsuji, S. and Obata, F. (2002) A new locus for Parkinson's disease (PARK8) maps to chromosome 12p11.2-q13.1. *Ann Neurol*, **51**, 296-301.
113. Wszolek, Z.K., Pfeiffer, R.F., Tsuboi, Y., Uitti, R.J., McComb, R.D., Stoessel, A.J., Strongosky, A.J., Zimprich, A., Muller-Myhsok, B., Farrer, M.J. *et al.* (2004) Autosomal dominant parkinsonism associated with variable synuclein and tau pathology. *Neurology*, **62**, 1619-22.
114. Mata, I.F., Wedemeyer, W.J., Farrer, M.J., Taylor, J.P. and Gallo, K.A. (2006) LRRK2 in Parkinson's disease: protein domains and functional insights. *Trends Neurosci*, **29**, 286-93.
115. Bosgraaf, L. and Van Haastert, P.J. (2003) Roc, a Ras/GTPase domain in complex proteins. *Biochim Biophys Acta*, **1643**, 5-10.
116. Marin, I. (2006) The Parkinson disease gene LRRK2: evolutionary and structural insights. *Mol Biol Evol*, **23**, 2423-33.
117. Deng, J., Lewis, P.A., Greggio, E., Sluch, E., Beilina, A. and Cookson, M.R. (2008) Structure of the ROC domain from the Parkinson's disease-associated leucine-rich repeat kinase 2 reveals a dimeric GTPase. *Proc Natl Acad Sci U S A*, **105**, 1499-504.
118. Gotthardt, K., Weyand, M., Kortholt, A., Van Haastert, P.J. and Wittinghofer, A. (2008) Structure of the Roc-COR domain tandem of *C. tepidum*, a prokaryotic homologue of the human LRRK2 Parkinson kinase. *Embo J*.
119. West, A.B., Moore, D.J., Biskup, S., Bugayenko, A., Smith, W.W., Ross, C.A., Dawson, V.L. and Dawson, T.M. (2005) Parkinson's disease-associated mutations in leucine-rich repeat kinase 2 augment kinase activity. *Proc Natl Acad Sci U S A*, **102**, 16842-7.
120. Giasson, B.I., Covy, J.P., Bonini, N.M., Hurtig, H.I., Farrer, M.J., Trojanowski, J.Q. and Van Deerlin, V.M. (2006) Biochemical and pathological characterization of Lrrk2. *Ann Neurol*, **59**, 315-22.
121. Biskup, S., Moore, D.J., Celsi, F., Higashi, S., West, A.B., Andrabi, S.A., Kurkinen, K., Yu, S.W., Savitt, J.M., Waldvogel, H.J. *et al.* (2006) Localization of LRRK2 to membranous and vesicular structures in mammalian brain. *Ann Neurol*, **60**, 557-69.
122. Simon-Sanchez, J., Herranz-Perez, V., Olucha-Bordonau, F. and Perez-Tur, J. (2006) LRRK2 is expressed in areas affected by Parkinson's disease in the adult mouse brain. *Eur J Neurosci*, **23**, 659-66.

123. Taymans, J.M., Van den Haute, C. and Baekelandt, V. (2006) Distribution of PINK1 and LRRK2 in rat and mouse brain. *J Neurochem*, **98**, 951-61.
124. Melrose, H.L., Kent, C.B., Taylor, J.P., Dachsel, J.C., Hinkle, K.M., Lincoln, S.J., Mok, S.S., Culvenor, J.G., Masters, C.L., Tyndall, G.M. *et al.* (2007) A comparative analysis of leucine-rich repeat kinase 2 (Lrrk2) expression in mouse brain and Lewy body disease. *Neuroscience*, **147**, 1047-58.
125. Melrose, H., Lincoln, S., Tyndall, G., Dickson, D. and Farrer, M. (2006) Anatomical localization of leucine-rich repeat kinase 2 in mouse brain. *Neuroscience*, **139**, 791-4.
126. Higashi, S., Moore, D.J., Colebrooke, R.E., Biskup, S., Dawson, V.L., Arai, H., Dawson, T.M. and Emson, P.C. (2007) Expression and localization of Parkinson's disease-associated leucine-rich repeat kinase 2 in the mouse brain. *J Neurochem*, **100**, 368-81.
127. Higashi, S., Biskup, S., West, A.B., Trinkaus, D., Dawson, V.L., Faull, R.L., Waldvogel, H.J., Arai, H., Dawson, T.M., Moore, D.J. *et al.* (2007) Localization of Parkinson's disease-associated LRRK2 in normal and pathological human brain. *Brain Res*, **1155**, 208-19.
128. Galter, D., Westerlund, M., Carmine, A., Lindqvist, E., Sydow, O. and Olson, L. (2006) LRRK2 expression linked to dopamine-innervated areas. *Ann Neurol*, **59**, 714-9.
129. Gloeckner, C.J., Kinkl, N., Schumacher, A., Braun, R.J., O'Neill, E., Meitinger, T., Kolch, W., Prokisch, H. and Ueffing, M. (2006) The Parkinson disease causing LRRK2 mutation I2020T is associated with increased kinase activity. *Hum Mol Genet*, **15**, 223-32.
130. Greggio, E., Jain, S., Kingsbury, A., Bandopadhyay, R., Lewis, P., Kaganovich, A., van der Brug, M.P., Beilina, A., Blackinton, J., Thomas, K.J. *et al.* (2006) Kinase activity is required for the toxic effects of mutant LRRK2/dardarin. *Neurobiol Dis*, **23**, 329-41.
131. Hatano, T., Kubo, S., Imai, S., Maeda, M., Ishikawa, K., Mizuno, Y. and Hattori, N. (2007) Leucine-rich repeat kinase 2 associates with lipid rafts. *Hum Mol Genet*, **16**, 678-90.
132. Paisan-Ruiz, C., Nath, P., Washecka, N., Gibbs, J.R. and Singleton, A.B. (2008) Comprehensive analysis of LRRK2 in publicly available Parkinson's disease cases and neurologically normal controls. *Hum Mutat*, **29**, 485-490.
133. Nichols, W.C., Pankratz, N., Hernandez, D., Paisán-Ruíz, C., Jain, S., Halter, C.A., Michaels, V.E., Reed, T., Rudolph, A., Shults, C.W. *et al.* (2005) Genetic screening for a single common LRRK2 mutation in familial Parkinson's disease. *Lancet*, **365**, 410-1.
134. Kachergus, J., Mata, I.F., Hulihan, M., Taylor, J.P., Lincoln, S., Aasly, J., Gibson, J.M., Ross, O.A., Lynch, T., Wiley, J. *et al.* (2005) Identification of a novel LRRK2 mutation linked to autosomal dominant parkinsonism: evidence of a common founder across European populations. *Am J Hum Genet*, **76**, 672-80.
135. Hernandez, D., Paisan Ruiz, C., Crawley, A., Malkani, R., Werner, J., Gwinn-Hardy, K., Dickson, D., Wavrant Devrieze, F., Hardy, J. and Singleton, A. (2005) The dardarin G 2019 S mutation is a common cause of Parkinson's disease but not other neurodegenerative diseases. *Neurosci Lett*, **389**, 137-9.
136. Di Fonzo, A., Rohé, C.F., Ferreira, J., Chien, H.F., Vacca, L., Stocchi, F., Guedes, L., Fabrizio, E., Manfredi, M., Vanacore, N. *et al.* (2005) A frequent LRRK2 gene mutation associated with autosomal dominant Parkinson's disease. *Lancet*, **365**, 412-4.

137. Deng, H., Le, W., Guo, Y., Hunter, C.B., Xie, W. and Jankovic, J. (2005) Genetic and clinical identification of Parkinson's disease patients with LRRK2 G2019S mutation. *Ann Neurol*, **57**, 933-4.
138. Paisan-Ruiz, C., Lang, A.E., Kawarai, T., Sato, C., Salehi-Rad, S., Fisman, G.K., Al-Khairallah, T., St George-Hyslop, P., Singleton, A. and Rogaeva, E. (2005) LRRK2 gene in Parkinson disease: mutation analysis and case control association study. *Neurology*, **65**, 696-700.
139. Ozelius, L.J., Senthil, G., Saunders-Pullman, R., Ohmann, E., Deligtisch, A., Tagliati, M., Hunt, A.L., Klein, C., Henick, B., Hailpern, S.M. *et al.* (2006) LRRK2 G2019S as a cause of Parkinson's disease in Ashkenazi Jews. *N Engl J Med*, **354**, 424-5.
140. Lesage, S., Ibanez, P., Lohmann, E., Pollak, P., Tison, F., Tazir, M., Leutenegger, A.L., Guimaraes, J., Bonnet, A.M., Agid, Y. *et al.* (2005) G2019S LRRK2 mutation in French and North African families with Parkinson's disease. *Ann Neurol*, **58**, 784-7.
141. Lesage, S., Durr, A., Tazir, M., Lohmann, E., Leutenegger, A.L., Janin, S., Pollak, P. and Brice, A. (2006) LRRK2 G2019S as a cause of Parkinson's disease in North African Arabs. *N Engl J Med*, **354**, 422-3.
142. Tan, E.K., Shen, H., Tan, L.C., Farrer, M., Yew, K., Chua, E., Jamora, R.D., Puvan, K., Puong, K.Y., Zhao, Y. *et al.* (2005) The G2019S LRRK2 mutation is uncommon in an Asian cohort of Parkinson's disease patients. *Neurosci Lett*, **384**, 327-9.
143. Lu, C.S., Simons, E.J., Wu-Chou, Y.H., Fonzo, A.D., Chang, H.C., Chen, R.S., Weng, Y.H., Rohe, C.F., Breedveld, G.J., Hattori, N. *et al.* (2005) The LRRK2 I2012T, G2019S, and I2020T mutations are rare in Taiwanese patients with sporadic Parkinson's disease. *Parkinsonism Relat Disord*, **11**, 521-2.
144. Goldwurm, S., Zini, M., Mariani, L., Tesei, S., Miceli, R., Sironi, F., Clementi, M., Bonifati, V. and Pezzoli, G. (2007) Evaluation of LRRK2 G2019S penetrance: relevance for genetic counseling in Parkinson disease. *Neurology*, **68**, 1141-3.
145. West, A.B., Moore, D.J., Choi, C., Andrabi, S.A., Li, X., Dikeman, D., Biskup, S., Zhang, Z., Lim, K.L., Dawson, V.L. *et al.* (2007) Parkinson's disease-associated mutations in LRRK2 link enhanced GTP-binding and kinase activities to neuronal toxicity. *Hum Mol Genet*, **16**, 223-32.
146. Smith, W.W., Pei, Z., Jiang, H., Dawson, V.L., Dawson, T.M. and Ross, C.A. (2006) Kinase activity of mutant LRRK2 mediates neuronal toxicity. *Nat Neurosci*, **9**, 1231-3.
147. Jaleel, M., Nichols, R.J., Deak, M., Campbell, D.G., Gillardon, F., Knebel, A. and Alessi, D.R. (2007) LRRK2 phosphorylates moesin at threonine-558: characterization of how Parkinson's disease mutants affect kinase activity. *Biochem J*, **405**, 307-17.
148. Li, X., Tan, Y.C., Poulou, S., Olanow, C.W., Huang, X.Y. and Yue, Z. (2007) Leucine-rich repeat kinase 2 (LRRK2)/PARK8 possesses GTPase activity that is altered in familial Parkinson's disease R1441C/G mutants. *J Neurochem*, **103**, 238-47.
149. Lewis, P.A., Greggio, E., Beilina, A., Jain, S., Baker, A. and Cookson, M.R. (2007) The R1441C mutation of LRRK2 disrupts GTP hydrolysis. *Biochem Biophys Res Commun*, **357**, 668-71.
150. Ito, G., Okai, T., Fujino, G., Takeda, K., Ichijo, H., Katada, T. and Iwatsubo, T. (2007) GTP binding is essential to the protein kinase activity of LRRK2, a



- causative gene product for familial Parkinson's disease. *Biochemistry*, **46**, 1380-8.
151. MacLeod, D., Dowman, J., Hammond, R., Leete, T., Inoue, K. and Abeliovich, A. (2006) The familial Parkinsonism gene LRRK2 regulates neurite process morphology. *Neuron*, **52**, 587-93.
152. Smith, W.W., Pei, Z., Jiang, H., Moore, D.J., Liang, Y., West, A.B., Dawson, V.L., Dawson, T.M. and Ross, C.A. (2005) Leucine-rich repeat kinase 2 (LRRK2) interacts with parkin, and mutant LRRK2 induces neuronal degeneration. *Proc Natl Acad Sci U S A*, **102**, 18676-81.
153. Plowey, E.D., Cherra, S.J., 3rd, Liu, Y.J. and Chu, C.T. (2008) Role of autophagy in G2019S-LRRK2-associated neurite shortening in differentiated SH-SY5Y cells. *J Neurochem*, **105**, 1048-56.
154. Dachselt, J.C., Taylor, J.P., Mok, S.S., Ross, O.A., Hinkle, K.M., Bailey, R.M., Hines, J.H., Szutu, J., Madden, B., Petrucelli, L. *et al.* (2007) Identification of potential protein interactors of Lrrk2. *Parkinsonism Relat Disord*, **13**, 382-5.
155. Wang, L., Xie, C., Greggio, E., Parisiadou, L., Shim, H., Sun, L., Chandran, J., Lin, X., Lai, C., Yang, W.J. *et al.* (2008) The chaperone activity of heat shock protein 90 is critical for maintaining the stability of leucine-rich repeat kinase 2. *J Neurosci*, **28**, 3384-91.
156. Gandhi, P.N., Wang, X., Zhu, X., Chen, S.G. and Wilson-Delfosse, A.L. (2008) The Roc domain of leucine-rich repeat kinase 2 is sufficient for interaction with microtubules. *J Neurosci Res*.
157. Greggio, E., Zambrano, I., Kaganovich, A., Beilina, A., Taymans, J.M., Daniels, V., Lewis, P., Jain, S., Ding, J., Syed, A. *et al.* (2008) The Parkinson Disease-associated Leucine-rich Repeat Kinase 2 (LRRK2) Is a Dimer That Undergoes Intramolecular Autophosphorylation. *J Biol Chem*, **283**, 16906-14.
158. Luzon-Toro, B., de la Torre, E.R., Delgado, A., Perez-Tur, J. and Hilfiker, S. (2007) Mechanistic insight into the dominant mode of the Parkinson's disease-associated G2019S LRRK2 mutation. *Hum Mol Genet*, **16**, 2031-9.
159. Sakaguchi-Nakashima, A., Meir, J.Y., Jin, Y., Matsumoto, K. and Hisamoto, N. (2007) LRK-1, a *C. elegans* PARK8-related kinase, regulates axonal-dendritic polarity of SV proteins. *Curr Biol*, **17**, 592-8.
160. Liu, Z., Wang, X., Yu, Y., Li, X., Wang, T., Jiang, H., Ren, Q., Jiao, Y., Sawa, A., Moran, T. *et al.* (2008) A *Drosophila* model for LRRK2-linked parkinsonism. *Proc Natl Acad Sci U S A*, **105**, 2693-8.
161. Wang, D., Tang, B., Zhao, G., Pan, Q., Xia, K., Bodmer, R. and Zhang, Z. (2008) Dispensable role of *Drosophila* ortholog of LRRK2 kinase activity in survival of dopaminergic neurons. *Mol Neurodegener*, **3**, 3.
162. Kolch, W. (2005) Coordinating ERK/MAPK signalling through scaffolds and inhibitors. *Nat Rev Mol Cell Biol*, **6**, 827-37.
163. Takai, Y., Sasaki, T. and Matozaki, T. (2001) Small GTP-binding proteins. *Physiol Rev*, **81**, 153-208.
164. Korr, D., Toschi, L., Donner, P., Pohlenz, H.D., Kreft, B. and Weiss, B. (2006) LRRK1 protein kinase activity is stimulated upon binding of GTP to its Roc domain. *Cell Signal*, **18**, 910-20.
165. Taylor, J.P., Hulihan, M.M., Kachergus, J.M., Melrose, H.L., Lincoln, S.J., Hinkle, K.M., Stone, J.T., Ross, O.A., Hauser, R., Aasly, J. *et al.* (2007) Leucine-rich repeat kinase 1: a paralog of LRRK2 and a candidate gene for Parkinson's disease. *Neurogenetics*, **8**, 95-102.
166. Cohen, O., Feinstein, E. and Kimchi, A. (1997) DAP-kinase is a Ca<sup>2+</sup>/calmodulin-dependent, cytoskeletal-associated protein kinase, with cell

- death-inducing functions that depend on its catalytic activity. *Embo J*, **16**, 998-1008.
167. Li, Y., Grupe, A., Rowland, C., Nowotny, P., Kauwe, J.S., Smemo, S., Hinrichs, A., Tacey, K., Toombs, T.A., Kwok, S. *et al.* (2006) DAPK1 variants are associated with Alzheimer's disease and allele-specific expression. *Hum Mol Genet*, **15**, 2560-8.
168. Bialik, S. and Kimchi, A. (2006) The death-associated protein kinases: structure, function, and beyond. *Annu Rev Biochem*, **75**, 189-210.
169. Manning, G., Whyte, D.B., Martinez, R., Hunter, T. and Sudarsanam, S. (2002) The protein kinase complement of the human genome. *Science*, **298**, 1912-34.
170. Leung, I.W. and Lassam, N. (1998) Dimerization via tandem leucine zippers is essential for the activation of the mitogen-activated protein kinase kinase kinase, MLK-3. *J Biol Chem*, **273**, 32408-15.
171. Farrar, M.A., Alberol, I. and Perlmutter, R.M. (1996) Activation of the Raf-1 kinase cascade by coumermycin-induced dimerization. *Nature*, **383**, 178-81.
172. Guo, L., Gandhi, P.N., Wang, W., Petersen, R.B., Wilson-Delfosse, A.L. and Chen, S.G. (2007) The Parkinson's disease-associated protein, leucine-rich repeat kinase 2 (LRRK2), is an authentic GTPase that stimulates kinase activity. *Exp Cell Res*, **313**, 3658-70.
173. Scott, P.G., McEwan, P.A., Dodd, C.M., Bergmann, E.M., Bishop, P.N. and Bella, J. (2004) Crystal structure of the dimeric protein core of decorin, the archetypal small leucine-rich repeat proteoglycan. *Proc Natl Acad Sci U S A*, **101**, 15633-8.
174. Kerppola, T.K. (2006) Visualization of molecular interactions by fluorescence complementation. *Nat Rev Mol Cell Biol*, **7**, 449-56.
175. Shyu, Y.J., Liu, H., Deng, X. and Hu, C.D. (2006) Identification of new fluorescent protein fragments for bimolecular fluorescence complementation analysis under physiological conditions. *Biotechniques*, **40**, 61-6.
176. Tanaka, S. and Hanafusa, H. (1998) Guanine-nucleotide exchange protein C3G activates JNK1 by a ras-independent mechanism. JNK1 activation inhibited by kinase negative forms of MLK3 and DLK mixed lineage kinases. *J Biol Chem*, **273**, 1281-4.
177. Terai, K. and Matsuda, M. (2006) The amino-terminal B-Raf-specific region mediates calcium-dependent homo- and hetero-dimerization of Raf. *Embo J*, **25**, 3556-64.
178. Garnett, M.J., Rana, S., Paterson, H., Barford, D. and Marais, R. (2005) Wild-type and mutant B-RAF activate C-RAF through distinct mechanisms involving heterodimerization. *Mol Cell*, **20**, 963-9.
179. Rushworth, L.K., Hindley, A.D., O'Neill, E. and Kolch, W. (2006) Regulation and role of Raf-1/B-Raf heterodimerization. *Mol Cell Biol*, **26**, 2262-72.
180. Westerlund, M., Belin, A.C., Anvret, A., Bickford, P., Olson, L. and Galter, D. (2008) Developmental regulation of leucine-rich repeat kinase 1 and 2 expression in the brain and other rodent and human organs: Implications for Parkinson's disease. *Neuroscience*, **152**, 429-36.
181. Biskup, S., Moore, D.J., Rea, A., Lorenz-Deperieux, B., Coombes, C.E., Dawson, V.L., Dawson, T.M. and West, A.B. (2007) Dynamic and redundant regulation of LRRK2 and LRRK1 expression. *BMC Neurosci*, **8**, 102.
182. Marin, I., van Egmond, W.N. and van Haastert, P.J. (2008) The Roco protein family: a functional perspective. *Faseb J*.


183. Greggio, E., Zambrano, I., Kaganovich, A., Beilina, A., Taymans, J.M., Daniels, V., Lewis, P., Jain, S., Ding, J., Syed, A. *et al.* (2008) The Parkinson's disease associated Leucine rich repeat kinase 2 (LRRK2) is a dimer that undergoes intra-molecular autophosphorylation. *J Biol Chem*.
184. Noble, M.E., Endicott, J.A. and Johnson, L.N. (2004) Protein kinase inhibitors: insights into drug design from structure. *Science*, **303**, 1800-5.
185. Knight, Z.A. and Shokat, K.M. (2005) Features of selective kinase inhibitors. *Chem Biol*, **12**, 621-37.
186. Fujino, G., Noguchi, T., Matsuzawa, A., Yamauchi, S., Saitoh, M., Takeda, K. and Ichijo, H. (2007) Thioredoxin and TRAF family proteins regulate reactive oxygen species-dependent activation of ASK1 through reciprocal modulation of the N-terminal homophilic interaction of ASK1. *Mol Cell Biol*, **27**, 8152-63.
187. Landon, L.A., Zou, J. and Deutscher, S.L. (2004) Is phage display technology on target for developing peptide-based cancer drugs? *Curr Drug Discov Technol*, **1**, 113-32.
188. Lin, Y., Stevens, C. and Hupp, T. (2007) Identification of a dominant negative functional domain on DAPK-1 that degrades DAPK-1 protein and stimulates TNFR-1-mediated apoptosis. *J Biol Chem*, **282**, 16792-802.
189. Pear, W.S., Nolan, G.P., Scott, M.L. and Baltimore, D. (1993) Production of high-titer helper-free retroviruses by transient transfection. *Proc Natl Acad Sci U S A*, **90**, 8392-6.



## Erklärung

Ich erkläre hiermit, dass ich die zur Promotion eingereichte Arbeit mit dem Titel: „*Functional characterization of leucine-rich repeat kinase 2 (LRRK2) dimerization*“ selbstständig verfasst, nur die angegebenen Quellen und Hilfsmittel benutzt und wörtlich oder inhaltlich übernommene Stellen als solche gekennzeichnet habe. Ich versichere an Eides statt, dass diese Angaben wahr sind und dass ich nichts verschwiegen habe. Mir ist bekannt, dass die falsche Abgabe einer Versicherung an Eides statt mit Freiheitsstrafe bis zu drei Jahren oder mit Geldstrafe bestraft wird.

Tübingen, im September 2008

A handwritten signature in black ink, appearing to read 'A. U.', is positioned to the right of the date.



## Danksagungen

Herrn **Prof. Dr. Tomas Gasser** möchte ich für die Bereitstellung des Arbeitsplatzes in seiner Arbeitsgruppe für Neurodegenerative Erkrankungen, die Erstellung des Erstgutachtens, sowie für die Vertretung der vorliegenden Dissertation an der Fakultät für Biologie und der medizinischen Fakultät der Eberhard-Karls-Universität Tübingen danken.

Herrn **Prof. Dr. Thilo Stehle** danke ich für die Bereitschaft, das Zweitgutachten für diese Dissertation zu erstellen.

Besonderer Dank gilt Herrn **Prof. Dr. Philipp Kahle**, der mir in zahlreichen wissenschaftlichen Diskussionen jederzeit mit fachmännischem Rat zur Seite stand und mit seinen interessanten und fundierten Anregungen zum Gelingen sowohl des experimentellen als auch des schriftlichen Teils dieser Dissertation beigetragen hat.

Bei den Mitgliedern der Arbeitsgruppe für Neurodegenerative Erkrankungen und der Arbeitsgruppe für Funktionelle Neurogenetik bedanke ich mich für die gute kollegiale Zusammenarbeit (und das Ertragen meines Musikgeschmackes 😊).

Ganz besonders bedanke ich mich bei meiner **Susi**, die mich immer bedingungslos unterstützt, mir viel Kraft gibt und jeden Tag ein Lächeln auf mein Gesicht zaubert.

Bedanken möchte ich mich auch bei meiner Familie: **Mama, Papa** und **Michi**, die immer an mich glauben und mich durch ihr liebevolles Verständnis in jeder erdenklichen Weise unterstützen. In großer Dankbarkeit denke ich an meinen verstorbenen Bruder **Jojo**, der mein Leben geprägt hat.

Darüber hinaus möchte ich den unzähligen Metalbands danken, die mit ihren Songs so manche Frustration im Laboralltag ertragbarer gemacht haben.





## CHRISTIAN KLEIN

Diplom-Molekularmediziner

Am Bronnen 15

72074 Tübingen

☎ 07071 856499

✉ ch.klein@uni-tuebingen.de



## CURRICULUM VITAE

### AUSBILDUNG

- 2004 – heute Promotionsstudium, Universität Tübingen  
Interfakultärer Studiengang Neuro- und Verhaltenswissenschaften  
(International Max Planck Research School)  
*voraussichtlicher Abschluss zum Dr. rer. nat. im Herbst 2008*
- 1999 – 2004 Studium der Molekularen Medizin, Universität Erlangen  
Diplom (Note 1,0 – mit Auszeichnung bestanden)
- 1998 – 1999 Studium der Biologie, Universität Erlangen
- 1988 – 1997 Gymnasium Neustadt a.d. Aisch, Abitur (Note 1,1)

### PRAKTISCH-BERUFLICHE ERFAHRUNG

- 12.2004 - heute Naturwissenschaftliche Dissertation  
Abteilung für Neurodegeneration, Hertie-Institut für klinische Hirnforschung,  
Universität Tübingen  
*Thema: "Functional characterization of leucine-rich repeat kinase 2  
(LRRK2) dimerization"*
- 07.2004 - 08.2004 6-wöchiges Praktikum im Biotech-Unternehmen  
responsif GmbH (Erlangen)
- 12.2003 - 06.2004 Diplomarbeit  
Labor für molekulare Neurobiologie, Universität Erlangen  
*Thema : "Characterization of soluble A $\beta$ -peptide-oligomers in vitro and  
investigation of complex-bound A $\beta$ -peptides in the lumbar  
cerebrospinal fluid in Alzheimer disease"*

### SONSTIGES

- Stipendien* seit Mai 2002: e-fellows Online-Stipendium
- PC* Adobe Photoshop – Experte  
Adobe Illustrator – sehr gute Kenntnisse  
Microsoft Office – sehr gute Kenntnisse
- Sprachen* Englisch – verhandlungssicher  
Französisch – Basiskenntnisse

### INTERESSEN

- Musik* Komponist, Sänger und Gitarrist der Metalband *ENCRYPTION*  
Veröffentlichung zweier selbst produzierter CDs (1997, 2000)  
Vorproduktion eigener Musikstücke am PC
- Digitales Design* Flyer, Poster, T-Shirts und CD-booklets für Encryption  
Erstellung von Panoramabildern
- Sport* Wandern, Volleyball